PN-ABH-394

FINAL REPORT

7.143

January 1991

APR 1 1991

FINAL REPORT

Project Title: Supercritical Fluid Extraction of Natural and Biological Products.

Proposal Number: 7.143.

Project Number: 936-5542.

Grant Number: DPE-5542-G-SS-7048-00.

Project Office: S&T/SCI.

Obligation Number: 7361213.

Grantee: Centro Quimica Estrutural
Instituto Superior Tecnico
Lisbon, Portugal.

Principal Investigator: Manuel Nunes da Ponte.

Period of Grant: From August 20, 1987 to March 31, 1991.

Period of Report: From August 20, 1987 to September 30, 1990.

Date of Raport: January 18, 1991.

List of Abbreviations Used in this Report:

AID = Agency for International Developmemt
CQE = Centro Quimica Estrutural
EOS = Equation of State
LDC = Less-Developed Country
SCF = Supercritical Fluid
VLE = Vapor-Liquid Equilibrium

Apr 1991

CONTENTS

1. Introduction 1

2. Research Activities 2
2.1. Introduction 2
2.2. Experimental 6
2.2.1. Solubility Apparatus with Opaque Cells 6
2.2.2. Solubility Apparatus with Visual Cells 8
2.2.3. Countercurrent Liquid-SCF Extraction Columns 9
2.3. Results 12
2.3.1. Measurement of Solubilities in SCF 12
2.3.1.1. Eucalyptus Oil 12
2.3.1.1.1. VLE in Carbon Dioxide 12
2.3.1.1.2. VLE of the Ternary Carbon Dioxide + Cineole + Limonene 14
2.3.1.1.3. VLE in Carbon Dioxide + Ethane Mixtures 16
2.3.1.1.4. VLE in Supercritical Ethene 17
2.3.1.1.5. Solubility Measurements in Compressed Gaseous Ethene 18
2.3.1.1.6. VLE of the Ternary Ethene+Cineole+Limonene 20
2.3.1.2. Extraction of Lactic Acid 20
2.3.1.3. Solubilities of Olive Oil Components in Supercritical Carbon Dioxide 21
2.3.2. Thermodynamic Modelling of the Phase Behavior 25
2.3.2.1. EOS Model 25
2.3.2.2. Statistical Thermodynamics-Based Model 28
2.3.2.2.1. Molecular Thermodynamics of SCF 29
2.3.2.2.2. Statistical Thermodynamics Considerations 31
2.3.2.2.3. Calculation of Solid Solubilities 34
2.3.2.2.4. Data Reduction 35
2.3.2.2.5. Extension to the Calculation of Solubilities of Liquids 37
2.3.2.2.6. Conclusions 37
2.3.3. New Directions 37

3. Scientific Collaboration 38

4. Training Programme 40

5. Comparison of Actual Accomplishments with Goals Established 42

6. List of Equipment Appraised Over $1,000 44

7. Concluding Remarks 45

7.1. Introduction 45

7.2. Relevance of this Work to LDC's 46

8. List of Publications 47

9. Annex: Pictures of the Experimental Apparatuses 50

10. Reprints of the Publications 55

1. INTRODUCTION

This Grant from AID was aimed to provide assistance and support to the research to be carried out at Centro Quimica Estrutural (hereinafter referred to as "CQE") towards the study of supercritical fluid extraction of valuable natural and biological products.

The life of the Grant was from August 20, 1987 through August 19, 1990. The completion date was later extended to March 31, 1991, as authorized by the Project Officer in his letter of January 4, 1991.

As stated in the Grant document, this research had the following specific objectives:

a) The measurement of the solubilities of the substances to be extracted in supercritical carbon dioxide (pure or mixed with an entrainer). These substances included the components of eucalyptus oil and others obtained from fermentation broths.

b) The thermodynamic modelling of the phase behavior of multicomponent mixtures that include carbon dioxide to obtain the best conditions of extraction.

c) The design and operation of a countercurrent extraction column, with optimization of the process parameters.

This research work involved the collaboration of the following Institutions and Investigators:

<u>From</u> <u>CQE</u> (Instituto Superior Tecnico and New University of Lisbon):

Manuel Nunes da Ponte (Principal Investigator).
Edmundo Gomes de Azevedo (Investigator).
Manuel T. Carrondo (Investigator).
Susana F. Barreiros (Investigator).
Henrique A. Matos (Graduate Student).
Pedro C. Simões (Graduate Student).

Margarida Gonçalves (Graduate Student).

From the University of Sierra Leone (Freetown, Sierra Leone, West Africa):
Daniel A. Jonah.

From the University of California (Berkeley, USA):
John M. Prausnitz.

From Cornell University (Ithaca, New York, USA):
William B. Streett.
John Zollweg.

The following Sections present the principal findings of this AID-sponsored research, as well as a comparison between the actual accomplishments with the goals established in the proposal and a report of the scientific collaboration and of the training programme developed during the life of this Grant.

2. RESEARCH ACTIVITIES

2.1. Introduction

In recent years attention has been paid worldwide to the experimental and theoretical aspects of SCF extraction.

SCF have unique physico-chemical and transport properties that make them specially interesting solvents. More particularly, the properties (e.g. density) of a compressed substance in the vicinity of its critical point can be modified by changes in pressure and/or temperature in such a way that the substance behaves either as a normal low-density gas or as liquid, thus changing greatly its solubility power. Therefore these substances have potential use as solvents in extraction or separation processes .

At the time of presentation of our proposal (August 1986) there were already a few well-known industrial processes which used SCF carbon dioxide as solvent (e.g, decaffeination of coffee and hops extraction). These processes took advantage of some of the characteristics presented by SCF, namely the absence of toxic residues in the final product and (possible) energy savings. However, industrial process designers claimed that this technique demanded high capital costs and posed safety problems due to the high pressures involved. Moreover, they were somehow skeptical about what appeared to them as a relatively untried technology with limited thermodynamic models which they needed for design and scale-up. This was particularly important in the food (or related) industries which didn't use routinely high pressure technology.

It is very likely that SCF extraction can solve important separation problems in many areas, namely in food, flavor, and fragances industries, and in specific separations of thermally labile pharmaceuticals. This means that this technique is more suitable in difficult separations, especially those involving relatively low-volume, high-value products.

We must point out, however, that environmental concerns (substitution of toxic solvents) and governamental regulations (absence of toxic residues in food and related products) make supercritical extraction potentially more attractive than conventional separations.

Since then, research activities centered in this new separation process have considerably expanded worldwide. Two recent Symposia on this subject, one in Europe, (*International Symposium on Supercritical Fluids*), held in Nice, France, in October 1988, and the other in the U.S.A., (*Symposium on Supercritical Fluid Extraction, American Institute of Chemical Engineers Annual Meeting*), held in Washington, D.C., in December 1988, were very successful, with an attendance of several hundred scientists and engineers and hundreds of communications. A recent survey of the

most promising separation processes in Chemical Engineering[1] rated SCF extracton among the top ten. Krukonis[2] has recently claimed that, after a decade of commercial applications, supercritical extraction should not be regarded any longer as a non-conventional process.

The course of events in this field has strongly influenced our research program. The knowledge base formed in our research group during the execution of this program has allowed us to accompany the main directions of change in this field and to develop it accordingly. Changes were introduced in the natural product extraction program as well as in the projected research on extraction from fermentation broths.

Eucalyptus oil was our model system for the purification of natural products using supercritical fluids. As carbon dioxide and carbon dioxide based mixtures revealed themselves not useful to this purpose (see Publication 3), we had to experiment with different solvents. Ethene (ethylene) seemed a logical choice due to the presence of carbon-carbon double bonds in the main impurity to remove from the oil, limonene. One of the main thrusts in our work was therefore a complete characterization of the phase diagrams of mixtures of ethene with eucalyptus oil components.

Meanwhile, and as a result of new collaboration with Portuguese and foreign groups, and also following an earlier suggestion by one of our American partners, research work was started on olive oil, another natural product abundant in the Mediterranean area and important for the Portuguese economy. Applications of supercritical fluids in the processing of food oils have been described in the literature and were summarized in

---

[1] J.L. Bravo, J.R. Fair, J.L. Humphrey, C.L. Martin, A.F. Seibert, S. Joshi, *Fluid Mixture Separation Technologies for Cost Reduction and Process Improvement*, 1986, Noyes Publications.

[2] V.J.Krukonis, "Supercritical Fluid Processing: Current Research and Operations", *Proc. Int. Symp. on Supercritical Fluids*, 1988, p.541, Nice, France.

the book by Stahl and collaborators[3]. However, until recently, no work on olive oil had been reported. We performed laboratory measurements that indicate the feasibility of deacidifying olive oils with supercritical carbon dioxide, without affecting the organoleptic qualities of those oils.

As to the fermentation broth processing, we were informed shortly after the beginning of this work, that a research project in the same lines that we were contemplating was near completion[4]. We decided therefore to change our main subject in this area to the investigation of lactic acid separation, as one of us was studying the biotechnological production of this substance, and also due to the economic importance of the subject in less-developed countries (LDC's). Phase behaviour studies were performed on mixtures of carbon dioxide, racemic lactic acid and water, and a new vapor-liquid equilibrium apparatus was assembled for a more complete description of this system.

Later in the program, a new development was the study of reverse micelles in supercritical media, to investigate the possibility of extracting biological molecules from aqueous solution. This line of work has been recently pursued by a number of authors[5]. A new high pressure apparatus with a view cell has been assembled for the study of micelle formation in supercritical carbon dioxide and ethylene. Solubilization of the surfactant AOT (sodium di-2-ethylhexyl sulfosuccinate) in supercritical carbon dioxide and ethylene and in supercritical and liquid propane is currently being examined.

---

[3] E.Stahl, K.-W. Quirin, D. Gerard, *Dense Gases for Extraction and Refining*, 1987, Springer-Verlag, Berlin.

[4] R.C. Willson, "Fermentation Product Recovery by Supercritical Fluid Extraction: Microbiological and Phase Equilibrium Aspects", *PhD. Thesis*, 1988, M.I.T.

[5] R.D. Smith, J.L.Fulton, J.P. Blitz, J.M. Tingley, *J. Phys. Chem., 1989, 93: 4193*; T.Klein, J.M. Prausnitz, *ibid., 1990, 94: 8811*; K.P. Jonhston, G.J. McFann, R.M. Lemert, *in Supercritical Fluid Science and Technology*, 1989, ACS Symposium Series 406.

2.2. Experimental

In the course of this project, a series of different measurements were performed. These were designed to examine the feasibility of useful separation processes involving supercritical fluids. Most of them can be classified as vapor-liquid equilibrium or solubility measurements, but a few and more recent ones involve either chemical reaction kinetics or mass transfer measurements. Several apparatuses (whose pictures are presented in the Annex) have been built and constantly improved. We started with the one described in our research proposal[6] and we end up with six different experimental set-ups, each of them being used for different purposes. One of them is a technical or semi-pilot scale apparatus, described below under the sub-title "Countercurrent Liquid-SCF Extraction Columns". The others are of the laboratory-scale type, and will be divided for description purposes according to whether the core of the apparatus, the equilibrium cell, is an opaque or a transparent, see-through cell.

2.2.1. Solubility Apparatus with Opaque Cells

The versions of this type of apparatus used in this work were essentially an upgrading of the apparatus for measuring solubilities in supercritical fluids described in our proposal. Successive modifications were introduced to this primitive version. Some of them were described in detail by Gomes de Azevedo et al. and by Matos et al. (see Publications 1 and 3). A schematic diagram of this apparatus is shown in Figure 1.

The main modifications introduced in the original apparatus were:

(i) A new pressure generating system (a piston pump).

---

[6] M.Nunes da Ponte, E. Gomes de Azevedo, M.T. Carrondo, *Supercritical Fluid Extraction of Natural and Biological Products*, Research Proposal submitted to AID, August 1986.

(ii) A different top cover for the equilibrium cell, with two outlets.

(iii) A modified sampling system, whereby the solute is deposited directly into a glass trap.

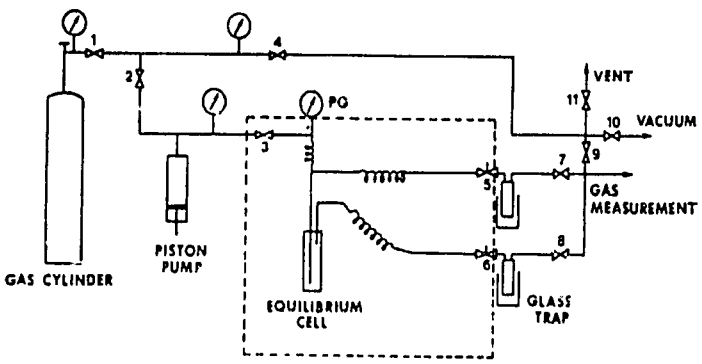

Figure 1: Schematic diagram of the VLE apparatus.

The main shortcomings of this design are related to the small volume of the cell and to the sampling system. A small volume of 30 cm^3, as we used, allows for perturbation of the equilibrium pressure condition inside the cell while sampling. On the other hand, the sampling system of directly depositing the solute in a cold glass trap is simple and quick, but not very precise. This is due specially to the liquid condensation in the walls of the tubing between the sampling valve and the trap. To overcome these limitations, a second apparatus was later assembled, following essentially the diagram of Figure 1, but with a 100 cm^3 cell and a different sampling system. This is closer to our original one, where a liquid solvent washes the deposition loop of a liquid chromatography valve. Instead of analysing the resulting liquid samples by refractometry, as was our original intention, we adopted for gas chromatography. This is a more versatile analytical method, that we also used for analysis of ternary mixtures involving eucalyptus oil components or multi-

component analysis of other natural products, as described later in this report. A picture of this apparatus is shown in the Annex.

2.2.2. Solubility Apparatus with Visual Cells

As described below, our work with ethylene as a supercritical solvent revealed a more complex phase behaviour than we had previously encountered with carbon dioxide or carbon dioxide-based mixtures. It quickly became apparent that it would be very useful to be able to see the different phases present in the equilibrium cell and to identify those we were sampling from. We therefore built transparent cells, following essentially two types of design. In the first one, glass or sapphire windows were attached to the ends of a stainless steel hollow cylinder by means of an unsupported area seal with teflon O-rings. A diagram of this type of cell is given in Figure 2.

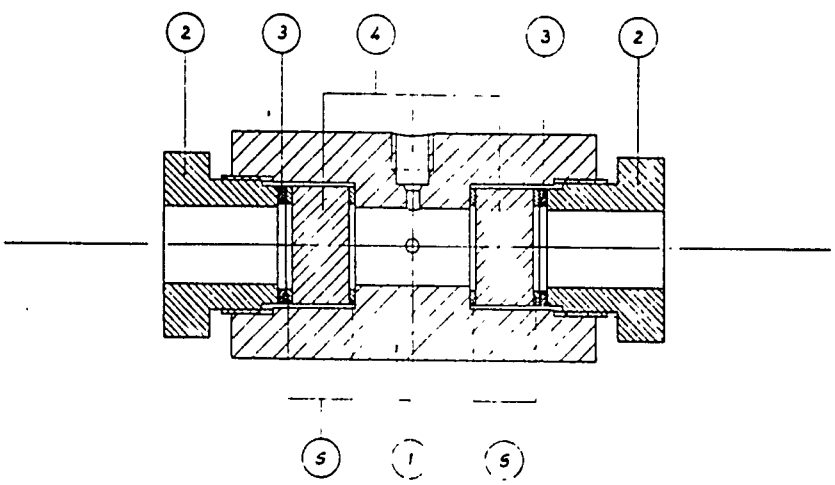

Figure 2. Visual cell with sapphire windows. 3: O-ring; 4: sapphire windows.

A second type of visual cell was also built using a sapphire tube as the main piece. The diagram of Figure 3 shows the closures on both ends, that consist of mushroom-shaped tubing supported by teflon O-rings. The principle of unsupported area is used in the same way as in the other type of cell to ensure a sufficient compression of the O-ring at high pressure.

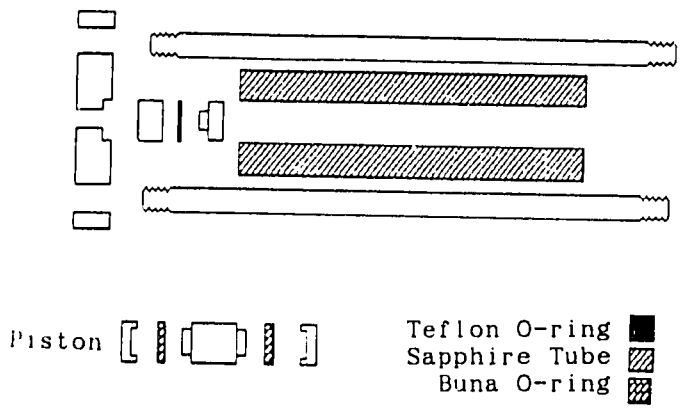

Figure 3. Sapphire tube cell.

Critical points and two and three-phase equilibria were easily observed with these cells. However an important shortcoming remained: isothermal pressure changes must be obtained by gas addition to the cell, because the available volume is constant. A further development of the design was the replacement of one of the closures (Figure 3) by a stainless steel piston, sealed by two O-rings, that can be moved by pressurization on the outer side with a suitable liquid (water, for instance). A picture of this sapphire cell can be seen in the Annex.

2.2.3. Countercurrent Liquid-SCF Extraction Columns

Finally, a semi-pilot scale apparatus was built. This apparatus was design to simulate extraction processes under

favourable pressure and temperature conditions, as indicated by previous laboratory experiments and by thermodynamic modelling. The main properties to be measured in this set-up are some of those necessary for scale-up and design of supercritical extraction processes, and in particular mass transfer coefficients as a function of several operational variables, like pressure, temperature, concentration, and flow. The design followed some suggestions given by Gerard[7] and also by Brunner and Peter[8].

A schematic view of this apparatus is presented in Figure 4 and its picture is shown in the Annex.

The main pieces of equipment are two one-meter long, 2.5 cm internal diameter stainless steel columns. In Figure 4, EC is the extraction column and SC the separation column. Sampling devices are provided at the top and bottom of each and a high precision Rheonik mass-flowmeter (MFM in the same figure) was placed between them. The circulating supercritical solvent is driven by a high-pressure gas compressor (C), while a high pressure liquid metering pump (MP_L) injects the liquid feed into the extraction column. The liquid flow is measured bv direct weighing of the liquid reservoir at regular time intervals, in a precision balance of 1000 g capacity.

Auxiliary equipment includes two back-pressure regulators, several temperature and pressure indicators, and a piston pump, to compensate for the solvent withdrawn during sampling. The columns are of the packed type, filled with Sulzer corrugated gauze. This is a very efficient packing, as demonstrated by Seibert et al.[9]

During operation, pressure in the extraction columns controlled with a back-pressure regulator (BPR_{EC}) and measured by two gauges (PG_1, PG_2). The pressurized solvent is preheated or

---

[7] D.Gerard, *PhD. Thesis*, 1985, University of Saarbrukrn, Germany.

[8] G. Brunner, S. Peter, *Ger. Chem. Eng., 1982, 5: 1981.*

[9] A.F. Seibert, D.G. Moosberg, J.L. Bravo, K.P. Jonhston, *Proc. Int. Symp. on Supercritical Fluids*, 1988, Nice, France.

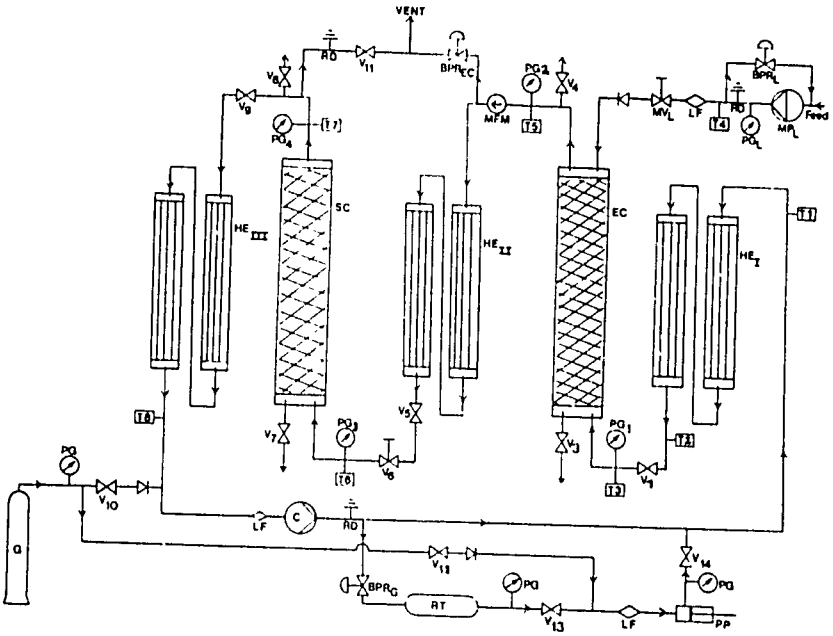

Figure 4: Flow diagram of the continuous countercurrent extraction apparatus. BPR: back pressure regulator; C: compressor; EC: extraction column; G: gas cylinder; HE: heat exchanger; LF: line filter; MFM: mass flowmeter; MP: metering pump; PG: pressure gauge; PP: piston pump; RD: rupture disk; SC: separation column; T : temperature sensor;

cooled to the desired temperature in a heat exchanger (HE_I), by circulating thermostated water.

A run starts with the solvent circulating through the apparatus for about two hours, without liquid feed injection, to obtain the desired pressures and temperatures in the extraction and the separation columns. The pressure drop between the two is regulated manually with a heated regulating valve (V6). Two pressure gauges (PG_3 and PG_4) read pressure at the top and bottom of the separation column and two heat exchangers (HE_{II} and HE_{III}) control its temperature.

When the desired pressures and temperatures are obtained, the injection at the top of the extraction column of the liquid mixture to separate starts. The extract, precipitated in the

separation column, and the raffinate, that is, the liquid not solubilized by the gaseous solvent, are collected at the bottoms of the separation and the extraction columns, respectively. The solvent loading (the solute concentration of the solvent flow exiting EC) is measured by sampling through valve V4.

2.3. Results

We report next the principal experimental results we obtained using the apparatuses described above. These results involve solubility and VLE data of natural products (the main components of eucalyptus oil and olive oil) and of products from fermentation broths (lactic acid) in different supercritical solvents.

2.3.1. Measurement of Solubilities in SCF

2.3.1.1. Eucalyptus Oil

To investigate the possibility of using SCF to the separation of 1,8-cineole (the most valuable component of eucalyptus oil) from d-limonene we obtained VLE data on mixtures involving these compounds and different SCF solvents, namely carbon dioxide, an azeotropic mixture carbon dioxide+ethane, and ethene.

2.3.1.i.1. VLE in Carbon Dioxide

Our work started with a full characterization of the vapor-liquid equilibrium in binary mixtures of carbon dioxide (above its critical temperature) and each of the two main components of eucalyptus oil, 1,8-cineole and d-limonene. A thorough description of these results is given in Publications 1

and 3 .

Some representative results are shown in Figure 5.

In addition to the new solubility data which became available, our data unveiled that previously published results on the solubility of terpenes in supercritical carbon dioxide were wrong, as shown in Figure 6. This figure compares our solubility data at 313 K of limonene in supercritical carbon dioxide with results obtained by different authors. As shown, our data for the

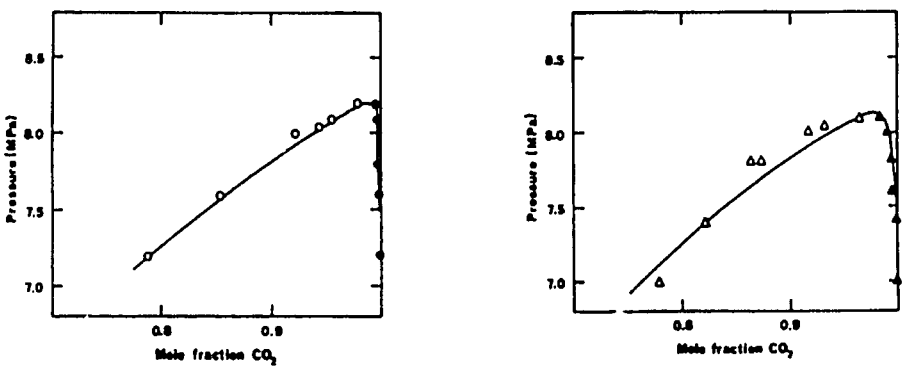

Figure 5. Experimental and calculated (from Peng-Robinson EOS) VLE for CO_2+limonene (left) and CO_2+cineole (right) at 313 K.

liquid and vapor phases are in good agreement with the equilibrium data of Coppella and Barton[10]. Agreement is also found between the data of Stahl and Gerard[11] and our results for the vapor phase. However, these authors' results show significant

---

[10] S.J. Coppella, P. Barton, in *Supercritical Fluids*, 1987, ACS Symposium Series 329.

[11] E. Stahl, D. Gerard, *Perfumer & Flavorist*, 1985, 10: 29.

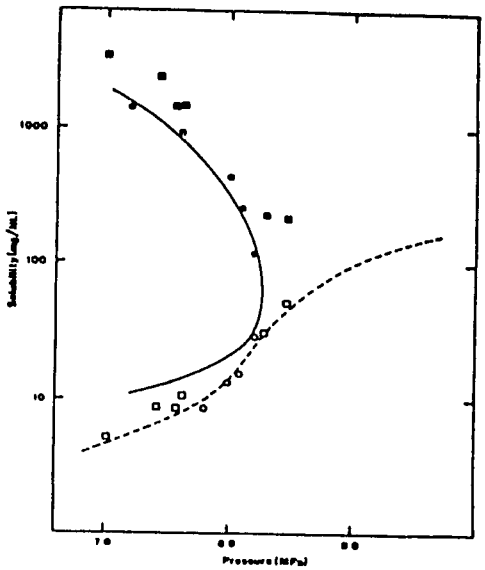

Figure 6. Comparison of our solubility data for limonene in dense CO_2 at 313 K with results from other authors.

Experimental: Our data (• liquid; o vapor);
Coppella, Barton (■ liquid; □ vapor);
Sthal, Gerard (-----).

Calculated: Peng-Robinson EOS with k_{12}=0.080 (———).

discrepancies at pressures above 8.3 MPa (the mixture critical pressure at 313 K). We attributed these differences to th experimental technique the authors have used (the dynamic flow principle) which could not detect the mixture critical point. Therefore their data above 8.3 MPa are meaningless.

2.3.1.1.2. VLE of the Ternary Carbon Dioxide+ Cineole+Limonene

The same apparatus was used to obtain VLE data on the ternary carbon dioxide + cineole + limonene. The measurements were made at 40 °C (or 313.15 K) for different pressures and for a mixture of overall mass ratio of about 0.80

cineole to 0.20 limonene, a composition chosen to simulate eucalyptus oil as obtained commercially in the first step of purification. The results are given in Table 1.

At this stage, these results clearly indicated that super critical CO_2 could not selectively extract either limonene or cineole from a mixture of the two of them. The reason for this behavior is quite obviously seen in Figure 7 which compares the

Table 1 - Liquid (x) and vapor (y) equilibrium compositions at 40°C for a ternary mixture of carbon dioxide + cineole + limonene, at different pressures.

P(MPa)	$x(CO_2)$	x(lim.)	x(cin.)	$y(CO_2)$	y(lim.)	y(cin.)
7.4	0.888	0.025	0.087	0.996	0.001	0.003
7.6	0.859	0.030	0.111	0.993	0.002	0.005
7.75	0.867	0.031	0.102	0.986	0.004	0.010
8.0	0.914	0.023	0.063	0.996	0.000	0.004
8.2	0.950	0.012	0.038	0.990	0.003	0.007

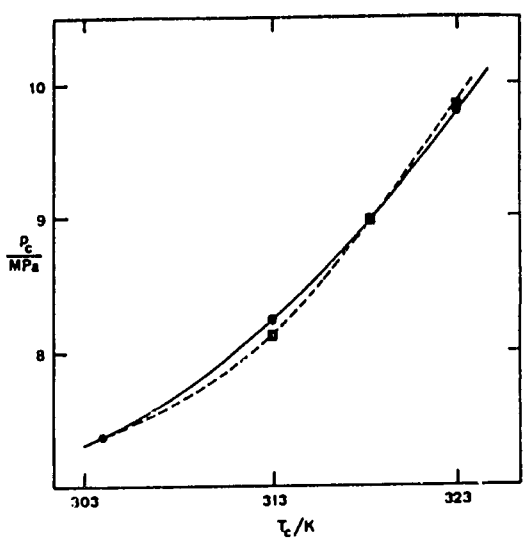

Figure 7. Critical pressures and temperatures of mixtures of CO_2 with limonene (•) and with cineole (■). The symbol * indicates the critical point of pure CO_2.

critical pressures and temperatures of mixtures of CO_2 with limonene and with cineole. There is almost no distinction between the two mixtures.

2.3.1.1.3. VLE in Carbon Dioxide + Ethane Mixtures

Our search for solvents with a better selectivity towards mixtures of cineole and limonene led us to mixtures of azeotropic composition of ethane with carbon dioxide. As explained in Publication 3, the main reason for the choice was that we were looking for a solvent which could enrich the vapor phase in limonene, the impurity to be removed.

The results are presented in Publication 3 and they are similar to those previously obtained with pure carbon dioxide. This is illustrated in Figure 8, which compares the VLE data we obtained at 303.2 K for the (supercritical) azeotropic mixture $CO_2+C_2H_6$ with limonene and with cineole. Again, the phase diagrams for the two (pseudo) binaries are very similar.

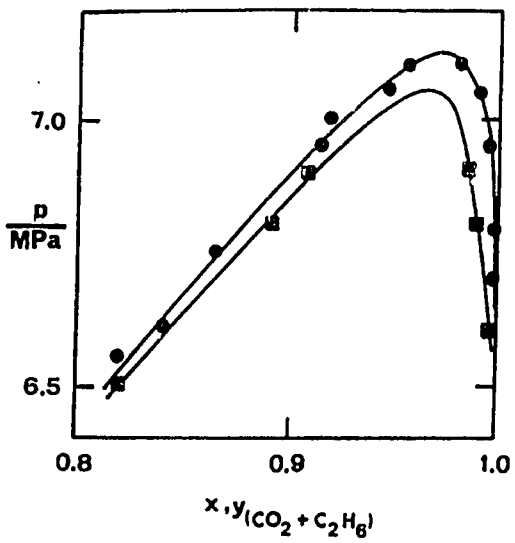

Figure 8. VLE data of the azeotropic mixture $CO_2+C_2H_6$ with limonene (•) and with cineole (■) at 303.2 K.

2.3.1.1.4. VLE in Supercritical Ethene

The failure of carbon dioxide or carbon dioxide-rich mixtures to selectively extract the main impurity in the preparation of cineole from eucalyptus oil led us to select ethene (ethylene), due to its possible affinity to limonene, a hydrocarbon with a carbon - carbon double bond.

The observed phase behavior for binary mixtures of ethene and limonene was quite different from our previous results. Three phases in equilibrium, a vapor phase, a limonene-rich liquid phase, and an ethylene-rich liquid phase were observed. This phase behavior, and in particular the existence of an intermediate, limonene-rich liquid phase, strongly indicated the possibility of an enhanced solubility of this compound in a limited range of temperatures and pressures. The thorough investigation of the coexistence limits of those phases was therefore the next step in our work on eucalyptus oil.

As sensitive methods were required to detect the phenomena under study, important changes had to be introduced in our experimental program. We built transparent cells of various kinds, as described in Section 2.2.2 above, for visual detection of three-phase coexistence and critical points, and some precise solubility measurements in a different apparatus were carried out at the Technical University of Berlin, Germany, by one of our collaborators. These results are briefly described in the next Section.

As mentioned above the phase diagrams for ethene + limonene are of a different kind from previous results in this work. A second liquid phase was formed, resulting in a three-phase equilibrium surface, that spanned from below 15 °C to above at least 25 °C, as shown in Figure 9. These results were obtained by combining vapor-liquid composition measurements, done as in previous cases, with transparent cell determination of mixture critical points and three-phase equilibria (see photographs in the Annex).

The second liquid phase was richer in limonene than the

vapor at lower pressures, especially at the lower temperatures, around 15 °C, and suggested the possibility of finding a pressure and temperature region where limonene would be definitely more soluble than cineole.

Three-phase equilibrium has also shown up in ethene + cineole, but on a much shorter temperature range, around 25 °C, and was much harder to detect. Our results with transparent cells

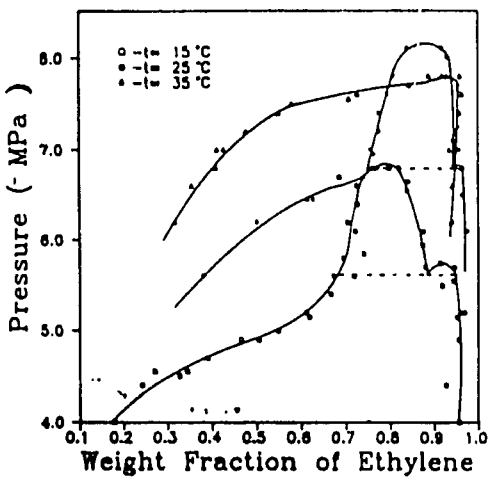

Figure 9. Pressure-composition diagram for the system ethene + limonene at 15, 25, and 35 °C.

around 25 °C indicate the presence of three phases. A liquid-liquid critical point was observed at 6.64 MPa and 25.2 °C, while the liquid-vapor separation remained. The phase coexistence in this system is therefore clearly different from what was previously observed with ethene+limonene.

2.3.1.1.5. Solubility Measurements in Compressed Gaseous Ethene.

These solubility measurements were carried out at the Technical University of Berlin, Germany, during a training one month visit of one of us (H. Matos). They were

performed in a high pressure apparatus (up to 20 MPa or 200 bar), using the dynamic continuous accumulative method. In this method the gaseous sample passes continuously through a series of saturation cells. The gas dissolves a certain amount of the solute contained in the first cell, and the solute is absorbed in the remainer cells filled with a suitable solvent (N-methyl pyrrolidinone). The total amount of the gas is measured by a gasmeter, and the concentration in each of the vessels determined by gas chromatography.

Figure 10 presents the measured solubilities at 25 °C of limonene and of cineole in ethene as a function of pressure. As shown the solubility of limonene is markedly higher than that of cineole.

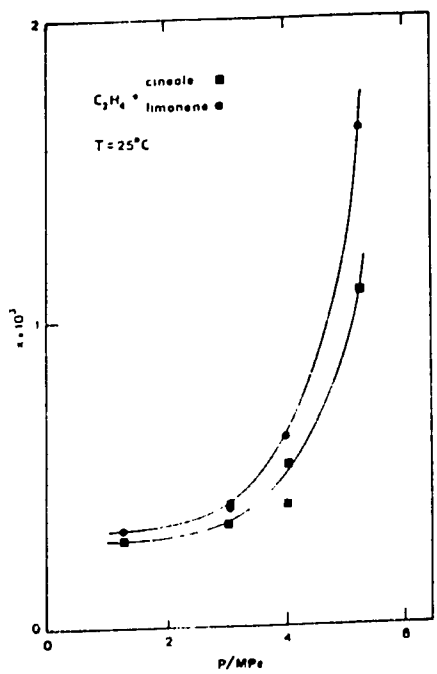

Figure 10. Solubility of limonene (•) and of cineole (■) at 25°C in gaseous ethene at several pressures.

2.3.1.1.6. VLE of the Ternary Ethene+ Cineole+Limonene

We proceeded to investigate the phase equilibria in ternary mixtures of ethene with limonene and cineole, using (as in the case of the study with carbon dioxide) a 20% limonene + 80% cineole liquid mixture as starting point. Phase compositions were measured with a gas chromatograph, as described in Section 2.2.1. Results indicated that in the gas phase there are limonene/cineole ratios between 1 and 1.5, while in the starting mixture this ratio was 0.25. Considerable enrichment of the more volatile phase in limonene was therefore obtained.

2.3.1.2. Extraction of Lactic Acid

Preliminary VLE data on mixtures containing SC CO_2 and an aqueous solution with 60% racemic lactic acid were obtained in an apparatus of the type described in Section 2.2.1. These results, summarized in Figure 11, indicated that a vapor-liquid critical point was reached at 38 °C and 175 bar.

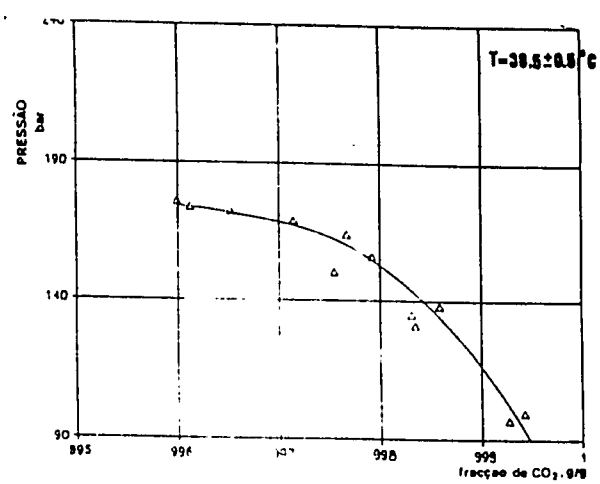

Figure 11. Vapor phase solubility of lactic acid in supercritical CO_2 at 38.5 °C.

These preliminary findings were encouraging as to the possibility of separating lactic acid, and a more thorough investigation was started. However, due to the specific characteristics of this system a new apparatus was designed and built (see picture in the Annex). In fact, and apart from the corrosive action of lactic acid, one had to take into account that while mixtures of the two optical isomers have melting points that can come down to 20 °C, the pure isomers only melt around 51 °C. This required a temperature control at higher temperatures than we had used before. An oven was specially built for this purpose, and it has recently come into operation.

2.3.1.3. Solubilities of Olive Oil Components in Supercritical Carbon Dioxide

The assessment of the possibility of deacidification of olive oils by supercritical extraction requires the knowledge of the solubilities of its main components. We have therefore performed experiments on pure glycerol trioleate, the main edible component of olive and husk oils, and on a highly acidic husk oil. The results are given in Publication 9. Figure 12 compares our data (at 35°C) for the solubility of glycerol trioleate (usually known as triolein which is the main component of olive oil) in CO_2 with measurements reported by different authors. As shown, the data of Brunetti et al.[12] are in notorious disagreement with our and other authors results[13].

We have also measured husk oil solubilities in supercritical CO_2 from previously hexane extracted crude husk oil (hexane is

---

[12] L. Brunetti, A. Daghetta, E. Fedeli, I. Kikic, L. Zanderighi, *J. Am. Oil Chem. Soc., 1989, 66: 209.*

[13] J. Chrastil, *J. Phys. Chem., 1982, 86: 3016*; M.B. King, T.R. Bott, M.J. Barr, R.S. Mahmud, *Separation Science & Technology, 1987, 22: 1103.*

the solvent commonly used in the conventional extraction process). For comparison the same extraction was performed from solid olive husk flakes. We noticed that in the latter case the solubilities values were lower than those obtained with liquid husk oil. We attributed this (significative, specially at high pressures) difference to the fact that some of the components extracted with hexane were less (or even non) extracted by SCF carbon dioxide from the solid matrix.

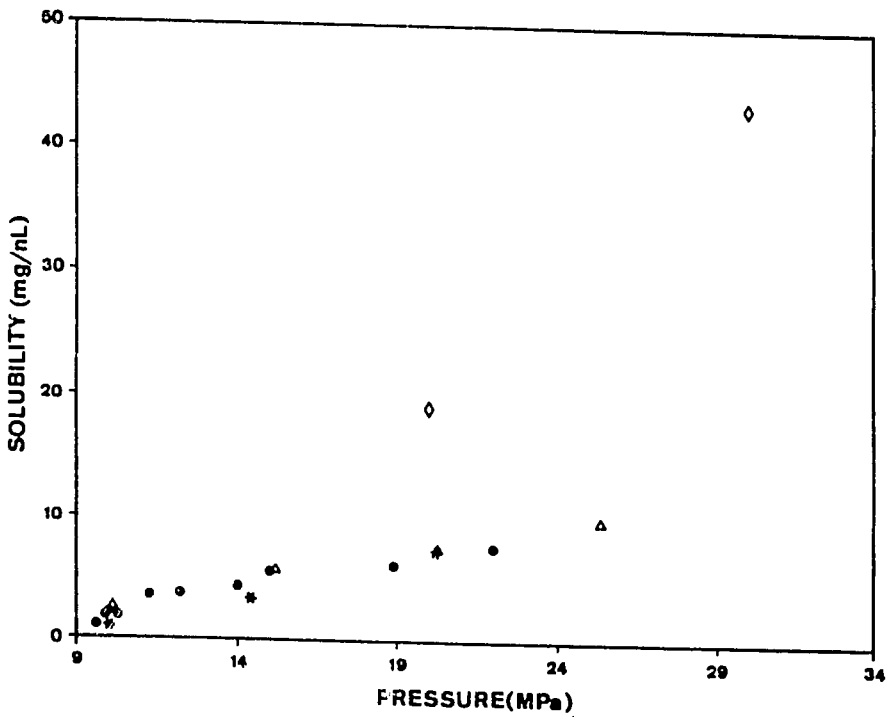

Figure 12. Solubility of glycerol trioleate in CO_2 at 308.6 K. Comparison of our measurements (•) with those reported in the literature: King et al. (*); Chrastil (Δ) and Brunetti et al. (◊) at 313.15 K.

Using capillary gas chromatography we analyzed the hexane extracted husk oil (crude husk oil) and the corresponding SCF CO_2 extracts. In both cases high contents of free fatty acids were found, being oleic acid the major constituent (about 60% in weight) followed by palmitic and linoleic acids.

We have also found that free fatty acids were more easily extracted than triglycerides from olive oil. This is shown in Figure 13 which gives the solubilities in SCF CO_2 at 313.6 K of crude husk oil, the free fattv acid, and the triglyceride fractions from the same oil.

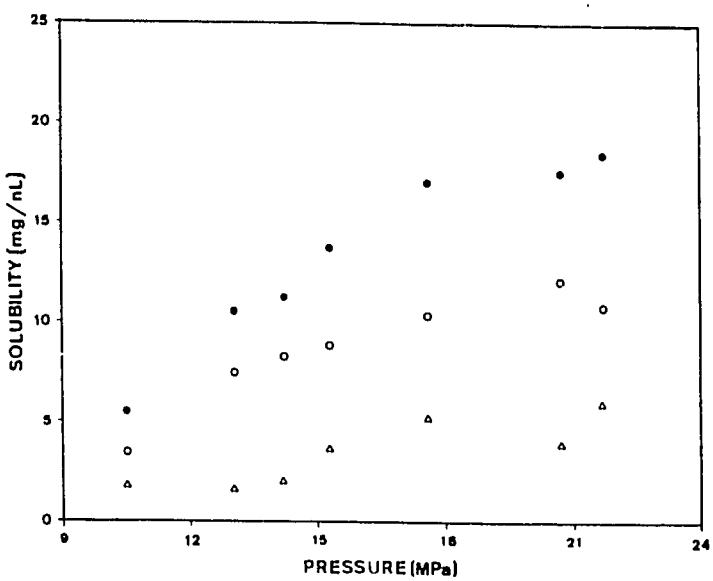

Figure 13. Solubility at 313.16 K in supercritical CO_2 of crude husk oil (•), the free fatty acid (o) and the triglyceride (Δ) fractions from the same oil.

The enrichment in free fatty acids is clearly observed through the comparison of the chromatograms of crude and SCF CO_2-extracted oils. This gives us the indication that the application of SCF CO_2 extraction to deacidify vegetable oils, namely husk and olive oils, is technically feasible in in relatively mild operational conditions. In addition, contrarily to what is observed in the conventional refining processes use to deacidify either olive and husk oils which may introduce significant changes in the triglyceride composition (causing a

decrease in the nutritional qualities of the oil), the SCF CO_2-extracted husk, the crude, and the two (commercially available) olive oils have a similar triglyceride composition, as Figure 14 shows. As no detectable differences were found between the crude oil and the extracts, we assumed that contact with high pressure CO_2, oppositely to classic refining processes, did not affect the organoleptic qualities of husk oil.

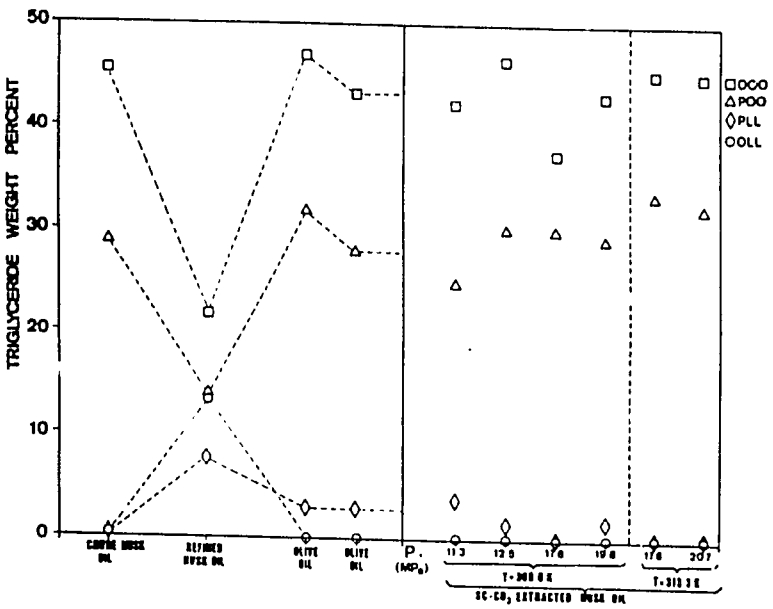

Figure 14. Triglyceride composition of supercritical CO_2 extracts obtained at different pressure and temperature conditions. Comparison with olive and husk oils.

Therefore our results indicated that SCF CO_2 extraction could achieve a deacidication of olive and husk oils, retaining their required triglyceride composition and consequently preserving their nutritional characteristics. The application of our findings to the industrial processes is now dependent from a complete economic feasibility study.

2.3.2. Thermodynamic Modeling of the Phase Behavior

As explained above, SCF are powerful solvents whose special thermodynamic and transport properties give them great potential for extraction processes in many areas where they can solve important, practical separation problems. However for process design, scale-up, and economic feasibility studies we need versatile molecular thermodynamic models to describe the phase equilibrium and to understand the molecular processes in SCF solutions. These models, which desirably are reliable, versatile, and theoretically-based predictive, assist the design engineer to model and predict the phase equilibria of complex systems as those usually found in SCF extraction processes.

Unfortunately there are two specific aspects of the SCF systems that makes them difficult to model. The first arises from the proximity of the critical point. The second is related with the large asymmetries (in size, shape, and polarity) of the molecules involved in typical SCF extraction processes.

In spite of its drawbacks (e.g. lack of precision in the critical region), equations of state have particular characteristics which make them very popular among thermodynamicists. For this reason we used first an equation of state to model our multicomponent supercritical systems.

To overcome the well-known limitations of the EOS, we developed a method, based on the one-fluid conformal solution theory, to correlate solubilities in SCF.

The findings using these two procedures are briefly described below.

2.3.2.1. EOS Model

For the quantitative description of the systems studied here, we selected the widely used Peng-Robinson EOS,

$$P = \frac{RT}{v - b} - \frac{a}{v(v - b) + b(v - b)} \quad (1)$$

where a and b are parameters related to the critical properties and acentric factors of the pure components (which are listed in Table 2). For mixtures, these parameters were defined by the conventional composition-dependent mixing rules,

$$a_m = \sum_i \sum_j x_i x_j a_{ij} \quad (2)$$

$$b_m = \sum_i x_i b_i \quad (3)$$

where x_i is the mole fraction of component i and a_{ij} is defined by

$$a_{ij} = (1 - k_{ij}) \sqrt{a_{ii} a_{jj}} \quad (4)$$

Table 2. Pure component data used in VLE calculations with the Peng-Robinson EOS.

Component	T_c(K)	P_c(MPa)	Acentric Factor
CO_2	304.2	7.38	0.225
Cineole	665†	2.77†	0.312
Limonene	654‡	2.75‡	0.327

† Estimated from the group contribution method of Lydersen.
‡ Estimated from the group contribution method of Nokay.

The binary interaction parameter k_{ij} is related to the mole-

cular interactions between components i and j, and is a characteristic parameter for each pair of the mixture constituents. This parameter was obtained from regression of the obtained binary phase equilibrium data at each temperature.

In spite of a slight temperature dependence of k_{12} has been always detected, the Peng-Robinson EOS could reproduce reasonably well the observed phase behavior as Figure 5 shows for the binaries CO_2+limonene and CO_2+cineole both at 313 K.

Moreover it was found that the same simple model could reproduce semi-quantitatively the ternary data of the system CO_2+limonene+cineole also at 313 K, using the interaction parameters obtained from the binary data only. As an example, Table 3 shows a comparison between calculated with experimental ternary data for the same system.

However, the agreement was less satisfactory for the systems with supercritical ethylene which exhibit a three phase equilibria, as shown above. Not with much success, the same equation of state was also used in the description of the phase behavior, namely in the prediction of the pressure-temperature projection

Table 3. Experimental and calculated (Peng-Robinson EOS with k_{12}=0.080, k_{13}=0.075, and k_{23}=0) liquid compositions for the ternary CO_2+limonene+cineole system at 313 K.

	x(CO_2)		x(limonene)		x(cineole)	
P (MPa)	exp.	calc.	exp.	calc.	exp.	calc.
7.4	0.888	0.819	0.025	0.081	0.087	0.100
7.6	0.859	0.856	0.030	0.024	0.111	0.120
7.75	0.867	0.888	0.031	0.012	0.102	0.100
8.0	0.914	0.942	0.023	0.008	0.063	0.050
8.2	0.950	0.972	0.012	0.008	0.038	0.020

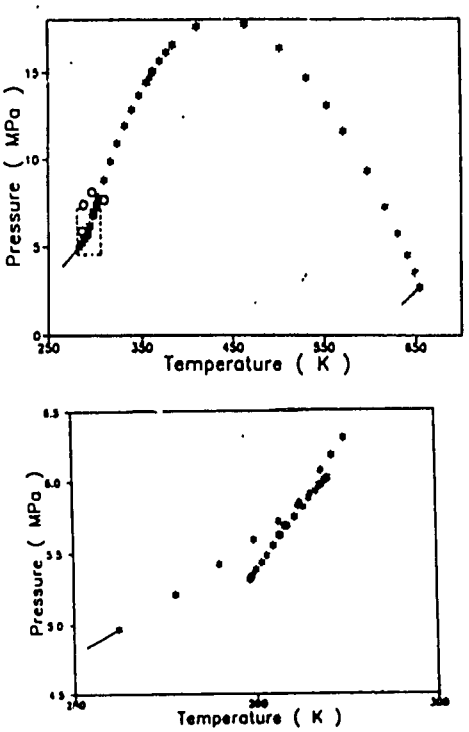

Figure 15. Experimental (o) and calculated (Peng-Robinson EOS with k_{12}=0.050) pressure-temperature projection for the limonene+ethylene system. The area marked above is shown enlarged below.

of the binary ethylene+limonene, as Figure 15 shows for this system (with k_{12}=0.050 obtained from regression of binary VLE data).

2.3.2.2. Statistical Thermodynamics-Based Model

Since there are well-known reasons that indicate that classical equations of state are only partially satisfactory in the thermodynamic modeling of mixtures involving supercritical fluids, we directed our efforts to more sophisticated treatments.

Based on the work performed by Dr. Daniel Jonah during his visits to CQE, we were able to develop a procedure to correlate and predict solid solubilities in supercritical solvents at different pressures and temperatures.

In this new method, based on the one-fluid conformal solution theory (see Publication No. 5) we shifted the emphasis from the properties of the gaseous *mixture* to those of the *pure* gaseous solvent, since this single-component properties are readily available.

The feasibility of this approach is a consequence of the fact that, in most systems, the solid is sparingly soluble in the gas phase and therefore the gas mixture is a dilute mixture in which solvent-solvent interactions play a dominant role. This assumption (which is very crude in the case of the solubility of liquids) greatly simplifies the proposed model. This was the reason why we first looked at the solubility of solids in SCF.

2.3.2.2.1. Molecular Thermodynamics of SCF

We started by considering a solid component *a* in equilibrium with a supercritical gaseous component *b*. The phase equilibrium equations are:

$$f_a^{solid} = f_a^{vap}, \tag{5}$$

$$f_b^{solid} = f_b^{vap}, \tag{6}$$

where f_a and f_b are the fugacities of components *a* and *b*, and the superscripts *solid* and *vap* refer to the solid and vapor phases, respectively.

Making the above mentioned (and usual) assumption of negligible solubility of the gas in the solid, the mole fraction y_a of the solid dissolved in the gas follows from Eq.(5):

$$f_a^{*solid} = y_a \, \phi_a^{vap} \, P, \tag{7}$$

ϕ_a and P denoting the fugacity coefficient of component *a* and the system pressure, respectively; in Eq.(7) the asterisk indicates a pure (solid) phase. Once the vapor phase is suitably modeled by an appropriate equation of state, the fugacity coefficient could then be readily calculated as a function of the (vapor) mole fraction y_a, the system temperature *T*, and pressure *P*. Calculation of the solid solubility in the supercritical gas could then be obtained through an iterative solution of Eq.(7).

The successful prediction and correlation of solid solubilities by this procedure depends to a large extent on the proper choice of mixing rules used in adapting the single component equation of state to a mixture situation.

However, an alternative route to solid solubility calculation is provided by the fact that the gaseous mixture is *dilute*, which means that solute-solute interactions can be neglected. This assumption of diluteness is supported by the existing experimental data. With such an assumption, we have invoked a *Henry'-law-like* relation for solubilities in a gas phase, for which the fugacity of the solute in the gas phase is taken as proportional to the solute concentration. Explicitly, we have

$$f_a^{vap} = K_{ab} \times \text{(solute mole fraction)}, \tag{8}$$

where K_{ab} denotes a generalized Henry's constant for solubility in any phase, resulting in a dilute mixture.

To take full advantage of the ready availability of single component properties, we have re-written Eq.(8) in a more convenient form:

$$f_a^{vap} = y_a \, f_b^* \exp\left(\frac{\mu_{ar}^{\infty} - \mu_{br}^*}{kT}\right), \tag{9}$$

where μ_{ar}^{∞} is the residual chemical potential of the solute *a* in an infinitely dilute mixture, and μ_{br}^* is the residual chemical

potential of the pure solvent b; f_b^* is the pure solvent fugacity and k is the Boltzmann constant.

In writing Eq.(9) we have simply used the identities,

$$ln \left(\frac{K_{ab}}{\rho kT}\right) = \frac{\mu_{ar}^{\infty}}{kT}, \tag{10}$$

$$ln \left(\frac{f_b^*}{\rho kT}\right) = \frac{\mu_{br}^*}{kT}, \tag{11}$$

where ρ is the number density of the pure solvent component b.

Making use of Eq.(5), we wrote for the solubility y_a,

$$y_a = \frac{f_a^{*solid}}{f_b^{*vap}} \exp \left(\frac{\mu_{br}^* - \mu_{ar}^{\infty}}{kT}\right). \tag{12}$$

We note that the right hand side of Eq.(12) is not mole-fraction dependent. Therefore, the problem of calculating the solubility y_a was reduced to that of obtaining a suitable expression for the difference between the residual chemical potentials ($\mu_{ar}^{\infty} - \mu_{br}^*$). This was done by using the framework of Statistical Mechanics.

2.3.2.2.2. Statistical Thermodynamics Considerations

A natural development for μ_{ar}^{∞} was a perturbation expansion, in which the reference system was taken as the pure solvent; then μ_{br}^* was the zeroth order term. Up to the second term we had:

$$\mu_{ar}^{\infty} = \mu_{br}^* + \langle \Delta U \rangle_{ps} - \frac{\beta}{2} \langle (\Delta U - \langle \Delta U \rangle)^2 \rangle_{ps} + O(\beta^2), \tag{13}$$

where

$$\Delta U = \sum_{j>1} [\, u_{ab}(1,j) - u_{bb}(1,j) \,]. \tag{14}$$

Here, $u_{ab}(1,j)$ denotes the pair potential between a solute molecule *a* at the position r_1, and a solvent molecule *b* at r_j in the infinitely dilute mixture; $u_{bb}(1,j)$ has an analogous meaning but for two solvent molecules. As usual, $\langle\ \rangle_{ps}$ denotes the canonical average over the *pure solvent* component.

The first order contribution $\langle \Delta U \rangle_{ps}$ in Eq.(13) was thermodynamically accessible and could readily be expressed in terms of the residual internal energy and compressibility factor of the pure solvent, for pair potentials of the Lennard-Jones type. However, the second order term was not thermodynamically accessible and needed to be approximated if it was to be expressed in terms of thermodynamic properties of the pure solvent.

An alternative and probably more convenient route to obtain μ_{ar}^{∞} was through a one-fluid mixture theory.

According to this theory the residual Helmholtz energy $A_r^{mix}(T,\rho,x_a)$ for the binary mixture at temperature T, density ρ, and of composition x_a, may be expressed in terms of the corresponding function A_{br}^{*} for a pseudo-pure component at reduced temperature T_R and reduced density ρ_R, as follows:

$$\frac{A_r^{mix}(T,\rho,x_a)}{T} = \frac{A_{br}^{*}(T_R,\rho_R)}{T_R}, \tag{15}$$

where

$$T_R = T\,\frac{\varepsilon_{bb}}{\varepsilon_m}, \tag{16}$$

and

$$\rho_R = \rho\,\frac{\sigma_m^3}{\sigma_{bb}^3}. \tag{17}$$

In the above equations, ε_m and σ_m are the molecular parameters for the pseudo-pure component.

Differentiation of Eq.(15) with respect to N_a (the number of solute molecules) at constant temperature, density, and N_b (the number of solvent molecules) lead to the desired expression for μ_{ar}:

$$\frac{\mu_{ar}(T,\rho,x_a)}{RT} = \frac{\mu^*_{br}(T_R,\rho_R)}{RT} + \left(\frac{N}{\varepsilon_m}\frac{\partial\,\varepsilon_m}{\partial\,N_a}\right)\frac{U^*_{br}(T_R,\rho_R)}{RT}$$

$$+ \left(\frac{N}{\sigma_m^3}\frac{\partial\,\sigma_m^3}{\partial\,N_a}\right) z^*_{br}(T_R,\rho_R). \qquad (18)$$

Writing Eq.(18) for an infinitely dilute solution gave at once μ^∞_{ar}:

$$\frac{\mu^\infty_{ar}(T,\rho)}{RT} = \frac{\mu^*_{br}(T_R,\rho_R)}{RT} + F_1\frac{U^*_{br}(T_R,\rho_R)}{RT} + F_2 z^*_{br}(T_R,\rho_R) \qquad (19)$$

where we have introduced the notations

$$F_1 = \lim_{x_a\to 0}\left(\frac{N}{\varepsilon_m}\frac{\partial\,\varepsilon_m}{\partial\,N_a}\right) \equiv \left(\frac{N}{\varepsilon_m}\frac{\partial\,\varepsilon_m}{\partial\,N_a}\right)^\infty, \qquad (20)$$

$$F_2 = \lim_{x_a\to 0}\left(\frac{N}{\sigma_m^3}\frac{\partial\,\sigma_m^3}{\partial\,N_a}\right) \equiv \left(\frac{N}{\sigma_m^3}\frac{\partial\,\sigma_m^3}{\partial\,N_a}\right)^\infty. \qquad (21)$$

Equations (18) and (19) are exact relations within the framework of the one-fluid conformal solution theory. Approximations are introduced only through the mixing rules relating ε_m and σ_m to the corresponding pure component parameters, and those pertaining to the solute-solvent interactions. Thus the successful performance of Eq.(19) very much depended on how well F_1 and F_2 were evaluated.

The most commonly used mixing rules are the so-called van der

Waals-1 (VDW-1) mixing rules, which lead to expressions for F_1 and F_2 exclusively in terms of the molecular parameter ratios σ_{ab}/σ_{bb} and $\varepsilon_{ab}/\varepsilon_{bb}$.

2.3.2.2.3. Calculation of Solid Solubilities

Since we already had an expression for $(\mu^{\infty}_{ar} - \mu^{*}_{br})$, the calculation of the solubility y_a was straightforward. Substitution of Eq.(19) in Eq.(12) gave:

$$y_a = \frac{f_a^{*solid}}{f_b^{*vap}} \exp\left[- F_1(s,t;T,\rho)\ \frac{U^{*}_{br}}{RT} - F_2(s,t;T,\rho)\ z^{*}_{br}\right], \quad (22)$$

where we have introduced the notations,

$$s \equiv \frac{\varepsilon_{ab}}{\varepsilon_{bb}} \qquad \text{and} \qquad t \equiv \frac{\sigma^3_{ab}}{\sigma^3_{bb}}\ . \quad (23)$$

In writing Eq.(22), we have assumed that the correct mixing rules are temperature- and density-dependent .

The fugacity of the pure solid at temperature T and pressure P is given by:

$$f_a^{*solid} = f_a^{*sat} \exp\ (\ Pv_a^{solid}\ /\ RT\ ), \quad (24)$$

where v_a^{solid} is the molar volume of the solid and f_a^{*sat} is the saturated fugacity of the solid.

Equation (22) can now be re-written in a more convenient form:

$$ln\ [f_a^{*solid}/(y_a f_b^{*vap})] = F_1(s,t;T,\rho)\ \frac{U^{*}_{br}}{RT} + F_2(s,t;T,\rho)\ z^{*}_{br}. \quad (25)$$

We used this equation to study solid solubilities in supercri-

tical gases by treating F_1 and F_2 as adjustable parameters. This approach didn't require any mixing rule.

2.3.2.2.4. Data Reduction

We have shown in Publication No. 5 that there were three ways in which Eqs.(22)-(25) could be employed in useful data-reduction processes, namely in extrapolation and interpolation at constant density or within small ranges of temperature and density. The third (and more important) use of those equations was in the construction of a solubility-temperature-density (y_a-T-ρ)-surface by fitting a set of (F_1,ρ)- and (F_2,ρ)-values to a suitable function of ρ. In this way, we were able to construct such a (y_a-T-ρ)-surface for the system adamantane/carbon dioxide, by fitting a set of (F_1,ρ) and (F_2,ρ) values to quadratic functions of density. Explicitly, we have for the solubility y_a the following expression:

$$y_a = \frac{p_a^{sat}}{f_b^{*vap}} \exp\left[\frac{P\, v_a^{solid}}{RT} - F_1(\rho)\, \frac{U_{br}^*}{RT} - F_2(\rho)\, z_{br}^*\right], \qquad (26)$$

with

$$F_1(\rho) = A + B\,\rho + C\,\rho^2, \qquad (27)$$

$$F_2(\rho) = A' + B'\rho + C'\rho^2. \qquad (28)$$

Using the relevant thermodynamic properties of pure carbon dioxide and adamantane, we have calculated from Eq.(26) the concentration c_a[14] of adamantane in supercritical carbon dioxide.

---

[14] The relationship between solute concentration c_a and mole fraction y_a is given by:

Calculated values are compared with experimental data in Figure 16, for 343 K and 382 K. As shown, the agreement between calculated and experimental results is good, within the range of temperature and density for which the surface (y_a-ρ-T) was constructed.

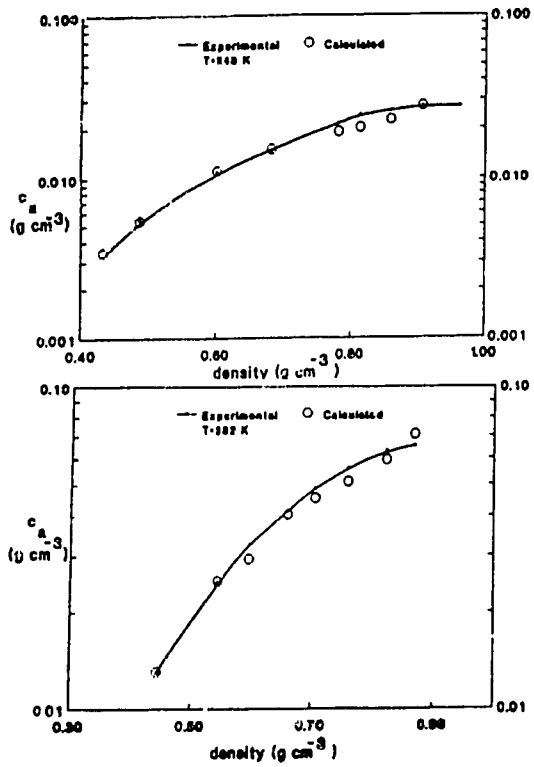

Figure 16. Experimental (Swaid et al., *Fluid Phase Equilibria, 1985, 21:95*) and calculated from Eqs. (26) and (29) solubilities of solid adamantane in SCF CO_2 at 343 and 382 K.

$$c_a = \frac{y_a \rho_b^* M_a}{M_b(1 - y_a)} \tag{29}$$

where ρ_b^* refers to the density of the pure solvent gas, and M_a and M_b are the molecular weights of the solute *a* and of the solvent *b*, respectively.

2.3.2.2.5. Extension to the Calculation of Solubilities of Liquids

We briefly observe that with suitable replacements in Eqs.(22) and (25), namely by replacing f_a^{*solid} by f_a^{liq}, these equations may still be used, provided the liquid is sparingly soluble in the supercritical gas.

However, contrarily to what is observed for solids, there is usually an appreciable solubility of the supercritical gas in the liquid. Hence, f_a^{liq} is function of the mole fraction of the gas dissolved in the liquid. Once we have modeled this composition dependence of the liquid phase fugacity, the procedure can be carried out as for solid solubilities.

The collaboration with Dr. Daniel Jonah is still going on and we hope to address the subject of liquid solubilities in a near future.

2.3.2.2.6. Conclusions

Our study indicated that the one-fluid conformal solution theory could be successfully applied to the correlation, interpolation, and extrapolation of solid solubilities in supercritical fluids. Of particular importance is the fact that linear isochores could be obtained, thus leading to the possibility of interpolating and extrapolating sparse data along constant-density paths; further, with a few isochores selected over a given density range, it became possible to construct a temperature-density-solubility surface valid for that range.

2.3.3. New Directions

Supercritical fluid science and its technological applications have developed and evolved quite considerably since we submitted in August 1986 the proposal for this project. The knowledge base formed in our research group by carrying it out

has allowed us to accompany the main directions of change in this field and get involved in new projects in supercritical extraction.

As mentioned in Section 2.3.1.3 we have measured the solubilities of olive oil components in supercritical carbon dioxide. The results are summarized in Publication N. 9, submitted for publication to the *Journal of American Oil Chemists Society*. The main conclusion is that the upgrading of lower quality olive oils is technically feasible. A more thorough evaluation will need the assessment of results obtained in a technical scale apparatus, such as the one we have assembled in the course of this project.

Simultaneously we have investigated the possibility of extracting biological molecules from aqueous solutions with SCF solvents, by use of reverse micelles formed in the supercritical phase. A new high pressure apparatus with a view cell was assembled (whose picture is presented in the Annex) for the study of micelle formation in supercritical carbon dioxide and ethylene. Solubilization of the surfactant AOT in supercritical ethylene is now being examined.

In a third project we examine the enzymatic catalysis in SCF solvents. This research includes enzyme stability studies, comparison with aqueous activity, study of the effects of carbon dioxide flowrate, pressure, water content, and co-solvent addition on reaction rate.

3. SCIENTIFIC COLLABORATION

This work had the contributions of researchers from University of Sierra Leone, Freetown, Sierra Leone (West Africa), University of California, Berkeley, and University of Cornell.

This Section describes the scientific collaboration given by the visitors during their (AID sponsored) stay at CQE. Funds for these visits were included in the item "Consultation".

The contributions from the visits of the members of the Portuguese team to the different locations are presented in the next Section.

Dr.Daniel A. Jonah from the University of Sierra Leone, Freetown, Sierra Leone, visited CQE twice.

Dr.Jonah's first visit took place from November 2, 1988, until January 27, 1989. This AID-sponsored visit was authorized by the Project Officer (letters of August 5, 1988 and February 27, 1989). During this stay, Dr.Jonah had the chance to contact with our experimental devices and with the techniques we were using. He give us a most valuable contribution in the theoretical treatment of our data, by developing a procedure (based on the one-fluid conformal solution theory) to correlate and predict the thermodynamic behavior in supercritical fluid extraction processes, namely of solid solubilities in supercritical solvents at different pressures and temperatures. This work produced Publication N. 5.

In the second visit, Dr.Jonah stayed four weeks with us, starting from September 29, 1990. He assisted us in the extension of our model (see Publication N. 5) which was developed for solid solubilities, to the more difficult problem of liquid solubilities in dense fluids. Although this problem has not been totally solved, significative progresses have been achieved. Moreover we discussed with Dr.Jonah our latest experimental results and future collaboration was planned, which is presently still going on.

Also under the AID grant funding, Dr. John Zollweg from Cornell University stayed with us from September 2, until September 8, 1990, as authorized by the letter of June 7, 1990 of the Project Officer. We discussed with Dr.Zollweg our experimental data and we have received important advices about the assessment and the usefulness of our results for industrial application. It was particularly interesting to exchange ideas with Dr.Zollweg since some of his present research projects are quite close to ours, fact which allowed us to compare our experimental data and techniques.

4. TRAINING PROGRAMME

This research involved several training periods of our graduate students and investigators at different Universities in USA and in Europe. Funds from AID used in this Training Programme were included in the item "Training & Travel".

Dr. Susana Barreiros spent a post-doctoral one-year leave (academic year 1987/88) at the University of California, Berkeley, working in the research group of Professor John Prausnitz. Her work was concerned mainly with the enzymatic catalysis in supercritical solvents and with the separation of biomolecule mixtures by extraction in aqueous-polymer systems. This stay did not involve funds from this Grant.

Also with Professor Prausnitz's group, the graduate student Margarida Gonçalves has spent a two-month (June-July 1988) training period. She gained experience in studies of enzymatic catalysis in supercritical solvents, namely enzyme stability studies, comparison with aqueous activity, and studies of the effects of carbon dioxide flowrate, pressure, water content, and co-solvent addition on reaction rate. This visit was partially funded by this Grant and was authorized by the Project Officer.

The graduate student H. Matos spent a two-month stay (September-October 1987) at the University of Erlangen-Nurenberg, Erlangen, West Germany. This is a well known university with a long tradition in high pressure work, which lately has dedicated much effort in research in supercritical fluid extraction processes.

Taking advantage of a collaboration link with the Technical University of Berlin, Germany, the same collaborator worked in the Summer of 1988 with the Group of Professor H. Knapp of the same University, where he measured the solubilities of limonene and of cineole in compressed gaseous ethylene (described in Section 2.3.1.1.5 above).

The same graduate student visited during five weeks (August-October 1989) the Department of Chemical Engineering of

the University of Delaware, Newark, Delaware. In this visit, this collaborator gained experience in high-pressure vapor-liquid measurements and in computer calculations of the thermodynamic modeling of mixtures involving supercritical fluids. He has applied equation of state models to our experimental results and important informations have been gained from these calculations. This work at Delaware was carried out under the supervision of Professor M.E. Paulaitis, a leading authority in supercritical extraction science.

These three training visits of the graduate student H. Matos were funded by sources other than AID.

The graduate student P.C. Simões spent the month of September 1989 at the University of Birmingham, England, where he had the opportunity to work in the Group of Drs. Bott and King in the operation of high-pressure countercurrent extraction columns. In this apparatus he measured particle-to-fluid mass transfer coefficients as function of pressure, temperature, solvent flowrate, and packed bed height, for the systems rape seed and benzoic acid in supercritical carbon dioxide. The results of this work have been presented at an international meeting (Publication No.8).

In addition, in his way back to Lisbon, this student attend ed in Holland a short training course provided by Aspen Technology, Inc., Cambridge, MA, on ASPEN PLUS, a process flowsheet simulator. This training was partially funded by AID (as authorized by the Project Officer in his letter of October 6, 1989).

The latest achievements of our research have been presented at the 2nd *Int. Symposium in High Pressure Chemical Engineering,* which took place in Erlangen, Germany, in September 1990. Present were the graduate students H. Matos and P.C. Simões and the investigator Edmundo Gomes de Azevedo. This was an important meeting attended by many experts in supercritical fluid extraction, from universities and industries alike. Fruitful discussions were carried out with many of the participants and a paper was presented by our Group (see Publication N. 7 of the

attached list). This trip was partially funded by this Grant, as authorized by the Project Officer in his letter of April 26, 1990.

With funds from AID and authorized (letter of June 7, 1990) by the Project Officer, Dr. Susana Barreiros has visited the Universities of California, Berkeley, and of Austin, Texas, from August 17 to September 6, 1990.

At Berkeley Dr.Barreiros met Professor J.Prausnitz with whom has discussed the main achievements of our research. The large experience of Prof. Prausnitz in molecular thermodynamics was of great help in showing us the adequate procedures to model and interpret our findings. Moreover, our collaborator has received valuable advices for the implementation of new directions of her research on enzymatic catalysis in supercritical fluids.

At the University of Texas at Austin, Dr. Barreiros had the chance of discussing with Professor Keith Johnston the possibilities of scale-up from our results to a pilot-plant scale process. In addition, in the apparatuses of Prof. Johnston's Laboratory she made a few experiments towards the formation of reversed micelles in supercritical carbon dioxide and propane. This was a very profitable visit to Austin (and Berkeley), which shed some light also towards the assessment studies of the extraction processes we have been studying in Lisbon.

5. COMPARISON OF ACTUAL ACCOMPLISHMENTS WITH GOALS ESTABLISHED

The bar diagram in Table 4 (taken from our initial proposal in 1987) indicates the estimated (1987) time schedule of the main goals established for this project. For comparison we represent also the actual (1990) accomplishments for each goal.

As Table 4 shows, most of the goals established in our proposal have been accomplished during the estimated time periods. However two remarks have to be made:

i) A few discrepancies occur for the final work to be

carried out with the countercurrent extraction columns, since some of the goals involving this apparatus have been partially accomplished only. More specifically, the last two goals indicated in Table 4 (*Optimization of Process Parameters in the Extraction of Model Systems* and the *Assessment Study*) are still being pursued. We predict they will be finished during the middle of 1991.

Table 4. Comparison of actual accomplishments (·····) with the goals established in our proposal (—).

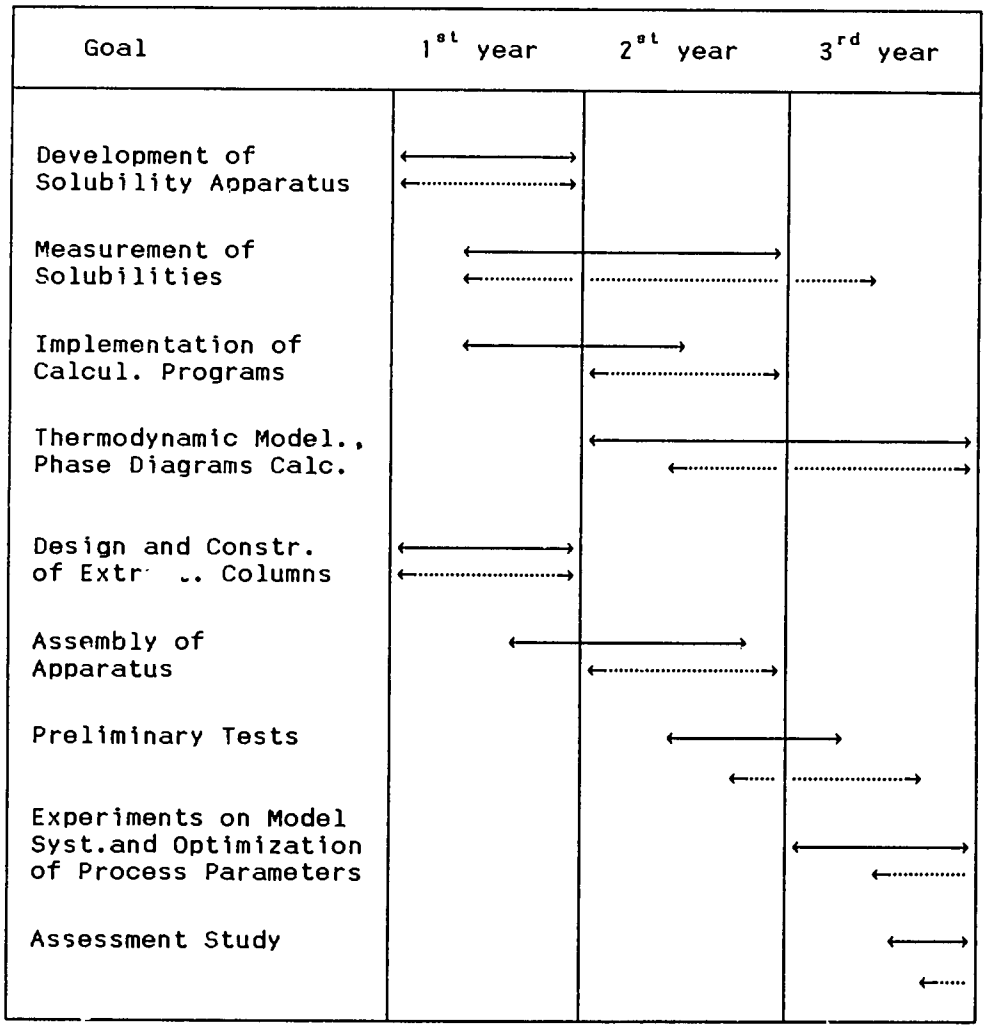

A couple of reasons have contributed to this delay, namely the complexity in the design of the apparatus and specially the difficulties related with the acquisition of part of the equipment. In the latter case, the contacts with American suppliers revealed troublesome. As an example (actually the worst), the first quotation for the acquisition of sapphire high pressure cells was dated December 4, 1987. We actually received them in March 19, 1990.

ii) Although is not shown in Table 4 we would like to mention that in addition to the work we were committed, we opened new directions in this project (as briefly mentioned in Section 2.3.3), e.g. the application of SCF to the refining and extraction of vegetable fatty edible oils. For example, our experimental data on the SCF extraction of soybean oil was have used by some of our colleagues (see Publication No.10) to study the application of high temperature capillary gas chromatography, associated with computerized pattern recognition techniques, for the rapid assessment of product quality in monitoring the extraction procedure.

6. LIST OF EQUIPMENT APPRAISED OVER US $1,000

With funds from this Grant different pieces of equipment have been acquired during the last three years. These items are now part of different apparatus which we used (and are currently still using) for our research.

As described above, in the course of our research three different experimental apparatuses have been assembled and the pieces of equipment (having an acquired unit value of $1,000 or more) listed in Table 5 are components of one of these apparatuses. It is our intention to keep these devices for further research work.

Table 5. List of equipment acquired with AID funds and appraised over US $1,000.

Item	Make	Date of Acquisition
Stainless steel cell	J.Simões	3/90
Automatic data acquisition system	Hewlett-Packard	6/90
Analytical balance	Mettler	3/90
Vacuum pump	Edwards	11/89
Gas compressor 10,000 psi	Newport Scientific	4/89
Multimeter	Keithley	8/89
Sapphire tubes	Union Carbide Co.	10/88
Mass Flowmeter	Rheonik GmbH	4/88
Microcomputer	Zenith	7/88
Gas compressor	Newport Scientific	1/88
Metering pump	Lewa GmbH	11/87

7. CONCLUDING REMARKS

7.1. Introduction

This research sponsored by AID has generated a large amount of experimental data, which has enriched our knowledge in terpene chemistry, namely the phase behavior of terpenes in SCF. We are pleased with our achievements that we shared with the world scientific community through our publications in international scientific journals.

Moreover, this work was the starting point of the graduate

work of our collaborators, H. Matos, P.C. Simões, and Margarida Gonçalves. They have carried out most of the work described above, and they are now close to the end of their Ph.D. Thesis. We hope that the graduate students H. Matos and P.C. Simões will have their dissertations ready for submission to approval during late 1991, and Ms. Gonçalves is likely to get her Ph.D. in early 1992. For this reason they are, more than anybody else, very grateful to the financial support from AID which has made it possible.

This grant was also rewarding for the international collaborations that we were able to support. Particularly gratifying was the collaboration with Dr.Jonah, of Sierra Leone, West Africa. During his visits to Lisbon, Dr.Jonah had the chance to contact with our apparatuses, and was introduced to the technical details of their operation. We had together many fruitful discussions which came out with our Statistical Thermodynamics-based method to model solubilities in SCF. Further collaboration is still in progress and we plan to extend our method to the more difficult problem of liquid solubilities in SCF.

7.2. Relevance of this Work to LDC's

In the course of this work we investigated the applicability of a novel separation process to natural (and biological) products abundant in many LDC's, particularly in the Mediterranean basin.

Our results show that this method could be useful for the upgrading of products that are usually sold by these countries as non-transformed raw materials of low-added value. Particularly promising is the applicability of the extraction with SCF to the refining of olive oils.

Our work has also demonstrated the usefulness of the collaboration among research groups in LDC's and more developed countries, Sierra Leone, Portugal and U.S.A. in the present case.

8. LIST OF PUBLICATIONS

The work described here produced several publications which are listed below. Part of the work was presented at scientific meetings and later published in refereed Journals or books of proceedings. A copy of the latter publications (corresponding to numbers 1, 3, 5, 7, 9 and 10) are attached.

1. "Phase Equilibria of Systems Containing Limonene, Cineole, and Supercritical Carbon Dioxide".
   E. Gomes de Azevedo, H. Matos, M. Nunes da Ponte, P.C. Simões.
   Proc. Int. Symposium on Supercritical Fluids, 1988, 135-142, Nice, France.

2. "Equilibrio de Fases de Sistemas Contendo Limoneno, Cineol e Fluidos Supercriticos Dioxido de Carbono e Mistura Dioxido de Carbono + Etano".
   E. Gomes de Azevedo, H. Matos, M. Nunes da Ponte, P.C. Simões.
   Presented at the *11th Annual Meeting of the Portuguese Chemical Society, 1988, Lisbon, Portugal.*

3. "Phase Equilibria of Natural Flavors and Supercritical Solvents".
   H. Matos, E. Gomes de Azevedo, M. T. Carrondo, P.C. Simões, M. Nunes da Ponte.
   Proc. of the 5th International Conference on Fluid Properties and Phase Equilibria for Chemical Process Design, 1989, 441-448, Banff, Canada.
   Published later in:
   Fluid Phase Equilibria, 1989, 52: 357-364.

4. "Supercritical Fluid Extraction of Eucalyptus Oil".
   P.C. Simões, M.T. Carrondo, M. Nunes da Ponte,

H. Matos, E. Gomes de Azevedo.
Presented at the 5th *International Chemical Engineering Conference, ChemPor, 1989, Lisbon, Portugal.*

5. "Statistical Thermodynamics of Solid Solubilities in Supercritical Fluids - a One-Fluid Conformal Theory Approach."
D.A. Jonah, E. Gomes de Azevedo, M. Nunes da Ponte.
Presented the 4th *Int. Conf. on Thermodynamics of Solutions of Non-Electrolytes, 1989, Santiago de Compostela, Spain.*
Published later in:
J. Supercritical Fluids, 1989, 2: 97-105.

6. "Phase Equilibria of Complex Systems".
E. Gomes de Azevedo.
Plenary Lecture at the 4th *Int. Conf. on Thermodynamics of Solutions of Non-Electrolytes, 1989, Santiago de Compostela, Spain.*

7. "Application of Supercritical Fluid Extraction to the Purification of Eucalyptus Oil".
P.C. Simões, M. Nunes da Ponte, H. Matos, and E. Gomes de Azevedo.
Proc. of the 2nd Int. Symposium in High Pressure Chemical Engineering, 1990, 401-405, Erlangen, Germany.

8. "Film Transfer Coefficients for Separation Processes Using Near-Critical CO_2".
O. Catchpole, P.C. Simões, M.B. King, T.R. Bott.
Proc. of the 2nd Int. Symposium in High Pressure Chemical Engineering, 1990, 153-158, Erlangen, Germany.

9. "On the Application of Supercritical Fluid Extraction to the Deacidification of Olive Oils".
M. Gonçalves, A.M.P. Vasconcelos, E.J.S. Gomes de Azevedo, H.J Chaves das Neves, M. Nunes da Ponte.
Submmitted to *J.Am. Oil Chem. Soc. (1990).*

10. "Use of Computerized Pattern Recognition of Triglyceride Profiles in Monitoring SCF-CO_2 Extraction of Fatty Oils".
A.M.P. Vasconcelos, M. Gonçalves, E. Gomes de Azevedo, M. Nunes da Ponte, H.J. Chaves das Neves.
J. High Resolution Chromatography, 1989, 12: 243-247.

9. ANNEX: PICTURES OF THE EXPERIMENTAL APPARATUSES

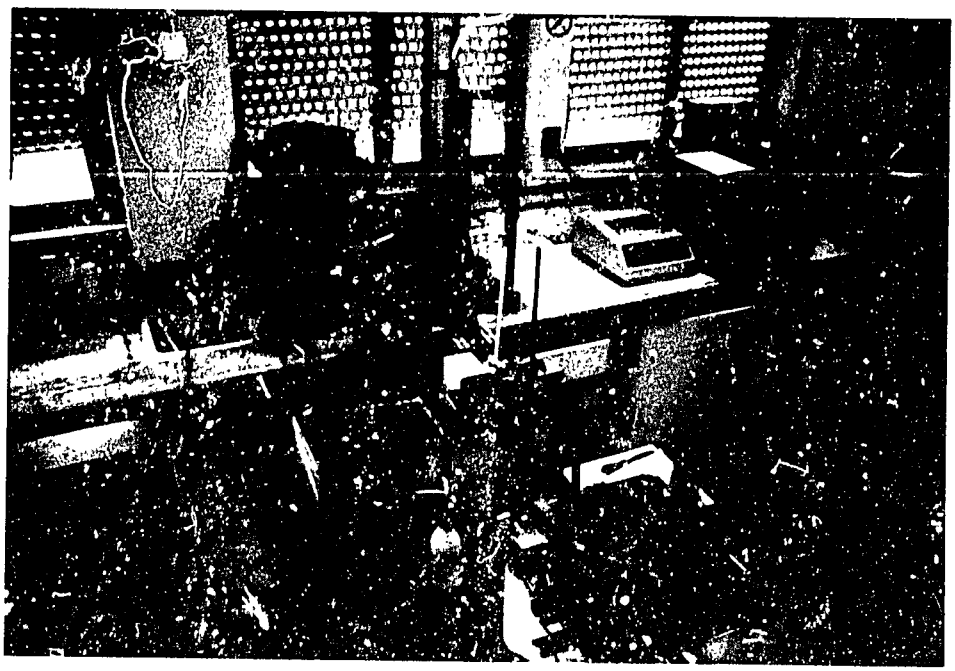

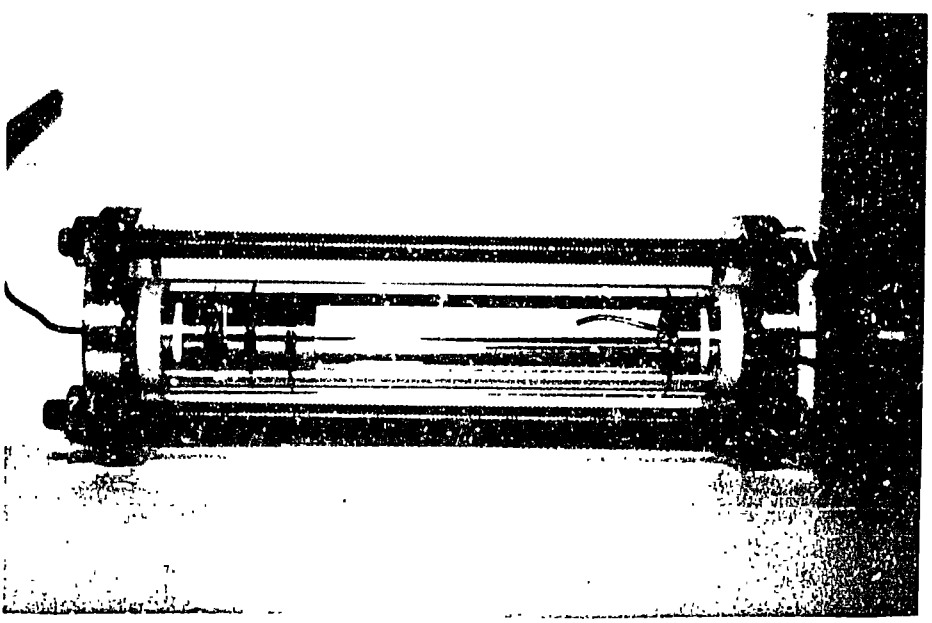

Top: VLE apparatus. Bottom: Variable volume sapphire tube cell.

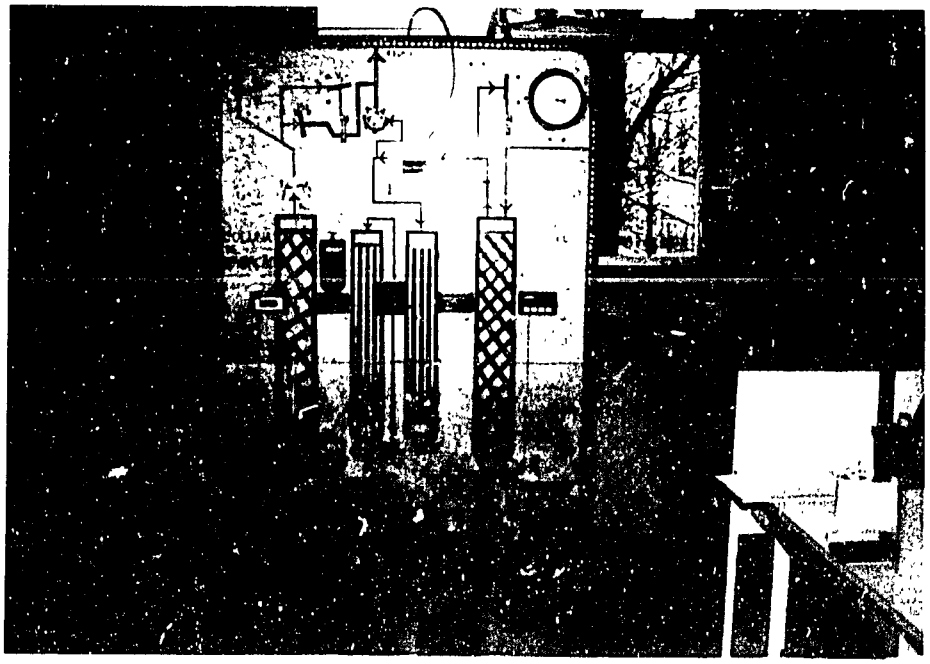

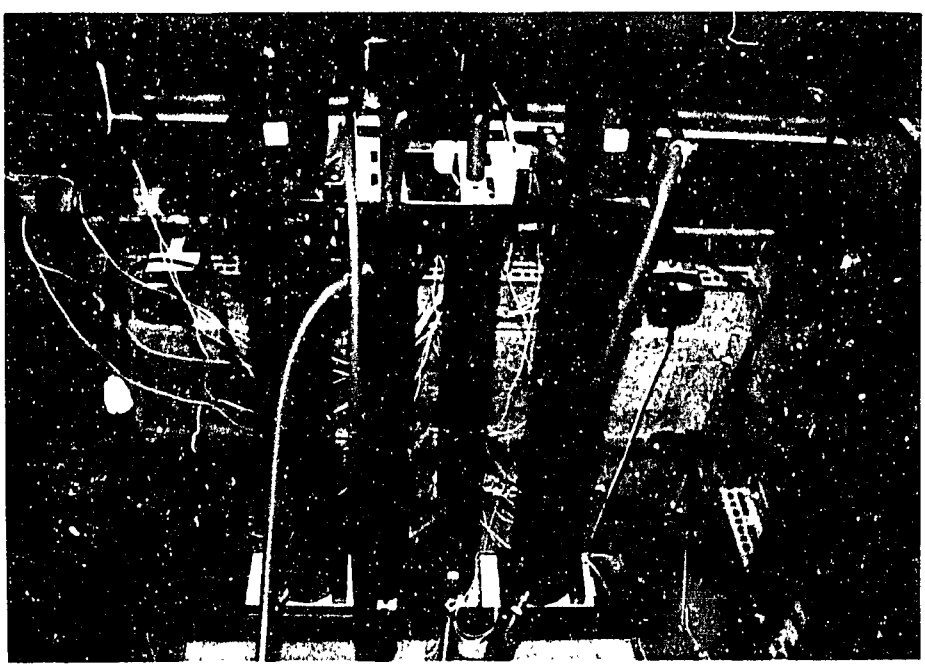

High-Pressure Countercurrent Liquid-SCF Extraction Columns

1)

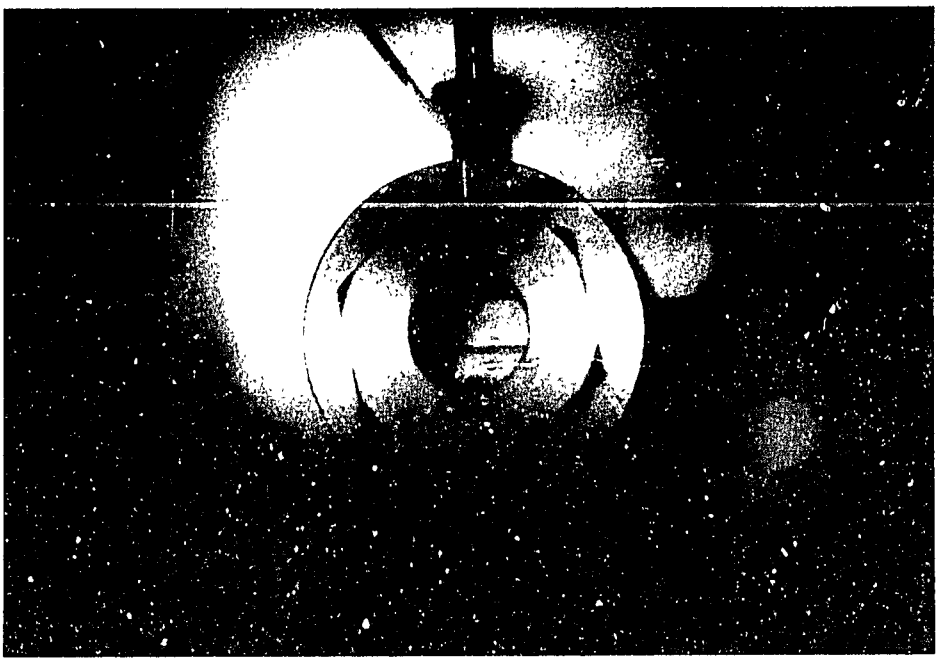

2)

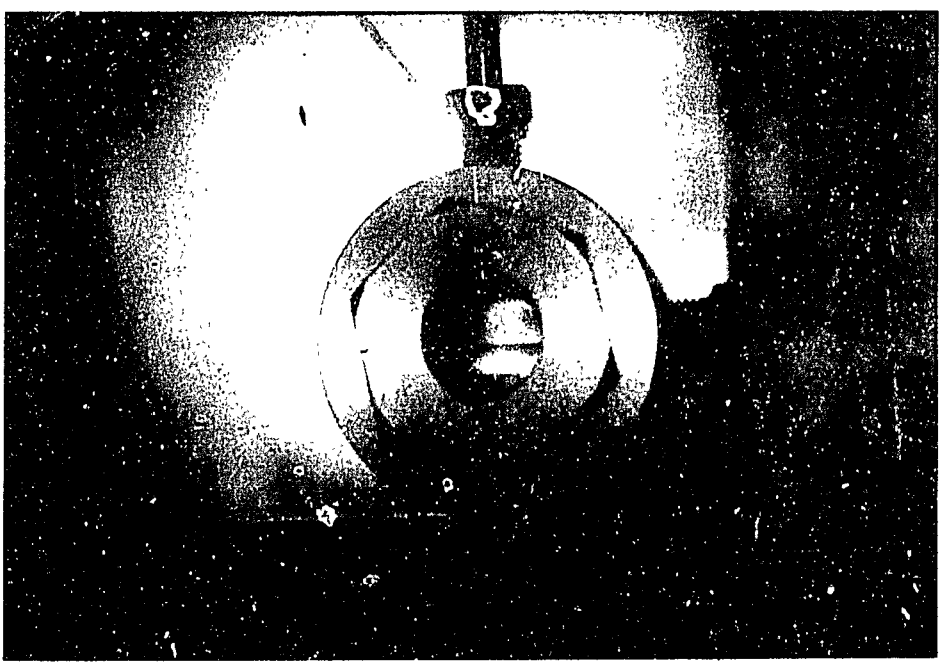

3)

4)

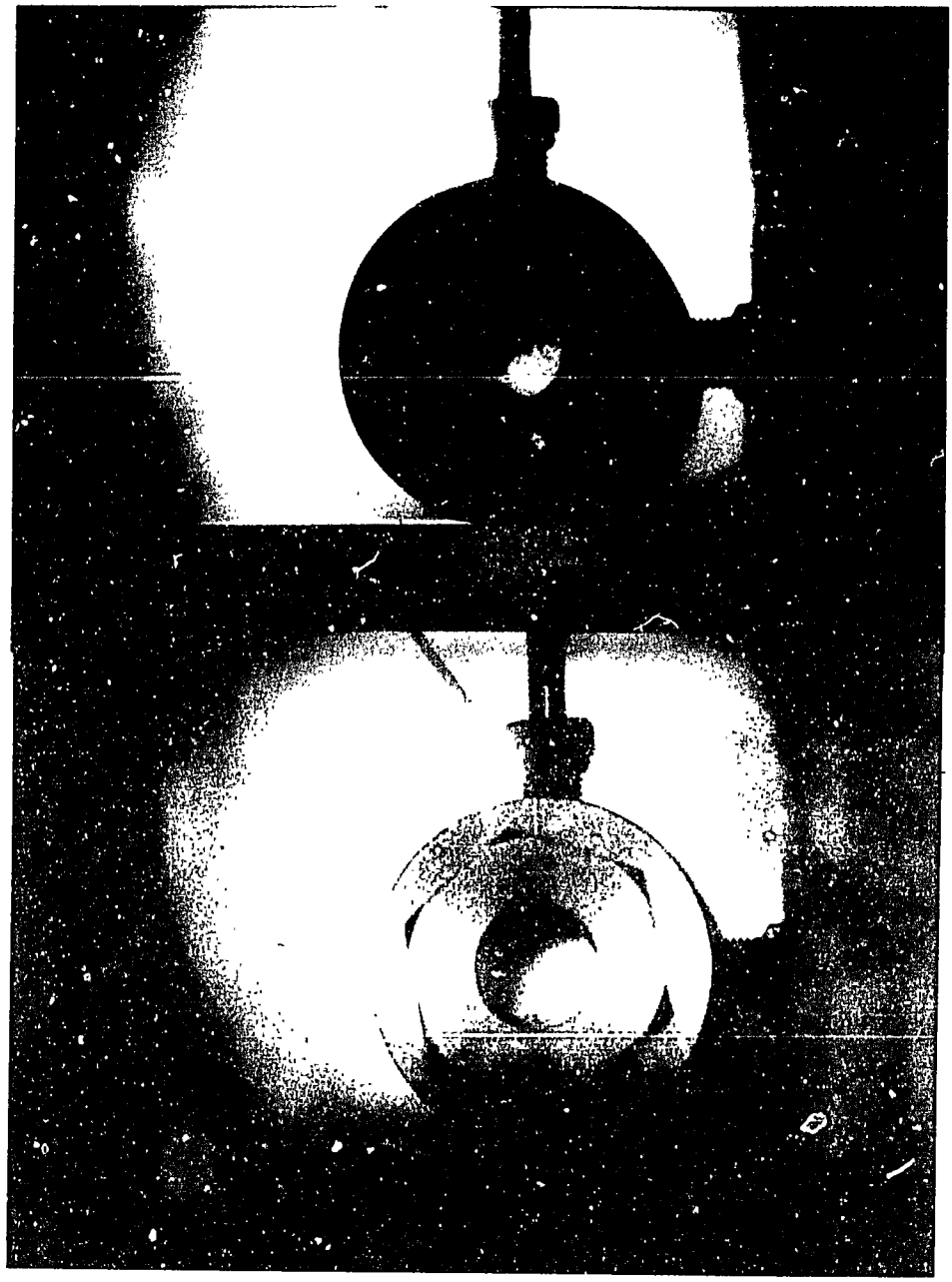

Sequence of a Mixture Critical Point: 1) Two-phase (vapor+liquid) in equilibrium; 2) By changing the pressure the mixture approaches the critical point (meniscus becomes ill defined); 3) Mixture at the critical point: meniscus has disappeared and critical opalescence is observed; 4) Mixture is above its critical point (supercritical): there is only one (dense) fluid phase.

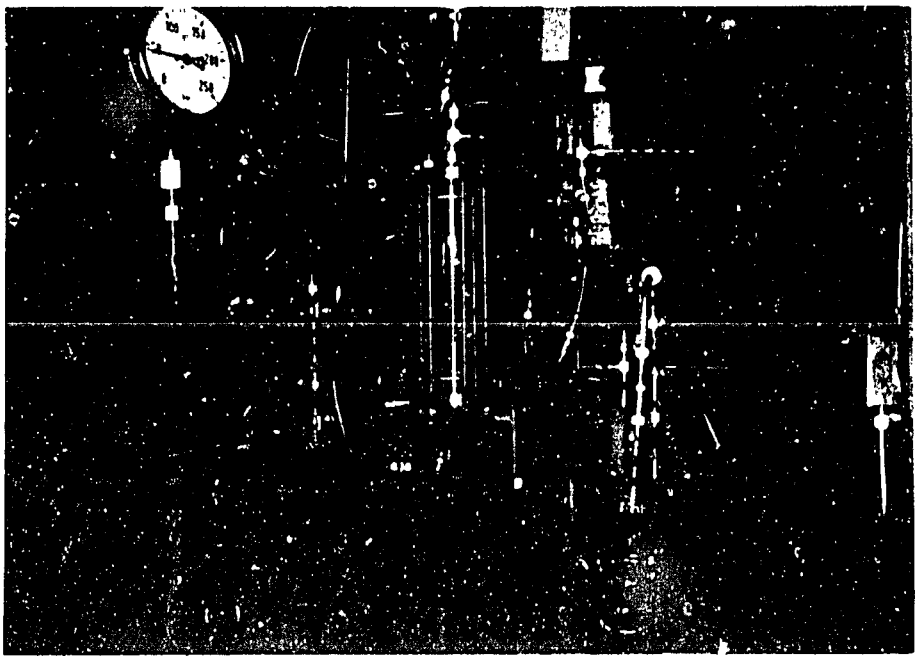

Lactic Acid Extraction Apparatus

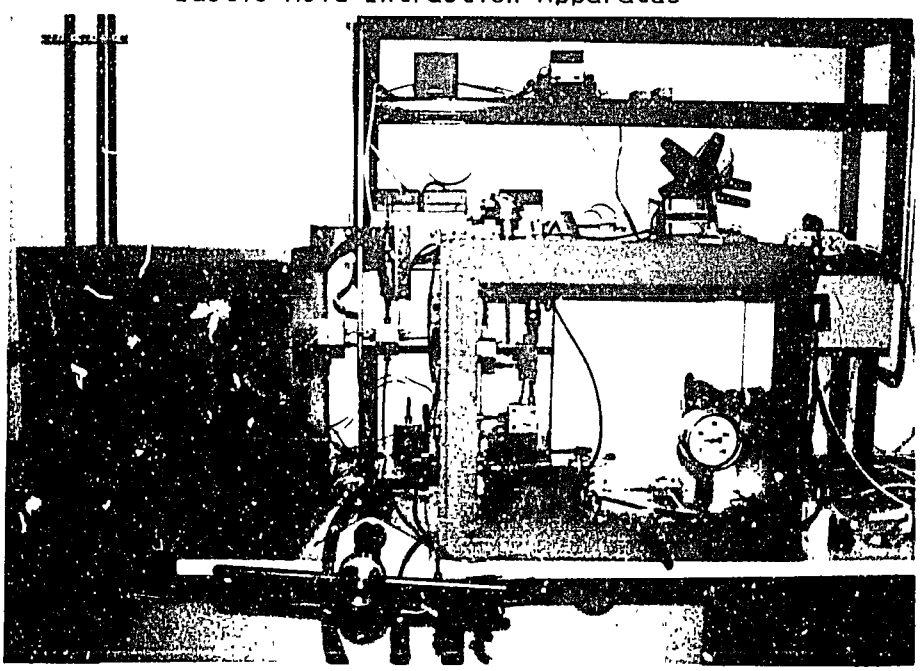

High-Pressure Apparatus for the Extraction of Bioproducts Using Reversed Micelles. It includes a Variable Volume Sapphire Cell.

10. REPRINTS OF THE PUBLICATIONS

Part of the work described in this report has been published in refereed Journals or in books of proceedings of scientific meetings.

Attached are copies of these publications which are listed in Section 8.

Table III. Relative Mean per cent Deviations $\delta(H_{12})/H_{12}$ between Experimental and Calculated Henry's Constants of Carbon Dioxide in Different Solvents. Comparison between Correlation of Data using the MLCSVDW, SRK and PR Equation of State and Prediction from the GCEOS Group Contribution Method. (References for experimental data are given in the original paper: Neau et al., 1988)

Compound 1	Range of T/K	N	MLCSVDW	RKS	PR	GCEOS
n-Hexane	293-303	3	0.31	0.33	0.42	7.27
n-Heptane	283-313	7	1.30	1.25	1.25	5.14
n-Octane	283-313	6	0.53	0.62	0.80	4.73
n-Decane	283-323	7	1.45	1.72	1.96	3.74
n-Dodecane	283-323	7	1.44	1.87	*	2.95
n-Tetradecane	298-343	4	2.41	3.71	*	4.21
n-Hexadecane	298-375	26	2.61	*	*	7.38
n-Eicosane	313-375	6	2.58	*	*	10.55
Cyclohexane	284-313	8	2.53	2.20	2.35	2.28
Methylcyclohexane	284-313	3	2.31	2.67	2.44	5.71
Cis-1,2-dimethylcyclohexane	298-313	2	0.56	0.60	0.39	6.57
Trans-1,2-dimethylcyclohexane	298-313	2	0.24	0.28	0.47	4.84
Benzene	293-307	7	0.69	0.58	0.60	2.24
Toluene	284-313	5	1.56	1.29	1.35	5.51
o-Xylene	283-313	5	0.99	0.43	0.55	0.28
m-Xylene	283-313	5	0.86	0.66	0.69	2.67
p-Xylene	283-313	5	0.74	0.63	0.66	1.62
Ethylbenzene	296-335	5	2.51	2.32	2.51	35.65
1-Methylnaphtalene	298-375	20	6.21	6.22	6.36	6.44
Diphenylmethane	300-375	10	1.63	2.04	*	41.96
Methanol	273-298	3	10.96	13.41	13.56	8.88
Ethanol	298-348	3	15.09	15.44	15.12	12.96
Propanol	283-313	5	10.41	10.25	10.24	12.91
2-Propanol	283-313	4	2.87	3.45	3.21	44.26
Octanol	283-384	3	2.14	1.49	*	20.00

PHASE EQUILIBRIA OF SYSTEMS CONTAINING LIMONENE, CINEOLE AND SUPERCRITICAL CARBON DIOXIDE

E. GOMES de AZEVEDO, H.A. MATOS, M. NUMES da PONTE, P.C. SIMOES
Instituto Superior Tecnico, Lisboa, Portugal

SUMMARY

Using a constant-volume, static cell we measured the vapour-liquid equilibrium at 313 K for the mixtures carbon dioxide + limonene and carbon dioxide + cineole in the vicinity of the mixture critical point (pressures up to 8.2 MPa). Data were also obtained for the ternary CO_2+ limonene + cineole at the same temperature and for a fixed overall mass ratio of approximately 0.80 cineole to 0.20 limonene.

The solubility behaviour of limonene and cineole in supercritical carbon dioxide was found to be quite similar. The results obtained with the ternary mixture show no selectivity in extraction of either component from a liquid sample with carbon dioxide.

Our data were well correlated with the Peng-Robinson equation of state using one interaction parameter obtained from regression of the binary vapour-liquid equilibrium data.

I. INTRODUCTION

The well-known characteristics of supercritical fluids, namely their suitability to the extraction of heat-labile biochemical and natural products, no residues being left in either extract or raffinate, make them adequate to the extraction of essential oil components.

Essential oils are largely used in food, pharmaceutical, and cosmetic industries. Numerous processes for supercritical extraction of oils have been presented. In particular, the high solubility of terpenes in supercritical carbon dioxide has been reported by a number of authors

Stahl and collaborators [1,2] measured solubilities as a function of pressure in a flow apparatus for a diversity of essential oil components. Coppella and Barton [3] and Kalra et al [4] measured the vapour-liquid equilibrium of lemon oil, a multicomponent mixture that includes several terpenes. However no vapour-liquid equilibrium data are available for mixtures of carbon dioxide with pure

PUBLICATION 1

56

terpenes.

The main purpose of this work is to examine the possibility of purifying eucaliptus oil by supercritical fluid extraction. The main component of this oil is 1-8 cineole ($C_{10}H_{18}O$). In the final stages of purification it must be separated from d-limonene ($C_{10}H_{16}$), a process usually carried out by fractional crystallization. Relevant thermodynamic data are needed to evaluate the feasibility of replacing this extraction process by supercritical fluid extraction.

We report here measurements of vapour-liquid equilibrium at 313 K for the binaries CO_2 + limonene and CO_2 + cineole in the vicinity of the mixture critical point. Data are also presented at the same temperature for the ternary CO_2 + limonene + cineole with a fixed overall mass ratio of approximately 0.80 cineole to 0.20 limonene.

II. EXPERIMENTAL

Measurements were performed in the apparatus schematically shown in Figure 1.

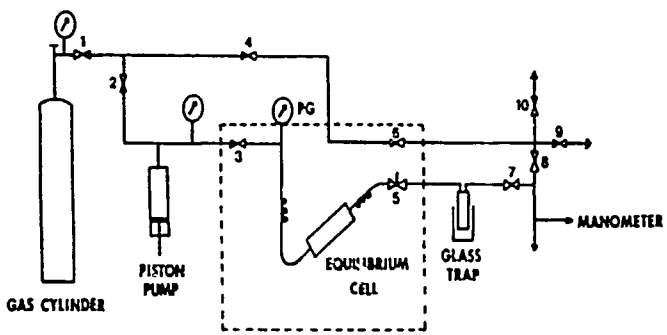

Figure 1. Schematic diagram of the experimental apparatus.

The main piece of equipment is a static vapour-liquid equilibrium cell of approximately 30 cm^3. It is connected to the rest of the apparatus through flexible tubing that allows considerable freedom of movement of the cell for a convenient mixing of its contents.

Samples can be withdrawn from the phases on top and bottom of the cell through a capillary line. These samples are collected by depressurization and expansion through the micrometering valve 5 into a small glass trap connected to

large steel bottles of calibrated volume. When valve 5 is open, the liquid solute condenses in the cold glass trap while the carbon dioxide expands into the steel bottles. Pressure in these bottles is measured with a mercury manometer and is used to calculate the amount of solvent gas, while the amount of the liquid solute is obtained by weighing of the glass trap. In the case of measurements with ternary mixtures, the ratio cineole/limonene is subsequently obtained by gas chromatography.

After filling at atmospheric pressure with a small amount (about 6 cm^3) of liquid (limonene, cineole, or limonene + cineole), the cell is closed and connected to the apparatus in a thermostated water bath.

Carbon dioxide is pressurized by a piston hand pump into the cell through valves 2 and 3, and equilibrium between liquid and vapour is attained after about 40 minutes of vigorous stirring of the whole cell. After about the same time of rest (no stirring), the pressure is read on a Bourdon tube manometer of 50 kPa precision, and the temperature is measured with a calibrated mercury thermometer of 0.1 K precision.

A sample from the top of the cell (gas phase) is then withdrawn and the amount of substances obtained using the procedure described above. Since these amounts were always very small, they were corrected for the vapor pressures of the solutes The cell is inverted, stirring of the system is resumed to restore equilibrium, and then allowed to settle again for 40 minutes and a new sample is taken from the bottom of the cell (liquid phase).

The carbon dioxide used in this work was 99.998 mole % pure supplied by Air Liquide, d-limonene was 99 mole % pure supplied by Sarsyntex, and 1-8 cineole was also 99 % pure supplied by EGA-Chemie.

III. RESULTS AND DISCUSSION

Experimental vapour-liquid equilibrium results at 313 K are shown in Figure 2 for CO_2 + limonene and in Figure 3 for CO_2 + cineole.

As shown in Figures 2 and 3, the vapour pressures read for the liquid samples are slightly lower than for the gas samples. This pressure drop is the result of the adopted sequence of experiments, as described in the preceding section.

Above the highest measured pressure indicated for each system, samples taken from top and bottom of the cell had the same composition (within experimental error), an indication of the existence of one (supercritical) phase only inside the cell.

The results show that the solubility behaviour of limonene and cineole in dense carbon dioxide is quite similar. This is confirmed by the results obtained for the ternary system which indicate that dense CO_2 dissolves equally well both components. Actually, the ratio cineole/limonene in the liquid and vapour phases in equilibrium is the same within experimental error, indicating no selectivity for either of them in an extraction process.

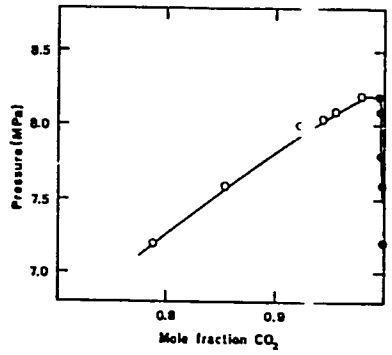

Figure 2. Experimental and calculated . .pour-liquid equilibria for CO_2+limonene at 313 K:
o liquid ; ● vapour
—— calculated from Peng :obinson equation with k_{12}=0.080.

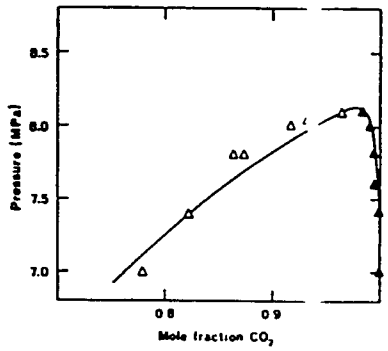

Figure 3. Experimental and calculated . pour-liquid equilibria for CO_2+cineole at 313 K:
Δ liquid ; ▲ vapour
—— calculated from Peng Robinson equation with k_{12}=0.075.

Figure 4 compares solubility data (expressed in mg of limonene per NL of CO_2, 1 NL corresponding to 1 dm^3 of CO_2 at 100 kPa and 293.15 K) for limonene in supercritical carbon dioxide obtained by several authors. As shown, our results for the liquid and the vapour phases are in good agreement with the equilibrium data obtained by Coppella and Barton for lemon oil, a mixture of terpenes with approximately 70 mole % of limonene. Agreement is also found between the data of Stahl and Gerard and our results for the vapour phase. However, since the latter authors have determined the solubilities by means of the dynamic flow principle, they could not detect the mixture critical point (about 8.3 MPa for CO_2 + limonene at 313 K). It makes no sense to define solubilities above it as at these conditions CO_2 and limonene have one (supercritical) phase only. Their curve above 8.3 MPa

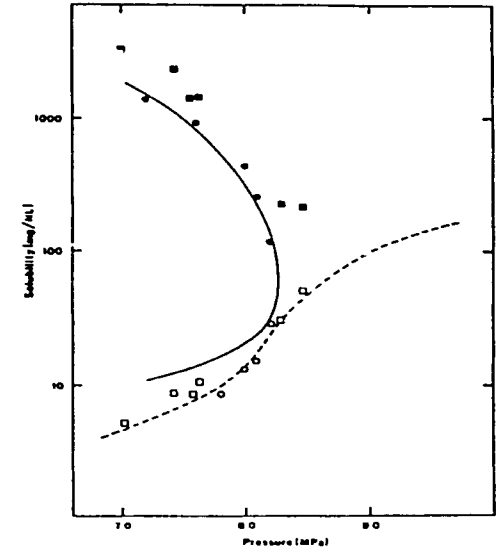

Figure 4. Solubility of limonene in dense carbon dioxide at 313 K.
Experimental
Coppella and Barton. ■ liquid, □vapour.
This work· ● liquid, 0 vapour.
Stahl and Gerard: - - -
Calculated. ——Peng-Robinson equation with k_{12}=0.080.

is therefore meaningless, as can be seen by comparison with our results and Coppella and Barton's for the liquid phase.

For a quantitative description of the phase equilibrium of the systems studied we used the Peng-Robinson equation of state.

For the pure components, equation of state parameter **b** was obtained from critical data. Parameter **a** was calculated at a given temperature from critical data and acentric factor.

For limonene and cineole T_c and P_c were estimated by the methods of Nokay and Lydersen [5,6], respectively. The acentric factor was estimated by the method of Pitzer et al. [6]. Table 1 shows the pure component constants used in this work.

	Molecular Weight	Critical Pressure (MPa)	Critical Temperature (K)	Acentric Factor
CO_2	44.01	7.38	304.2	0.225
Limonene	136.24	2.75	654.4	0.327
Cineole	154.25	2.77	665	0.312

Table 1. Pure component constants.

For mixtures, **a** and **b** are composition dependent and obtained from the usual quadratic mixing rules. The binary constant a_{12} is given by $a_{12}=(1-k_{12})(a_{11}a_{22})^{1/2}$, being k_{12} an adjustable parameter which characterize the interactions of unlike molecules. This parameter was obtained from regression of the binary phase equilibrium data.

As shown in Figures 2, 3, and 4 the Peng-Robinson equation of state can reproduce quantitatively the observed phase equilibrium behaviour with a binary interaction parameter determined from the binary data.

It was also found that the same thermodynamic model can reproduce semi-quantitatively the ternary data, using the interaction parameters obtained from the binary data (and assuming $k_{23}=0$ for the binary limonene+cineole). As an example, Table 2 shows a comparison between experimental ternary data at 313 K and the predictions of the Peng-Robinson equation of state using $k_{12}=0.080$, $k_{13}=0.075$ and $k_{23}=0$.

P (MPa)	x(CO_2) exp	x(CO_2) calc.	x(limonene) exp	x(limonene) calc.	x(cineole) exp.	x(cineole) calc.
7.4	0.888	0.819	0.025	0.081	0.087	0.100
7.6	0.859	0.856	0.030	0.024	0.111	0.120
7.75	0.867	0.888	0.031	0.012	0.102	0.100
8.0	0.914	0.942	0.023	0.008	0.063	0.050
8.2	0.950	0.972	0.012	0.008	0.038	0.020

Table 2. Experimental and calculated liquid compositions for the ternary CO_2 + limonene + cineole at 313 K.

IV. ACKNOWLEDGEMENTS

The authors are grateful to Professor M. Paulaitis and Dr.C.-P. Kao (University of Delaware, Newark, U.S.A.) for helpful discussions and to JNICT, Franco-Farmaceutica, Favorita (Lisboa, Portugal) and A.I.D. (Washington D.C., U.S.A.) for financial support.

V. REFERENCES

[1] STAHL,E., SCHILZ,Z., Chem.-Ing.-Tech., 48, 1976, 773.

[2] STAHL,E., GERARD,D., Perfumer & Flavorist, 10, 1985, 29.

[3] COPPELLA,S.J., BARTON,P., Supercritical Fluids, 1987, edited by T.G Squires, M.E.Paulaitis, ACS Symposium Series 329, p.202.

[4] KALRA, H., CHUNG, S.Y.-K., CHEN, C.-J., Fluid Phase Equilibria, 36, 1987, 263.

[5] DAUBERT,T.E., DANNER,R.P., Eds., "Technical Data Book - Petroleum Refining", 1983, 4th. ed., American Petroleum Institute, Washington D.C.

[6] REID,R.C., PRAUSNITZ,J.M., POLING,B.E., "The Properties of Gases and Liquids", 1987, 4th. ed., McGraw-Hill Book Co., New York.

HIGH PRESSURE VAPOR-LIQUID EQUILIBRIA FOR THE SUPERCRITICAL CO_2+ETHANOL+WATER SYSTEM

K. NAGAHAMA, J. SUZUKI, T. SUZUKI
Tokyo Metropolitan University, Japan

Summary

Using a static type of apparatus vapor-liquid equilibrium (VLE) data have been measured for the system CO_2+ethanol at 313 and 333 K, and for the system CO_2+ethanol+water at 313 K and pressures of 3.86,5.79, and 9.98 MPa. To predict the ternary system from the binary data only, VLE data of three constituent binaries including the literature data have been correlated by use of the Peng-Robinson equation of state(PR-EOS).

As a result of testing several mixing rules, at least two interaction binary parameters were needed to represent the VLE data for every binary system sufficiently.

Employing a total of six binary parameters VLE of the CO_2+ethanol+water mixture have been predicted and compared with the experimental data. The agreement is good at low pressures but there is some inconsistency in the region close to the critical point of the ternary.

1. INTRODUCTION

Supercritical carbon dioxide can be used as a solvent for recovery of ethanol from aqueous solutions. To design such a rational separation process and equipment, phase equilibrium data at high pressures for the ternary CO_2+ethanol+water system are needed.

In the present paper, the results of experimental VLE data for the CO_2+ethanol system as well as for the CO_2+ethanol+water system are presented. Next we describe the calculated results of the ternary VLE from binary data using the Peng-Robinson equation of state coupled with a two-parameter combining rule.

Previous experimental studies of VLE for the CO_2+ethanol were made by Takishima et al.(304.2 and 308.2 K)[1] and Panagiotopoulos and Reid(308.1,323.1 and 338.1 K)[2],but the latter reported graphically only. Gupta et al.[3] measured the vapor composition for this binary at 298.15,323.15 and 348.15 K. Baker and Anderson[4] reported the critical locus in the region close to the pure CO_2.

For the CO_2+ethanol+water system, Kuk and Montagna[5] measured solubilities of CO_2 and ethanol+water in liquid

Fluid Phase Equilibria, 52 (1989) 357–364
Elsevier Science Publishers B.V., Amsterdam — Printed in The Netherlands

PHASE EQUILIBRIA OF NATURAL FLAVOURS AND SUPERCRITICAL SOLVENTS

HENRIQUE A. MATOS, EDMUNDO GOMES DE AZEVEDO
Centro de Química Estrutural, Instituto Superior Técnico,
P-1096 Lisboa (Portugal)
PEDRO C. SIMOES, MANUEL T. CARRONDO and MANUEL NUNES DA PONTE
Faculdade de Ciências e Tecnologia, Universidade Nova de Lisboa,
P-2825 Monte da Caparica (Portugal)

ABSTRACT

To study the possibility of separation of cineole from limonene (two of the main components of eucalyptus oil) we measured the vapour-liquid equilibrium of the systems containing either d-limonene or 1,8-cineole in the supercritical solvents carbon dioxide (at 318.2 and 323.2 K) and an azeotropic mixture of ethane+carbon dioxide (at 303.2 K). The results obtained show that both solutes have similar solubilities in the supercritical solvents studied here.

INTRODUCTION

The main purpose of this work is to examine the possibility of purifying eucalyptus oil by supercritical fluid extraction. The main component of this oil is 1-8 cineole ($C_{10}H_{18}O$). In the final stages of purification it must be separated from d-limonene ($C_{10}H_{16}$), a process usually carried out by fractional crystallization. Relevant thermodynamic data needed to evaluate the feasibility of replacing this process by supercritical fluid extraction are essentially vapour-liquid equilibrium results.

Practically all available data of this kind involving essential oils have been obtained with supercritical carbon dioxide (Stahl and Schilz, 1976; Stahl and Gerard, 1985; Coppella and Barton, 1987). In a previous publication (Azevedo et al.,1988), we presented results obtained with mixtures of carbon dioxide and limonene and of carbon dioxide and cineole, at 313.2 K and relatively close to the critical pressure of the mixture. In this work, we extend those measurements to 318.2 K and 323.2 K, and, in addition, we report results on the carbon dioxide+ethane+ (limonene or cineole) systems, at 303.2 K.

At this temperature, both carbon dioxide and ethane are subcritical, but most binary mixtures of these two substances are

0378-3812/89/$03.50 © 1989 Elsevier Science Publishers B.V.

61

already supercritical. In fact , due to the existence of a positive azeotrope, the critical temperatures of the mixtures are lower than those of the pure components (Fredenslund et al., 1974). In this work, we used a CO_2+C_2H_6 mixture close to the azeotropic composition, in an attempt to obtain improved selectivity for limonene over pure carbon dioxide solvent.

EXPERIMENTAL

The vapour-liquid equilibrium measurements were performed in the apparatus schematically shown in Figure 1.

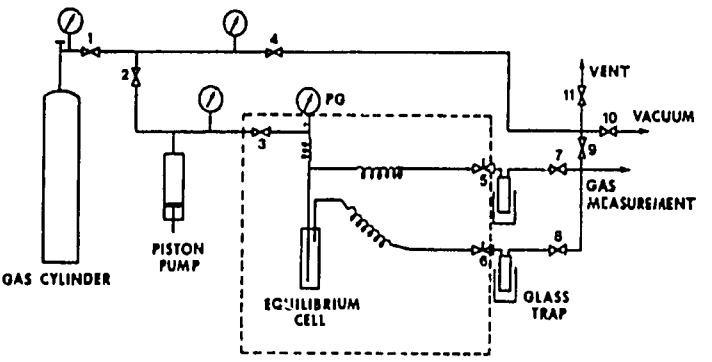

Figure 1. Schematic diagram of the experimental apparatus.

The main piece of equipment is a static vapour-liquid equilibrium cell (immersed in a thermostated water bath) of approximately 30 cm^3, connected to the apparatus through flexible tubing that allows considerable freedom of movement of the cell for a convenient mixing of its contents.

Operation starts with filling of the cell,at atmospheric pressure, with a small amount (about 5 cm^3) of liquid (limonene or cineole). The solvent gas is then pressurized by a piston hand pump into the cell through valves 2 and 3. After about 40 minutes of vigorous stirring of the whole cell and the same time of rest, the pressure is read on a Bourdon tube manometer (which was previously

calibrated against a dead-weight gauge) of 50 kPa precision, and the temperature is measured with a calibrated mercury thermometer of 0.1 K precision. A sample is then taken either from top or bottom of the cell.

These samples are collected by depressurization and expansion through valves 5 and 6 into small glass traps connected to large steel bottles of calibrated volume, in a thermostated bath. When one of these valves is open, the solute condenses in the respective cold glass trap, while the solvent gas expands into the steel bottles, through valves 7 or 8 . These bottles have an overall volume of approximately 900 cm^3, calibrated to ± 0.1 cm^3. The pressure of the gas is read with a mercury manometer associated with a precision cathethometer, and is used to calculate the amount of gas present in the sample. The amount of liquid deposited in the glass trap is measured by weighing.

With this set up, the amounts sampled can be obtained with a high precision, except in the limit of very low solubility, at low pressures in the vapour phase.

The accuracy of the obtained composition results is limited by the disturbances introduced in the phase equilibrium by the sampling procedure itself. A sufficient amount of each of the phases has to be withdrawn from the cell to deposit a measurable mass of limonene or cineole in the cold trap. Observed pressure drops in the cell were between 0.1 and 0.2 MPa when sampling from the vapour and between 0.05 and 0.1 MPa when sampling from the liquid. The mass taken out in each sample does not exceed, in the worst cases, 1.5% of the estimated total mass inside the cell.

Another source of error in this procedure is the existence of dead volumes between the cell and the sampling valves 5 and 6. To minimize these errors, the lines leading from the cell to those valves were made of capillary stainless steel tubing of 0.20 mm internal diameter. The amount of substance in the dead volumes represents less than 3% of the total amount of each sample. Moreover, a purge of the capillary lines is performed half-way through the stirring process, filling them with a fluid of composition similar to that of the final vapour or liquid.

The reproducibility of the composition results was checked by several measurements under the same conditions of pressure and temperature. From these we estimate their precision to be ± 1.5 mole percentage.

The carbon dioxide used in this work is 99.998 mole % pure supplied by Air Liquide. The carbon dioxide+ethane mixture was also supplied, in the gas phase, by Air Liquide, with a composition of 0.232 ± 0.005 mole fraction of ethane. d-Limonene is 99 mole % pure supplied by Sarsyntex, and 1-8 cineole is also 99 mole % pure supplied by EGA-Chemie.

RESULTS

The vapour-liquid equilibrium results obtained for CO_2+limonene at 318.2 K and 323.2 K are given in Table 1. The results for CO_2+cineole are shown in Table 2.

The vapour-liquid equilibrium results obtained at 323.2 K for both CO_2+limonene and CO_2+cineole are compared in Figure 2.

Figure 3 shows the critical pressure of the mixtures as a function of temperature, obtained graphically from p-x-y plots like those in Figure 2.

Table 3 gives the vapour-liquid equilibrium results obtained at 303.2 K for either limonene or cineole with carbon dioxide and ethane. In this case, the supercritical solvent is a mixture of composition close to that of the critical azeotrope, as given by Fredenslund et al. (1974). The ratio CO_2 / C_2H_6 was not measured in any of the two phases, and therefore only an overall composition, x (CO_2+C_2H_6), was obtained.

TABLE 1

Vapour-liquid equilibrium results for CO_2+limonene at 318.2 and 323.2 K. p is the total pressure and x and y are the mole fractions of CO_2 in the liquid and in the gas, respectively.

p/MPa	x(CO_2)	y(CO_2)	p/MPa	x(CO_2)	y(CO_2)
T=318.2 K			T=323.2 K		
8.5	0.857	-	8.7	0.807	0.994
8.6	0.859	0.996	9.1	0.851	0.996
8.7	-	0.997	9.3	0.858	-
8.7	0.908	0.991	9.4	-	0.994
8.8	0.916	0.993	9.5	-	0.991
8.9	0.954	0.992	9.6	0.905	0.987
8.9	0.940	-	9.65	0.913	-
9.0	-	0.984	9.7	-	0.985
			9.75	-	0.985
			9.8	-	0.967

64

TABLE 2

Vapour-liquid equilibrium results for CO_2+cineole at 318.2 and 323.2 K. Symbols as in Table 1.

p/MPa	$x(CO_2)$	$y(CO_2)$	p/MPa	$x(CO_2)$	$y(CO_2)$
T=318.2 K			T=323.2 K		
8.0	0.809	0.995	7.75	-	0.994
8.4	0.859	0.995	8.0	0.763	0.995
8.6	0.875	0.991	8.4	-	0.995
8.8	0.920	0.992	8.8	0.834	0.995
8.9	0.939	-	9.2	0.888	0.996
8.95	-	0.982	9.4	0.904	0.996
9.0	-	0.970	9.5	0.913	-
9.0	0.956	0.979	9.6	0.932	0.988
			9.8	0.943	0.977

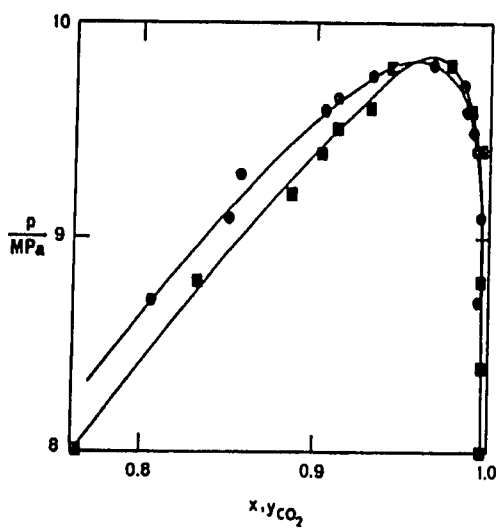

Figure 2. Vapour-liquid equilibria for CO_2+limonene (●) and CO_2+cineole (■) at 323.2 K.

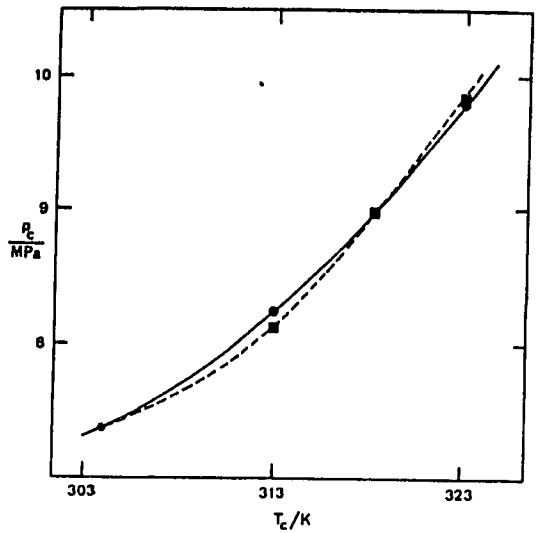

Figure 3. Critical temperatures and pressures of mixtures of CO_2 with limonene (●) and with cineole (■). The symbol ✱ indicates the critical point of pure CO_2.

TABLE 3

Vapour-liquid equilibrium results at 303.2 K for mixtures containing either limonene or cineole and (carbon dioxide + ethane) of overall composition 0.232 mole fraction of ethane. p is the pressure and x and y are the mole fractions of CO_2+C_2H_6 in the liquid and gas phases, respectively.

p(MPa)	x	y	p(MPa)	x	y
Limonene			Cineole		
6.55	0.816	-	6.5	0.831	-
6.6	0.839	-	6.6	-	0.993
6.7	-	0.991	6.8	0.895	0.986
6.75	0.860	-	6.9	0.911	0.982
6.8	-	0.991			
6.95	0.910	0.986			
7.0	0.912	-			
7.05	0.939	0.983			
7.1	0.947	0.973			

The results of Table 3 are plotted in Figure 4.

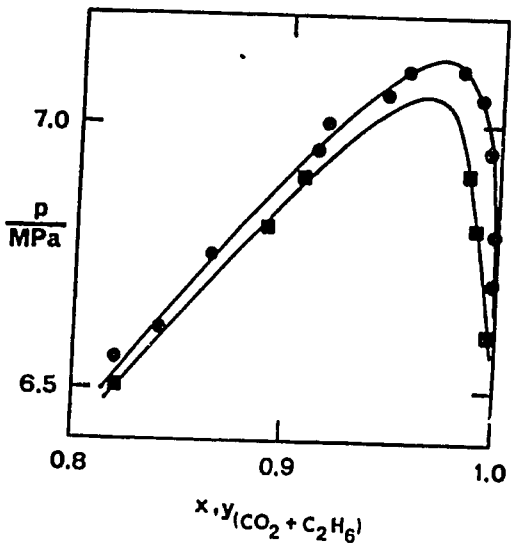

Figure 4. Vapour-liquid equilibria of the azeotropic mixture C_2H_6+CO_2 with limonene (●) and with cineole (■) at 303.2 K.

DISCUSSION

Azevedo et al. (1988) compared results obtained in the presently described apparatus with results of other authors. In particular, good agreement was reached with the gas phase solubilities of limonene in carbon dioxide presented by Stahl and Gerard (1985), in the short range of superposition of the two sets of data.

The results obtained in this work confirm the earlier conclusion of Azevedo et al.(1988) that limonene and cineole are readily soluble in supercritical carbon dioxide. But, although cineole is an ether and limonene a hydrocarbon, their thermodynamic behaviour is so similar that no selectivity towards any of them can be obtained. Figures 2 and 3 show very similar patterns

61

of phase behaviour in mixtures with supercritical carbon dioxide. The differences observed between the two mixtures are of the same order of magnitude of the combined uncertainties of our measurements.

Another attempt carried out in this work to devise a method of separation was the use of a mixed solvent. A mixture of carbon dioxide and ethane was used to investigate whether the presence of a hydrocarbon would increase the solubility of (hydrocarbon) limonene relatively to that of (ether) cineole.

Carbon dioxide and ethane form positive azeotropes that go up into the critical region. We selected a mixture of composition (0.232 mole fraction in ethane) very close to the critical azeotrope composition, assuming that this would minimize differences in the CO_2/C_2H_6 ratio between phases in equilibria containing the liquid solutes. Other advantages presented by the mixture relatively to pure carbon dioxide are the lower critical pressure, due to the much lower critical pressure of ethane, and also a lower critical temperature, induced by the presence of the azeotrope. Actually, although the critical temperatures of carbon dioxide and ethane are respectively 304.2 K and 305.5 K, the critical azeotrope occurs at a temperature of about 293 K.

Figure 4, however, shows that the presence of ethane does not introduce any meaningful difference between the solubilities of the two solutes.

ACKNOWLEDGEMENTS

For financial support the authors are grateful to J.N.I.C.T., Lisbon, Portugal, and to A.I.D., Washington, D.C., U.S.A.

REFERENCES

Azevedo, E.J.S.G., Matos, H.A., Nunes da Ponte, M., Simoes, P.C., 1988. Proc. Int. Symp. on Supercritical Fluids, Nice, Vol. I, 135-142.
Coppella, S.J., Barton, P., 1987, Supercritical Fluids, Edited by T.G. Squires, M.E. Paulaitis, ACS Symposium Series 329, 203-212.
Fredenslund A., Mollerup, J., 1974, J. Chem. Soc., Faraday Trans., 70: 1653-1660.
Stahl, E., Schilz, Z., 1976, Chem. Ing. Tech., 48: 773.
Stahl, E., Gerard, D., 1985, Perfumer & Flavorist, 10: 29-37.

68

The Journal of Supercritical Fluids 1989, 2, 97–105

Statistical Thermodynamics of Solid Solubilities in Supercritical Fluids — A One-Fluid Conformal Theory Approach

D. A. Jonah,† E. Gomes de Azevedo,* and M. Nunes da Ponte

Centro de Química Estrutural, Instituto Superior Técnico, 1096 Lisboa, Portugal

Received August 17, 1989; accepted in revised form November 28, 1989

Supercritical fluid extraction involves highly asymmetric mixtures at conditions close to the critical point. The thermodynamic modelling of these mixtures is therefore inconveniently described by the conventional methods, namely the analytical equations-of-state with conventional mixing rules (which are poorest in the near supercritical region).

Based on the one-fluid conformal solution theory, we present here a procedure to correlate (and ultimately to predict) the thermodynamic behavior in supercritical fluid extraction processes. The method described in this work allows the correlation (as well as interpolation and extrapolation) of solid solubilities in supercritical solvents at different pressures and temperatures.

Keywords: solubility, correlation, prediction, supercritical fluid, one-fluid conformal solution theory

INTRODUCTION

The application of supercritical fluids in industrially important separation processes of chemical components and in the processing of natural products has motivated, in recent years, large amounts of work in both the theoretical and the experimental aspects of supercritical fluid mixtures.

The design of separation processes involving these fluids requires the knowledge of transport and thermodynamic properties of the compressed fluid mixtures. The development of predictive modelling and correlation techniques which enable the quantitative understanding of the phase equilibria of the strongly asymmetric mixtures involved in supercritical fluid extraction processes are, therefore, of great importance.

The proximity to the critical region and the large differences in size, shape, and polarity commonly found in mixtures involving supercritical fluids, make the analytical equations-of-state with the conventional mixing rules inadequate to calculate the thermodynamic properties of these mixtures, namely to describe the solubilities of solids in supercritical solvents.

The modelling of solid solubilities in supercritical fluid solvents depend crucially on a good equation-of-state for the gaseous phase mixture. Once such an equation is available, the solute fugacity coefficient in the gas mixture can be calculated and the phase equilibrium equations solved for the solubility.

At moderate densities, that is, densities not close to the critical density of the gas, there is available the virial equation-of-state for mixtures, which is exact and with a well-known composition dependence. The only limitation to its application is the limited availability of experimental data, namely of cross-virial coefficients and of virial coefficients higher than the third.

At higher densities, however, it has been common practice to use empirical or semi-empirical equations-of-state for the pure fluids, whose parameters are then modified using mixing rules to make them applicable to mixtures. As pointed out by Prausnitz et al.,[1] the calculated solubility is sensitive not only to the equation-of-state used, but also to a large extent, to the mixing rules. Nonetheless, several reasonable correlations based on empirical equations-of-state and mixing rules have been obtained by the standard procedure of calculating solute fugacity coefficients in the gas phase from semi-empirical equations-of-state with chosen mixing rules. Examples are given in the works by Mackay and Paulaitis,[2] Kurnik et al.,[3] Johnston and Eckert,[4] and Wong et al.[5]

Alternative approaches include the mean-field lattice–gas model as developed by Kleintjens and Koningsveld.[6,7] This model provides useful physical insight; however, the

†Permanent address: Department of Mathematics, Fourah Bay College, University of Sierra Leone, Freetown, Sierra Leone, West Africa

0896-8446/89/0202-0097$4.00/0 © 1989 PRA Press

69

interaction constants involved must be obtained empirically. In most of the available methods, the solubility is extremely sensitive to the unlike pair interaction constant since the solution is highly nonideal.

In this paper, we wish to shift the emphasis from the properties of the gaseous mixture to those of the pure gaseous solvent, taking advantage of the ready availability of single-component properties as compared with mixture properties. The latter will enter the picture only through the residual solute chemical potential at infinite dilution. In the common approach, the most important mixture property is the solute partial molar volume, as it is required in the evaluation of the solute fugacity coefficient.

The feasibility of the approach presented here is a consequence of the fact that, in the majority of systems, the solid is sparingly soluble in the gas phase and therefore the gas mixture is a dilute mixture in which the solvent–solvent interactions play a dominant role. The method presented here is simple and correlates well the solubilities of solids in different supercritical solvents.

MOLECULAR THERMODYNAMICS OF SUPERCRITICAL FLUIDS

We consider a solid component a in equilibrium with a supercritical gaseous component b. The phase equilibrium equations are

$$f_a^{solid} = f_a^{vap} \tag{1}$$

and

$$f_b^{solid} = f_b^{vap} \tag{2}$$

where f_a and f_b are the fugacities of components a and b and the superscripts *solid* and *vap* refer to the solid and vapor phases, respectively.

Making the usual assumption of negligible solubility of the gas in the solid, the mole fraction, y_a, of the solid dissolved in the gas follows from eq 1

$$f_a^{*solid} = y_a \phi_a^{vap} P \tag{3}$$

where ϕ_a and P denote the fugacity coefficient of component a and the system pressure, respectively; in eq 3, the asterisk indicates a pure (solid) phase. Once the vapor phase is suitably modelled by an appropriate equation-of-state, the fugacity coefficient can then be readily calculated as a function of the (vapor) mole fraction (y_a), the system temperature (T), and pressure (P). Calculation of the solid solubility in the supercritical gas is now obtained through an iterative solution of eq 3.

The successful prediction and correlation of solid solubilities by this procedure depends to a large extent on the proper choice of mixing rules used in adapting the single component equation-of-state to a mixture situation. However, an alternative route to solid solubility calculation is provided by the fact that the gaseous mixture is dilute, which means that solute–solute interactions can be neglected. This assumption of diluteness is supported by the existing experimental data. With such an assumption, we may invoke a Henry's law-like relation for solubilities in a gas phase, for which the fugacity of the solute in the gas phase is taken as proportional to the solute's concentration. Explicitly, we have

$$f_a^{vap} = K_{ab} \times (\text{solute mole fraction}) \tag{4}$$

where K_{ab} denotes a generalized Henry's constant for solubility in any phase, resulting in a dilute mixture.

To take full advantage of the ready availability of single component properties, we may rewrite eq 4 in a more convenient form

$$f_a^{vap} = y_a f_b^* \exp\left(\frac{\mu_{ar}^{\infty} - \mu_{br}^*}{kT}\right) \tag{5}$$

where μ_{ar}^{∞} is the residual chemical potential of the solute a in an infinitely dilute mixture, μ_{br}^* is the residual chemical potential of the pure solvent b, f_b^* is the pure solvent fugacity, and k is the Boltzmann constant.

In writing eq 5, we have simply used the identities

$$\ln\left(\frac{K_{ab}}{\rho kT}\right) = \frac{\mu_{ar}^{\infty}}{kT} \tag{6}$$

and

$$\ln\left(\frac{f_b^*}{\rho kT}\right) = \frac{\mu_{br}^*}{kT} \tag{7}$$

where ρ is the number density of the pure solvent component b.

Making use of eq 1, we can now write for the solubility

$$y_a = \left(\frac{f_a^{*solid}}{f_b^{*vap}}\right) \exp\left(\frac{\mu_{br}^* - \mu_{ar}^{\infty}}{kT}\right). \tag{8}$$

We note that the right hand side of eq 8 is not mole fraction dependent. Therefore, the problem of calculating y_a is reduced to that of obtaining a suitable expression for the difference between the residual chemical potentials ($\mu_{ar}^{\infty} - \mu_{br}^*$). This can be done by using the framework of statistical mechanics.

STATISTICAL THERMODYNAMICS CONSIDERATIONS

A natural development for μ_{ar}^{∞} is a perturbation expansion, in which the reference system is taken as the pure solvent; then, μ_{br}^* is the zeroth order term. Up to the second term we have

10

$$\mu_{ar}^{\infty} = \mu_{br}^{*} + \langle \Delta U \rangle_{ps} - \beta/2 \langle (\Delta U - \langle \Delta U \rangle)^2 \rangle_{ps} + O(\beta^2) \tag{9}$$

where

$$\Delta U = \sum_{j>1} [u_{ab}^{(1,j)} - u_{bb}^{(1,j)}] . \tag{10}$$

In the above equation, $u_{ab}^{(1,j)}$ denotes the pair potential between a solute molecule a at the position r_1 and a solvent molecule b at r_j in the infinitely dilute mixture; $u_{bb}^{(1,j)}$ has an analogous meaning but for two solvent molecules. As usual, $\langle\ \rangle_{ps}$ denotes the canonical average over the pure solvent component.

Equation 9 follows by taking the infinite dilution limit of the corresponding expression for μ_{ar} at low dilution (see Jonah[8]). Equation 9 may also be obtained from Widom's[9] test-particle expression for the chemical potential.

The first order contribution, $\langle \Delta U \rangle_{ps}$, in eq 9 is thermodynamically accessible and can readily be expressed in terms of the residual internal energy and compressibility factor of the pure solvent for pair potentials of the Lennard–Jones type. However, the second order term is not thermodynamically accessible and needs to be approximated if it is to be expressed in terms of thermodynamic properties of the pure solvent. Such an approximate use of eq 9 has been applied by Jonah[10] in the correlation of solid solubilities in supercritical gases. An alternative and probably more convenient route to obtain μ_{ar}^{∞} is through a one-fluid mixture theory.

According to this theory (see, e.g., Scott[11]) the residual Helmholtz energy $A_r^{mix}(T, \rho, x_a)$ for the binary mixture at temperature T, density ρ, and of composition x_a, may be expressed in terms of the corresponding function A_{br}^{*} for a pseudo–pure component at reduced temperature (T_R) and reduced density (ρ_R) as follows:

$$\frac{A_r^{mix}(T, \rho, x_a)}{T} = \frac{A_{br}^{*}(T_R, \rho_R)}{T_R} \tag{11}$$

where

$$T_R = T \frac{\varepsilon_{bb}}{\varepsilon_m} \tag{12}$$

and

$$\rho_R = \rho \frac{\sigma_m^3}{\sigma_{bb}^3} . \tag{13}$$

In the above eqs, ε_m and σ_m are the molecular parameters for the pseudo-pure component.

In terms of the residual Gibbs energy (G_r^{mix}), the analogous relation to eq 11 is

$$\frac{G_r^{mix}(T, P, x_a)}{T} = \frac{G_{br}^{*}(T_R, P_R)}{T_R} \tag{14}$$

where T_R is still defined by eq 12 and P_R is given by

$$P_R = P \frac{\sigma_m^3}{\sigma_{bb}^3} \frac{\varepsilon_{bb}}{\varepsilon_m} . \tag{15}$$

Differentiation of eq 11 with respect to N_a (the number of solute molecules) at constant temperature, density, and N_b (the number of solvent molecules) leads to the desired expression for μ_{ar}

$$\frac{\mu_{ar}(T, \rho, x_a)}{RT} = \frac{\mu_{br}^{*}(T_R, \rho_R)}{RT} + \left(\frac{N}{\varepsilon_m} \frac{\partial \varepsilon_m}{\partial N_a}\right) \frac{U_{br}^{*}(T_R, \rho_R)}{RT} + \left(\frac{N}{\sigma_m^3} \frac{\partial \sigma_m^3}{\partial N_a}\right) z_{br}^{*}(T_R, \rho_R) . \tag{16}$$

Writing eq 16 for an infinitely dilute solution gives at once μ_{ar}^{∞}

$$\frac{\mu_{ar}^{\infty}(T, \rho)}{RT} = \frac{\mu_{br}^{*}(T_R, \rho_R)}{RT} + F_1 \frac{U_{br}^{*}(T_R, \rho_R)}{RT} + F_2 z_{br}^{*}(T_R, \rho_R) \tag{17}$$

where we have introduced the notations

$$F_1 = \lim_{x_a \to 0} \left(\frac{N}{\varepsilon_m} \frac{\partial \varepsilon_m}{\partial N_a}\right) = \left(\frac{N}{\varepsilon_m} \frac{\partial \varepsilon_m}{\partial N_a}\right)^{\infty} \tag{18}$$

and

$$F_2 = \lim_{x_a \to 0} \left(\frac{N}{\sigma_m^3} \frac{\partial \sigma_m^3}{\partial N_a}\right) \equiv \left(\frac{N}{\sigma_m^3} \frac{\partial \sigma_m^3}{\partial N_a}\right)^{\infty} . \tag{19}$$

Equations 16 and 17 are exact relations within the framework of the one-fluid conformal solution theory. Approximations are introduced only through the mixing rules relating ε_m and σ_m to the corresponding pure component parameters and those pertaining to the solute–solvent interactions. Thus, the successful performance of eq 17 very much depends on how well F_1 and F_2 are evaluated. The most commonly used mixing rules are the so-called van der Waals–1 (VDW–1) mixing rules, which lead to expressions for F_1 and F_2 exclusively in terms of the molecular parameter ratios σ_{ab}/σ_{bb} and $\varepsilon_{ab}/\varepsilon_{bb}$.

The VDW–1 mixing rules are known to be inadequate and several efforts have been made to improve them (Mansoori and Ely;[12] Deiters;[13] Hamad and Mansoori;[14] Meyer[15]). It would appear from these several modifications of the VDW–1 mixing rules that it is necessary to intro-

71

duce some state dependence to reproduce the (real or simulated) experimental data. As a consequence, F_1 and F_2 become functions of temperature and density, in addition to the molecular parameter ratios. For example, Meyer's version leads to a state dependence for F_1 and F_2 only through the density. However, the version of Mansoori and coworkers[12,14] indicates that F_1 and F_2 are both temperature and density dependent. In subsequent sections, we shall attempt to have some indications about the relative strengths of the temperature (and density) dependence of F_1 and F_2.

There is a very interesting relationship between eqs 9 and 17 for the residual infinite-dilution solute chemical potential. In eq 9, we have the leading terms of an exact infinite series expansion for μ_{ar}^{∞} in terms of reciprocal temperature. As already mentioned, we also have in eq 17 an exact expression (within the framework of the conformal solution theory) for μ_{ar}^{∞}, but in closed form.

The first order term $\langle \Delta U \rangle_{ps}$ in eq 9 for the case of the Lennard–Jones pair potentials may be expressed in terms of the two pure solvent thermodynamic properties occurring in eq 17, but with coefficients which are functions exclusively of the molecular parameter ratios. The closed expression in eq 17 may be regarded as the sum of the infinite series in eq 9 – provided the series is convergent – when the correct mixing rules are introduced and the infinite dilution limit is taken. Unfortunately, we do not know what the correct mixing rules are although good approximations can be given as exemplified by the choices of Hamad–Mansoori, Meyer, and Deiters. The effect of these choices from the point of view of approximating the sum of the series in eq 9 is rather interesting. Effectively, the series is truncated after the term $\langle \Delta U \rangle_{ps}$ and the remainder is taken into account by readjustment of the coefficients of U_r^*/RT and z_r^*, which are now made to be, not only functions of the potential parameters, but also state-dependent. In other words, the effect of a good mixing rule is that of telescoping the infinite series of eq 9 into its first order perturbation correction term.

CALCULATION OF SOLID SOLUBILITIES

Since we already have an expression for $(\mu_{ar}^{\infty} - \mu_{br}^{*})$, the calculation of the solubility, y_a, is straightforward. Substitution of eq 17 in eq 8 gives

$$y_a = \left(\frac{f_a^{*solid}}{f_b^{*vap}}\right) \exp\left[-F_1(s, t; T, \rho)\frac{U_{br}^*}{RT} - F_2(s, t; T, \rho)\, z_{br}^*\right] \tag{20}$$

where we have introduced the notations

$$s \equiv \frac{\varepsilon_{ab}}{\varepsilon_{bb}},$$

and

$$t \equiv \frac{\sigma_{ab}^3}{\sigma_{bb}^3}. \tag{21}$$

In writing eq 20, we have assumed that the correct mixing rules are temperature- and density-dependent.

The fugacity of the pure solid at temperature T and pressure P is given by the expression (Prausnitz et al.[1])

$$f_a^{*solid} = f_a^{*sat} \exp\left[v_a^{solid}(P - P_a^{sat}) / RT\right] \tag{22}$$

where v_a^{solid} is the molar volume of the solid; f_a^{*sat} and P_a^{sat} are, respectively, the saturated fugacity and pressure of the solid. Since $P_a^{sat} \ll P$, eq 22 takes the simpler form

$$f_a^{*solid} = f_a^{*sat} \exp(P v_a / RT)\,. \tag{23}$$

Equation 20 can now be rewritten in a more convenient form

$$\ln[f_a^{*solid} / (y_a f_b^{*vap})] = F_1(s, t; T, \rho)\frac{U_{br}^*}{RT} + F_2(s, t; T, \rho)\, z_{br}^*\,. \tag{24}$$

There are at least two ways in which we can use eq 24 to study solid solubilities in supercritical gases. One approach is to treat the molecular parameter ratios, s and t, as adjustable parameters. This approach would require a mixing rule to obtain F_1 and F_2 explicitly in terms of its arguments.

A second alternative is to treat F_1 and F_2 as adjustable parameters. This approach doesn't require any mixing rule. A proper molecular investigation would certainly require the first approach or some variant of it. However, in this paper we shall opt for the second approach, deferring a detailed molecular investigation to a later paper.

Meyer's mixing rules based on a comparison between exact hard-sphere equations-of-state for pure component and mixtures, add a density-dependent correction term to the well-known VDW–1 mixing rule. Use of Meyer's mixing rules leads, therefore, to density-dependent F_1 and F_2, but not to temperature dependence. Since tests against simulated and real experimental data show encouraging success, we believe that F_1 and F_2 might be weakly temperature dependent. This hypothesis can be easily tested by plotting at constant densities

$$Y \equiv \frac{1}{z_{br}^*}\ln[f_a^{*solid}/(y_a f_b^{*vap})] \quad \text{versus} \quad U \equiv \frac{U_{br}^*}{z_{br}^* RT} \tag{25}$$

where f_a^{*solid} is given by eq 23. A weak temperature dependence for F_1 and F_2 would result in linear graphs.

To test whether this linearity is obtained, we have examined several solubility data of solids in supercritical carbon dioxide and ethylene. Figure 1 shows representative plots calculated for the system adamantane/CO_2 (at ρ =

12

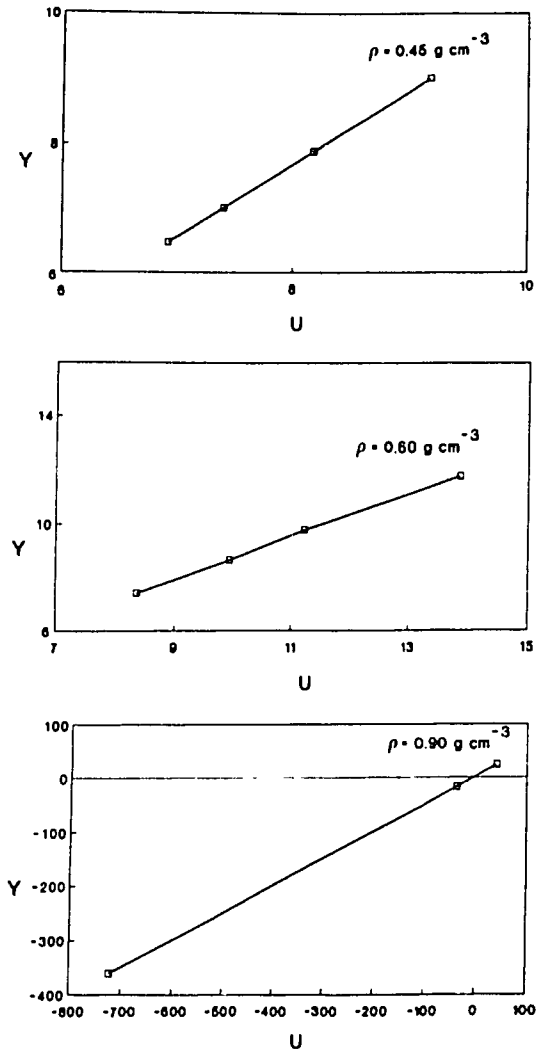

Figure 1. Quantity Y as function of U, as defined by eq 25, for the system adamantane/CO_2 at densities ρ = 0.45, 0.60, and 0.90 g cm^{-3}. Linearity is observed which indicates weak temperature dependence of F_1 and F_2, defined by eqs 18 and 19, respectively.

0.45, 0.60, and 0.90 g cm^{-3}). Similar plots were obtained for octacosane, squalane, 2,3- and 2,6-dimethylnaphthalene, benzoic acid, and phenanthrene in CO_2 and C_2H_4, but these are not shown. All these graphs reveal a weak temperature dependence for F_1 and F_2.

On the other hand, Meyer's mixing rules would lead to a linear density dependence for F_1 and F_2. Figure 2 shows a few representative plots (also for the system adamantane/CO_2) of F_1 and F_2 against density. As can be easily seen (from these and similar graphs, which are also not

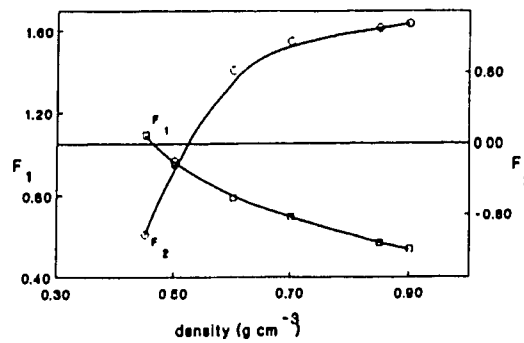

Figure 2. Dependence of F_1 and F_2 with density for the system adamantane/CO_2. Linearity is not observed.

shown), this linear dependence with density is not confirmed — at least not over the finite range of densities tested here.

DATA REDUCTION

There are at least three ways in which eqs 20–24 can be employed in a useful data reduction process:

1) Using the constant density plots of Y against U to smooth experimental data. More importantly, these plots can be used for extrapolation and interpolation of solid solubilities, y_a, between two temperatures, T_1 and T_2, at a given density $\rho = \rho_0$, when we know y_a for the states (T_1, ρ_0) and (T_2, ρ_0). Tables I and II illustrate this procedure for a couple of systems. For comparison, the same tables give in the last column values obtained by, respectively, direct linear interpolation and extrapolation of the given solubilities.

2) Since in a narrow range of densities, F_1 and F_2 are effectively linear functions of density, it should be possible to interpolate within a rectangular grid with vertices (T_1, ρ_1), (T_1, ρ_2), (T_2, ρ_1), and (T_2, ρ_2) for small values of $|\rho_1 - \rho_2|$.

Table III[††] illustrates such an interpolation for the system adamantane/carbon dioxide. Details of this calculation are presented in Appendix 1. For comparison, we have also obtained solubilities for these same states by direct linear interpolation; for example, we first interpolate linearly for y_a between [(T_1, ρ_1) and (T_2, ρ_1)], and [(T_1, ρ_2) and (T_2, ρ_2)] to obtain values at states (T, ρ_1) and (T, ρ_2). Finally, we interpolate linearly between these two states for y_a at state (T, ρ).

3) We can construct a solubility–temperature–density (y_a–T–ρ)-surface by fitting a set of (F_1, ρ)- and (F_2, ρ)- val-

[††] Using linear interpolation from (ln c_a, ρ)–plots instead of (c_a, ρ)–plots as given in Tables I to III, would make no difference in the results of Tables I and II (interpolation and extrapolation at constant density) and would give results which are not better than those presented in Table III.

The Journal of Supercritical Fluids, Vol. 2, Nos. 2&3, 1989

TABLE I

Comparison of Experimental Solubilities With Those Obtained by Interpolation According to Eq 20 and Those Obtained by Ordinary Interpolation, for Given Solubilities at States (T_1, ρ) and (T_2, ρ). Densities (ρ) in g cm^{-3}, Temperatures (T) in Kelvin, and Solubilities (c_a) in g cm^{-3} or in Mole Fractions (y_a).

ρ	T_1	T_2	Interpolated Temperature	Exp. c_a (× 10^3)	Interpolated c_a (× 10^3) eq 20	Linear
adamantane/CO_2 (data from Swaid et al.[16])						
0.5	343	402	362.5	10.5	11.0	15.1
			382.0	19.7	19.7	24.1
0.7	343	402	362.5	28.3	28.2	36.1
			382.0	48.3	47.1	56.0
0.9	343	382	362.5	38.0	39.7	43.7
2.6-dimethylnaphthalene/C_2H_4 (data from Kurnik et al.[3])						
				Exp. c_a (× 10^3)	Interpolated y_a (× 10^3) eq 20	Linear
0.336	308	328	318	5.4	5.9	6.8
0.364	308	328	318	9.0	9.3	11.7
0.384	308	328	318	12.8	12.9	16.7

TABLE II

Comparison Between Solubilities Extrapolated to Temperature T According to Eq 20 With Solubilities (c_a Expressed in g cm^{-3} or in Mole Fraction y_a) Obtained by Linear Extrapolation for Given Solubilities at State (T_1, ρ) and (T_2, ρ). Temperatures in Kelvin and Densities in g cm^{-3}.

ρ	T_1	T_2	Extrapolated Temperature	Exp. c_a (× 10^3)	Extrapolated c_a (× 10^3) eq 20	Linear
adamantane/CO_2 (data from Swaid et al.[16])						
0.5	343	362.5	382	19.7	17.6	14.9
			402	33.3	28.5	19.4
0.7	343	362.5	382	48.3	47.2	40.4
			402	76.34	76.2	52.8
0.9	343	362.5	382	60.2	55.5	48.8
2.6-dimethylnaphthalene/C_2H_4 (data from Kurnik et al.[3])						
				Exp. c_a (× 10^3)	Interpolated y_a (× 10^3) eq 20	Linear
0.336	308	318	328	10.6	8.9	7.8
0.364	308	318	328	18.4	17.3	13.0
0.384	308	318	328	26.8	26.6	19.1

TABLE III

Comparison of Solubilities for the System Adamantane/CO_2 Obtained by Direct Linear Interpolation with Solubilities Interpolated at State (T, ρ) Within a Rectangular Grid with Vertices (T_1, ρ_1), (T_2, ρ_1), (T_1, ρ_2), and (T_2, ρ_2) Using Eq 20. Densities (ρ) in g cm^{-3}, Temperatures (T) in Kelvin, and Solubilities (c_a) in g cm^{-3}.

ρ_1	ρ_2	T_1	T_2	T	ρ	Exp. c_a (× 10^3)	Interpolated c_a (× 10^3) eq 20	Linear
0.60	0.65	343	402	362.5	0.625	21.7	22.6	28.7
				382.0	0.625	36.8	38.1	44.8

TABLE IV
Solute (Adamantane) and Solvent (Carbon Dioxide) Properties at Selected States

T (K)	CO_2					Adamantane	
	ρ (g cm^{-3})	P (bar)	f (bar)	$-U_r^*/RT$	$-z_r^*$	v (cm^3 mol^{-1})	P^{sat} ($\times 10^3$ bar)
343	0.680	210	102.5	5.108	0.5233	0.127	4.33
343	0.906	500	177.5	6.648	0.1485		
362.5	0.695	290	143.5	4.819	0.3907	0.127	12.09
362.5	0.893	600	251.2	6.095	0.0184		
382	0.442	200	129.9	3.000	0.3730	0.127	30.35
382	0.703	370	194.2	4.534	0.2708		
382	0.821	550	268.9	5.244	0.0714		
402	0.457	240	160.0	2.867	0.3086	0.127	71.06
402	0.725	475	268.0	4.353	0.1369		

ues to a suitable function of ρ. In this way, we were able to construct such a (y_a–T–ρ) surface for the system adamantane/carbon dioxide, by fitting a set of (F_1, ρ) and (F_2, ρ) values to quadratic functions of density. [Appendix 2 summarizes the principal steps leading to the construction of a (y_a–T–ρ) surface]. Explicitly, we have for y_a the following expression:

$$y_a = \left(\frac{P_a^{sat}}{f_b^{*vap}}\right)\exp\left(\frac{Pv_a^{solid}}{RT} - F_1(\rho)\frac{U_{br}^*}{RT} - F_2(\rho)\, z_{br}^*\right) \quad (26)$$

with

$$F_1(\rho) = A + B\rho + C\rho^2 \quad (27)$$

and

$$F_2(\rho) = A' + B'\rho + C'\rho^2 . \quad (28)$$

Table IV lists relevant thermodynamic properties of pure carbon dioxide and adamantane at selected states. These values were used to calculate (from eq 26) the concentration c_a‡ of adamantane in supercritical carbon dioxide which are compared in Table V with experimental values. This comparison is shown in graphical form in Figure 3 for 343 K and 382 K. As shown, the agreement between calculated and experimental results is good, within the range of temperature and density for which the surface (y_a–ρ–T) was constructed.

‡ The relationship between solute concentration, c_a, and mole fraction, y_a, is given by

$$c_a = \frac{y_a \rho_b^* M_a}{M_b(1 - y_a)}$$

where ρ_b^* refers to the density of the pure solvent gas and M_a and M_b are the molecular weights of the solute a and of the solvent b, respectively.

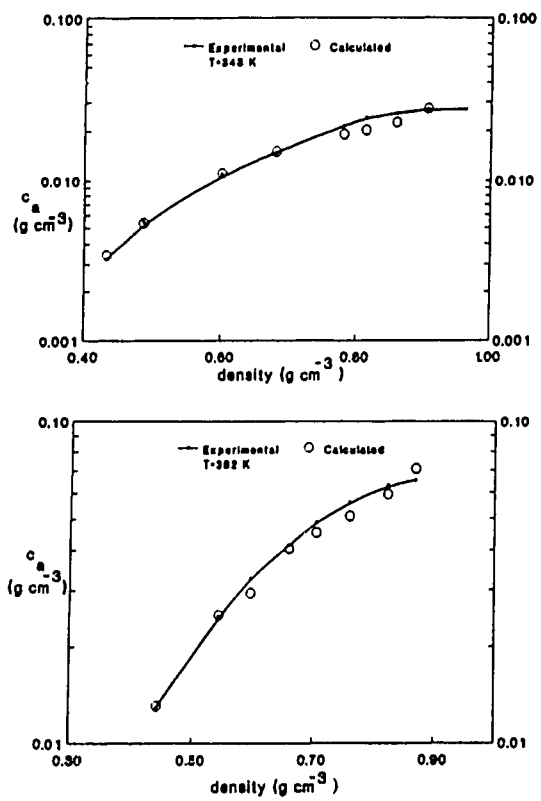

Figure 3. Experimental (Swaid et al.[16]) and calculated (this work, from eqs 26 and 29) solubilities of solid adamantane in supercritical carbon dioxide at 343 and 382 K.

EXTENSION TO THE CALCULATION OF SOLUBILITIES OF LIQUIDS

Without going into details, we briefly observe that with suitable replacements in eqs 20 and 24, namely by replacing f_a^{*solid} by f_a^{liq}, these equations may still be used, provided the liquid is sparingly soluble in the supercritical

TABLE V
Experimental (Swaid et al.[16]) and Calculated (from Eqs 26 and 29) Solubilities of Adamantane in CO_2

P (bar)	ρ (g cm^{-3})	$c_a \times 10^3$ (g cm^{-3}) Exp.	Calc.
T = 343 K (P_a^{sat} = 4.33 × 10^{-1} bar)			
135	0.4318	3.23	3.41
145	0.4848	5.44	5.35
175	0.6000	10.95	11.04
210	0.6800	14.90	14.97
290.5	0.7800	21.38	18.93
330	0.813	24.00	20.12
400	0.858	25.57	22.40
500	0.906	27.10	27.16
660	0.962	26.93	41.87*
T = 362.5 K (P_a^{sat} = 12.09 × 10^{-1} bar)			
200	0.5378	13.74	14.05
290	0.6950	27.74	27.00
360	0 7630	35.18	31.44
400	0.7925	37.53	33.42
500	0.8496	41.47	38.81
600	0.8926	42.74	46.72
750	0.9423	42.29	67.78*
T = 382 K (P_a^{sat} = 30.35 × 10^{-1} bar)			
200	0.442	12.81	12.91
246	0.543	25.00	25.11
277	0.595	32.54	29.35
326	0.659	41.58	40.41
370	0.703	48.80	45.43
440	0.758	56.11	51.05
550	0.821	63.15	59.31
660	0.868	65.53	70.79
T = 402 K (P_a^{sat} = 71.06 × 10^{-1} bar)			
172	0.3132	8.35	7.73*
211	0.3988	18.66	16.62*
228	0.4337	22.02	21.74*
240	0.457	25.79	25.75
259.5	0.492	31.82	32.20
332	0.597	51.96	53.68
475	0.725	82.26	76.10
600	0.795	94.48	89.06

* Values calculated for states outside the range of temperature and density for which surface is constructed: $0.45 \leq \rho \leq 0.90$.

gas. However, contrary to what is observed for solids, there is usually an appreciable solubility of the supercritical gas in the liquid. Hence, f_a^{liq} is a function of the mole fraction of the gas dissolved in the liquid. Once we have modelled this composition dependence of the liquid phase fugacity, the procedure can be carried out as for solid solubilities. In another paper, we shall address the subject of liquid solubilities.

CONCLUSIONS

The present study indicates that the one-fluid conformal solution theory can be successfully applied to the correlation, interpolation, and extrapolation of solid solubilities in supercritical fluids. Of particular importance is the fact that linear isochores can be obtained, thus leading to the possibility of interpolating and extrapolating sparse data along constant density paths; further, with a few isochores selected over a given density range, it becomes possible to construct a temperature–density–solubility surface valid for that range.

The successful use of the one-fluid conformal solution theory predictively, on the molecular level, depends crucially on the availability of a good combining rule and on the availability of a good mixing rule. Given these two prerequisites, we may expect to be able to predict the solubilities of solids in supercritical fluid solvents.

ACKNOWLEDGMENTS

For financial support the authors are grateful to A.I.D., Washington D.C., U.S.A.

REFERENCES

(1) Prausnitz, J. M.; Lichtenthaler, R. N.; Gomes de Azevedo, E. J. S. *Molecular Thermodynamics of Fluid-Phase Equilibria*, 2nd Ed.; Prentice-Hall: Englewood Cliffs, New Jersey, 1986.
(2) Mackay, M. E.; Paulaitis, M. E. *Ind. Eng. Chem. Fund.* **1979**, *18*, 149.
(3) Kurnik, R. T.; Holla, S. J.; Reid, R. C. *J. Chem. Eng Data* **1981**, *26*, 47.
(4) Johnston, K. P.; Eckert, C. A. *AIChE J.* **1981**, *27*, 773.
(5) Wong, J. M.; Pearlman, R. S.; Johnston, K. P. *J. Phys Chem.* **1985**, *89*, 2671.
(6) Kleintjens, L. A.; Koningsveld, R. *Colloid & Polym. Sci.*, **1980**, *258*, 711; *Ibid., J. Electrochem. Soc.*, **1980**, *127*, 2352; *Ibid., Sep. Sci. & Technol.*, **1982**, *17*, 215.
(7) Kleintjens, L. A. *Fluid Phase Equil.* **1983**, *10*, 183.
(8) Jonah, D. A. *Int. J Thermophys.* **1986**, *7*, 935.
(9) Widom, B. *J. Chem. Phys.* **1963**, *39*, 2808.
(10) Jonah, D. A. *Chem. Eng. Commun.* **1989**, (in press).
(11) Scott, R. L. *Physical Chemistry – An Advanced Treatise. Liquid State*, Vol. VIII, Academic Press: New York, 1971.
(12) Mansoori, G. A.; Ely, J. F. *J. Chem. Phys.* **1985**, *82*, 406.
(13) Deiters, U. K. *Fluid Phase Equil.* **1987**, *33*, 267.
(14) Hamad, E. Z.; Mansoori, G. A. *J. Chem. Phys.* **1987**, *87*, 6046.
(15) Meyer, E. C. *Fluid Phase Equil.* **1988**, *41*, 19.
(16) Swaid, I.; Nickel, D.; Schneider, G. M. *Fluid Phase Equil.* **1985**, *21*, 95.

APPENDIX 1

INTERPOLATION OF SOLID SOLUBILITIES

In the example presented in Table III for the system adamantane/CO_2, solubilities are given at states (T, ρ) represented by (343, 0.60), (343, 0.65), (402, 0.60), and (402, 0.65) where temperatures are in Kelvin and densities in g cm^{-3}; the solubility being calculated for the states (362.5, 0.625) and (382, 0.625).

To accomplish this interpolation, we first use the given data to obtain $F_1(\rho)$ and $F_2(\rho)$ at densities ρ_1 and ρ_2.

Thus, we obtain $F_1(0.60) = 0.8146$; $F_1(0.65) = 0.7471$; $F_2(0.60) = 0.6060$; and $F_2(0.65) = 1.003$.

By linear interpolation, we now obtain F_1 and F_2 at density 0.625 g cm^{-3}. Thus we find, $F_1(0.625) = 0.7809$ and $F_2(0.625) = 0.8045$.

The solubilities, y_a, for the states (362.5, 0.625) and (382, 0.625) are now calculated using eq 20. From these values, concentrations, c_a, are obtained from eq 29; they are presented in Table III.

APPENDIX 2

CONSTRUCTION OF THE (y_a–T–ρ) SURFACE

The construction of the (y_a–T–ρ) surface is performed from the following steps:

Step 1.

We start by choosing a density ρ_0^* and then calculate Y and U (as defined by eq 25) at this density and the various temperatures at which experimental solubility isotherms are available.

The input thermodynamic data for the pure components are the saturated vapor pressure and molar volume of the pure solid and the fugacity, the residual internal energy, and compressibility factor of the pure solvent gas.

Step 2.

With this data, we make a least-square fit of the calculated ($Y - U$) values to the equation

$$Y = a + bU$$

and identify a and b as

$$a \equiv F_2(\rho)$$

and

$$b \equiv F_1(\rho)\,.$$

Step 3.

Repeat steps 1 and 2 for other densities, $\rho_0^* = \rho_1, \rho_2$, etc.

Step 4.

Finally, we fit the set of (F_1, ρ)- and (F_2, ρ)-values so obtained to quadratic functions, as given by eqs 27 and 28. For the system adamantane/CO_2, the values obtained for the fitting constants of these equations are

$$A = 2.417533 \qquad A' = -10.99275$$

$$B = -3.893446\ \text{cm}^3\,\text{g}^{-1} \qquad B' = 31.20106\ \text{cm}^3\,\text{g}^{-1}$$

$$C = 2.004615\ \text{cm}^6\,\text{g}^{-2} \qquad C' = -19.55385\ \text{cm}^6\,\text{g}^{-2}.$$

We observe in this fitting process, that the states (generally the high density states) at which $|z_{br}^*| \ll 1$ can be given a smaller weight compared to other states, in fitting F_2, since this coefficient need not be known accurately.

Application of Supercritical Fluid Extraction to the Purification of Eucalyptus Oil

P.C. Simões, M. Nunes da Ponte, H. Matos(*), and E. Gomes de Azevedo(*)

Faculdade de Ciencias e Tecnologia, Universidade Nova de Lisboa P-2825 Monte de Caparica, Portugal, and (*) Centro de Quimica Estrutural, Instituto Superior Tecnico, P-1096 Lisboa, Portugal

Introduction

High solubilities of essential oils in supercritical fluids have been reported by several authors /1,2/. However, when dealing with complex mixtures, the main problem may be selectivity of extraction.

Eucalyptus oil has 1,8-cineole as its main component, mixed with smaller quantities of terpenic hydrocarbons, like pinenes and d-limonene. This last component is the most difficult to separate from cineole, due to the similarity in vapour pressures, that rules out distillation as a feasible separation process in this case. For example, their normal boiling points differ by 2°C only.

Results and Discussion

In this work, we began by examining the selectivity of some supercritical fluids towards the components of eucalyptus oil. Pure carbon dioxide, a quasi-azeotropic mixture of carbon dioxide and ethane, and pure ethene (ethylene) were examined in succession. The first two fluids were not selective /3,4/. With ethene, liquid-liquid-vapour equilibrium appeared at temperatures above the critical temperature of the pure solvent. As an example, Figure 1 shows the pressure-composition diagram showing the phase equilibria behavior of the mixture of d-limonene with supercritical ethene at 15, 25 and 35°C.

At the lower temperatures there is a three-phase line which indicates the coexistence of three phases in equilibrium: a gas, a limonene-rich liquid phase and a ethane-rich liquid phase. These measurements were made in a high-pressure experimental apparatus (previously described /4/) consisting mainly in a static vapor-liquid

equilibrium stainless steel cell.

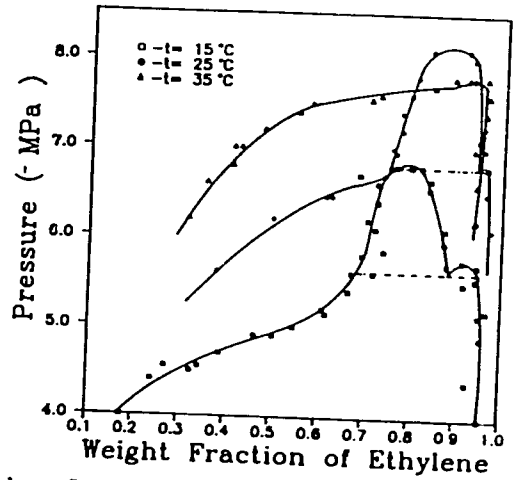

Figure 1: Pressure-composition diagram for the system d-limonene+ethene at 15, 25, and 35°C.

This three-phase behavior was confirmed by observation in a high pressure visual cell provided with borosilicate glass windows 15 mm thick, which was used for detailed measurements of phase equilibria in the critical and three-phase regions.

The resulting phase diagrams might be included in either Type III or V of the classification of van Konynenburg and Scott /5/. Our experimental results were supported by calculations using the Peng-Robinson equation of state. Using conventional mixing rules and one binary interaction parameter (k_{AB}=0.05) regressed from the fitting of vapor-liquid equilibrium data, we calculated the pressure-temperature projection for this binary. Figure 2 shows typical calculations for the pressure-temperature projection of d-limonene+ethene system, which are in reasonable agreement with our experimental data.

Similar studies for the system cineole with supercritical ethene indicate that there are significative differences between the

solubilities of cineole and of d-limonene, in a narrow range of pressures and at temperatures around 15°C. This feature opens up new possibilities in the design of a separation process involving terpene based essential oils. Toward this end, a continuous countercurrent extraction unit is being operated to examine the feasibility of obtaining high purity cineole by purification of eucalyptus oil with supercritical ethene. This unit is schematically shown in Figure 3 .

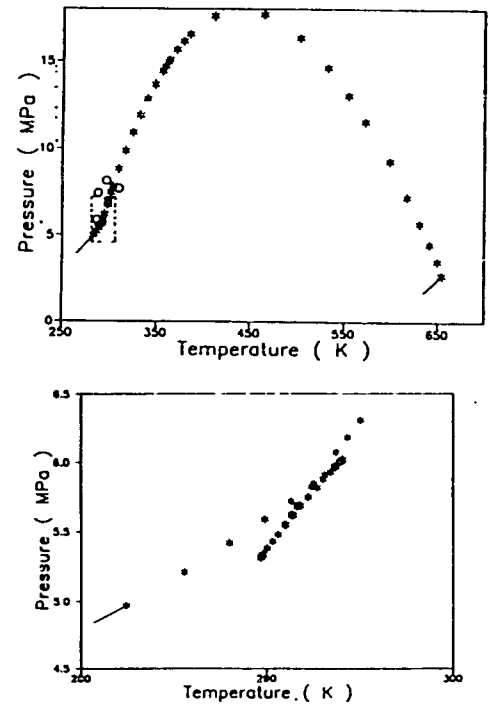

Figure 2: Experimental (O) and calculated (from Peng-Robinson equation of state with k_{AB}=0.05) pressure-temperature projection for the system d-limonene+ethene. The area marked above is shown enlarged in the bottom figure.

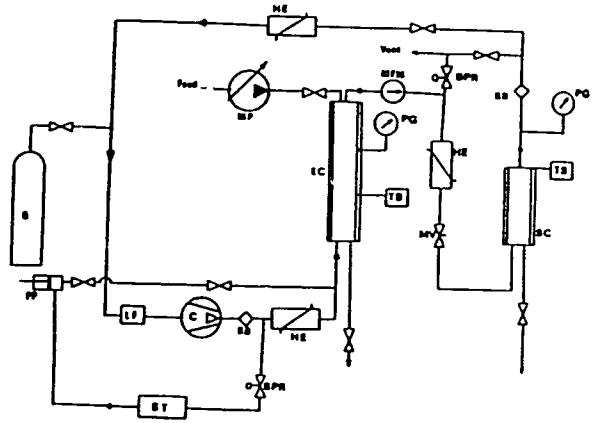

Figure 3: Flow diagram of the continuous countercurrent extraction apparatus. BPR: back pressure regulator; C: compressor; EC: extraction column; G: gas cylinder; HE: heat exchanger; LF: line filter; MFM: mass flowmeter; MP: metering pump; PG: pressure gauge; PP: piston pump; RD: rupture disk; SC: separation column; TS: temperature sensor;

It has two one-meter high pressure columns of 2.5 cm internal diameter, filled with structured metallic packing from Sulzer and is operated at temperatures between 12 and 15°C and pressures between 5.5 and 6.5 MPa. In addition to the separation studies, this equipment will be also used to obtain transport data, namely mass transfer coefficients and rates, and solvent loadings. It will also be studied the influence in the extraction efficiency of several parameters, namely pressure, temperature, and solvent rate.

Acknowledgements

For financial support the authors are grateful to AID, Washington DC, USA, and to NATO (Research Grant No. 328/80 and Science for Stability Programme), Brussels, Belgium.

References

/1/ E. Sthal, D. Gerard, Perfumer & Flavorist, 1985, 10: 29-37.

/2/ S. J. Copella, P. Barton, Supercritical Fluids, M.E. Squires, M.E. Paulaitis (Eds.), A.C.S. Symposium Series 329, 203-212.

/3/ H. Matos, E. Gomes de Azevedo, P.C. Simões, M. Nunes da Ponte, Proc. Int. Symposium on Supercritical Fluids, 1988, 135-142, Nice, France.

/4/ H. Matos, E. Gomes de Azevedo, P.C. Simões, M. T. Carrondo, M. Nunes da Ponte, Fluid Phase Equilibria, 1989, 52: 357-364.

/5/ P. H. Konynenburg, R. L. Scott, Phil. Trans. Roy. Soc., 1980, 298: 495-540.

On the application of supercritical fluid extraction to the deacidification of olive oils

M. Gonçalves, A.M.P. Vasconcelos, E.J.S. Gomes de Azevedo[a], H.J. Chaves das Neves and M. Nunes da Ponte
Departamento de Química, Faculdade de Ciências e Tecnologia, Universidade Nova de Lisboa, 2825 Monte da Caparica, Portugal

[a] Permanent address: Centro de Química Estrutural- Instituto Superior Técnico - 1096 Lisboa - Portugal

ABSTRACT

Application of supercritical fluid extraction to deacidify olive oils and olive husk oils has been subject to conflicting reports in the recent literature. In particular, basic data, like solubilities in supercritical carbon dioxide of some key compounds, vary wildly from author to author. In this work, we measured the solubilities of substances chosen for their importance in that extraction process, namely pure glycerol trioleate, the most abundant triglyceride in olive oil, and of a husk oil with a high acid content. Our results agree well with some of the previous reports on this subject. These are a trustworthy data base from which we may conclude that supercritical deacidification of olive oils is technically feasible.

1. INTRODUCTION

The use of supercritical fluid extraction in the vegetable oil industry has been suggested by several authors. For example, Friedrich et al. (1) and List et al. (2) compared the composition and stability of vegetable oils either obtained by supercritical carbon dioxide (SC-CO_2) extraction or recovered and purified by conventional methods. Stahl and collaborators (3-5) performed extensive studies of the solubilities of soybean oil up to very high pressures.

Vegetable oils have two major groups of constituents: triglycerides and free fatty acids. The solubilities in SC-CO_2 of pure compounds belonging to each of these classes have been reported in several literature references (6-9); unfortunately, lack of agreement between the various reports is still quite frequent, reflecting the need for additional work to be performed in this field. The accurate knowlege of these solubilities is an useful reference to the studies of supercritical fluid extraction applied to mixtures. Processes for deacidification and deodorization of natural fats and oils have actually been described in patents by Zosel (10) and by Coenen and Kriegel (11). Brunner and Peter (12) describe a deacidification method of palm oil using supercritical carbon dioxide as solvent and ethanol as entrainer.

Olive oil is a vegetable oil extracted by mechanical means from olives. Large quantities of oil are unsuitable for immediate consumption, due to a high free fatty acid content, and require refining. Conventional refining processes, however, may alter the

nutritional qualities of the oil, resulting in a lower price product. On the other hand, about 15% of the triglyceride content of olives remain trapped in the solid matrix, from where it is usually extracted with organic solvents. The end product is husk oil, which has a triglyceride composition slightly different from olive oil, and a much higher acid content.

Brunetti et al. (7) have recently suggested the use of SC-CO_2 extraction as a deacidification method of olive and husk oils; however, their data of solubilities of the pure components are in notorious disagreement with other results reported in the literature, like those of Chrastil (8) and King et al. (6). On the other hand, Di Giovacchino et al. (13) report preliminary measurements that seem to show that SC-CO_2 is not selective towards the free fatty acids present in olive oil.

In this work, we try and contribute to sort out between these conflicting results. We were concerned with two different aspects of the extraction of olive oils with SC-CO_2 : a) measurement of the solubility of pure compounds that are frequently found in these oils; b) evaluation of the selectivity of SC-CO_2 towards components of the oil that are usually removed by various methods in order to improve its quality .

We present measurements of the solubility in SC-CO_2 of a pure triglyceride - glycerol trioleate, usually known as triolein, the main component of olive oil - and compare our results with analogous results from other authors.

Additionally, the solubility behaviour of triglycerides and free fatty acids present in a husk oil of high acidity was investigated to evaluate the possibility of their separation by SC-CO_2 extraction.

Finally, the SC-CO_2 extraction of husk oil directly from the corresponding solid (husk flakes) was also performed and results are compared with similar data of King et al. (6) for rapeseed.

2. EXPERIMENTAL

2.1 MATERIALS

The CO_2 used in this work was 99.5 % (w/w) pure and supplied by Air Liquide,and glycerol trioleate (triolein) was 99% (w/w) pure, purchased from SIGMA. All solvents used in the chromatographic analysis were of analytical grade and obtained from E. MERCK. The husk flakes were milled to 0.5 to 1.5 mm thickness prior to use.

2.2 METHODS

2.2.1 Solubilities in supercritical Carbon Dioxide

The solubility measurements were performed in the apparatus schematically shown in figure 1. This is an improved version of the one used in previous studies (14), and is similar to the apparatus described by Matos et al. (15).

The main piece of equipment is a static vapour-liquid equilibrium cell, of approximately 30 cm^3 , immersed in a thermostated water bath.

A typical experiment starts with filling of the cell, at atmospheric pressure, with a small amount (about 2.5 cm^3), of liquid (crude husk oil or triolein) or solid (husk flakes). The CO_2 is then pressurized by a diaphragm compressor into the cell trough valves 2 and 3. After about 60 minutes of stirring (using a magnetic bar) and about the same time of rest, the pressure is read on a Bourdon tube manometer, with an accuracy of ± 100 kPa, and the temperature is measured with a mercury thermometer of 0.1 K precision. A sample is then taken from the top of the cell.

The samples are collected by depressurization and expansion trough valve 4 into a glass trap connected to a large steel bottle of calibrated volume, in the thermostated bath . When the valve is open, the solute condenses in the cold trap, while the solvent gas expands into the steel bottle (with a volume of approximately 1 dm^3 , calibrated to ± 0.1 cm^3). The pressure of the gas is read in a mercury manometer with a precision cathethometer, and is used to calculate the amount of gas present in the sample. The amount of liquid is measured by weighing.

The accuracy of the obtained composition results is limited by disturbances introduced in the phase equilibrium by the sampling procedure itself. A sufficient amount of the fluid phase has to be withdrawn from the cell to deposit a measurable amount of liquid in the cold trap. Observed pressure drops in the cell were between 0.2 and 1 MPa, depending on the pressure at wich the sampling is performed. The mass taken out in each sample is no more than 3 % of the total mass inside the cell.

Another source of error in this procedure is the existence of a dead volume between valve 4 and the cold trap, where some solute may condense. To minimize these errors, series of samples were successively taken in the same operating conditions and the average value of solubility was estimated. The standard deviations for each of the sets of measurements vary from 0.7 mg/nL to 3.2 mg/nL; the average value is 1.8 mg/nL.

2.2.2 Capillary Gas Chromatography

Gas chromatography of SC-CO_2 extracted husk oil, and of other oil samples we used for reference, was performed with a Carlo Erba instrument of the Mega Series, model 5300, equipped with a Carlo Erba MFA 515 injector and a flame ionization detector (FID). Quantitative calculations were made with a Shimadzu CR3A computing integrator equipped with a floppy disk unit and a CRT display.

GC-analysis of the samples were carried out in a home made glass capillary column coated with OV-17-OH, of 0.25 micrometer diameter.

Injection was performed at programmed temperature under the following conditions : FID temperature 400 °C ; injector temperatures - initial temperature 100 °C , final temperature 390 °C ; split of the solvent (n-pentane) during a period of 300 s. After the split period, the injector was ballistically heated to 390 °C, and followed a splitless

period of 180 s, at this temperature. The split valve flow rate was 340 ml/min. 0.1 ml aliquots of the non extracted oil samples and 3 ml aliquots of the SC-CO_2 extracted oil samples were injected. Hydreogen at a pressure of 100 kPa was the carrier gas.

The oven temperature was programmed as follows : initially set at 150 °C and after ballistic heating to 280 °C, it was linearly programmed at a heating rate of 8°/min until the final temperature of 370 °C was reached.

The reproducibility of injection was tested with samples of non extracted oil ; aliquots of different concentration were injected with eight replicates each , and the mean value deviation was of 1-2.5 % to the higher concentrations and of 4-5 % to the lower concentrations.

3. RESULTS

We measured the solubility of glycerol trioleate (usually refered to as triolein) in SC-CO_2, at (308.1 ± 0.2) K, over a pressure range of 9.6 to 22 MPa. The results are given in table 1, where the solubility units are mass of solute per normal liter of gaseous carbon dioxide (1 nL = 1000 cm^3 at 1 bar, 0 ° C = 1.977g of CO_2).

The solubility of crude husk oil (previously extracted with hexane from husk flakes), in SC-CO_2 was measured at (308.6 ± 0.3) K and (313.6 ± 0.1) K, in a pressure range of 9 to 22 MPa. Extraction of the husk oil from the husk flakes was performed in a pressure range from 10 to 18 MPa and at 308.6 K. The results of these measurements are presented in table 2.

We used capillary gas chromatography to obtain the composition profiles of some of the extracted husk oil liquid samples. By the same method, we analysed the composition of the crude husk oil from which the SC-CO_2 extraction was performed, and additionally a husk oil obtained by traditional refining processes and two olive oils with a good market acceptance.

Integrating the peak areas corresponding to the major groups of compounds present in the several samples analysed, we obtained their relative concentration in the samples. These groups were ,in all cases, triglycerides and free fatty acids.

The composition data thus obtained and the corresponding results for the oil solubility enabled us to calculate the sclubilities of the free fatty acid and of the triglyceride fractions of the oil, as a function of pressure. These are given in table 3 .

In tables 4 and 5 the composition of the free fatty acid and the triglyceride fractions of the SC-CO_2 extracted husk oil is discriminated into their individual elements. The triglycerides are identified by a group of three letters corresponding to the fatty acid moieties, present in the triglyceride molecule, for instance, PLO refers a triglyceride that results from the esterification of glycerol with palmitic acid, linoleic acid and oleic acid, respectively in the first, second and third carbon atoms of the glycerol molecule.The relative concentration of each free fatty acid or each triglyceride is defined as its weight percent within the corresponding fraction, for instance, oleic acid weight % is defined as the concentration of oleic acid in the free fatty acid fraction.

Table 5 also includes the composition of the triglyceride fractions of the crude and refined husk oils and of the two olive oils mentioned above.

4. DISCUSSION

The solubility of triolein, measured in this work at 308.6 K, is compared in figure 2 with data of other authors. Our results are in very good agreement with the solubility values obtained by King et al. (6), at 308.15 K. The results of Chrastil (8) are also within experimental error of ours. Although they were obtained at a 5 K higher temperature, 313.15 K, interpolation between results at different temperatures of King et al. suggest that this increase in temperature should lower the solubility by only about 0.6 mg/nL.

The data reported by Brunetti et al. at 313.15 K are also shown in figure 2. They are much higher than the above mentioned results and also than other published values of the solubilities of oils mainly composed by triglycerides, like those of Sthal et al. (4) for soybean oil and those of Klein et al. (16) for rapeseed oil.

We measured husk oil solubility in carbon dioxide from previously hexane extracted crude husk oil and also from solid olive husk flakes.

Our results of the SC-CO_2 extraction from the husk flakes are in good agreement with those of King et al. (6) on rapeseed (another triolein rich solid matrix). We verify that, in both cases, solubilities are slightly higher than the solubility of triolein in identical pressure and temperature conditions. This probably means that the seed extracted oil contains compounds other than triglycerides - King reports the presence of small amounts of free fatty acids in the rapeseed oil extracts.

When SC-CO_2 extraction is performed from the husk flakes, the solubility values are lower than when similar measurements are done on liquid husk oil. This difference is shown in figure 3 and indicates that some of the compounds extracted with hexane are less or even non extracted by SC-CO_2 from the solid matrix. The hexane extracted husk oil (crude husk oil), and the corresponding SC-CO_2 extracts, were analysed by capillary chromatography and in both cases high contents of free fatty acids were found .

The chromatographic analysis allowed the separate calculation of solubilities of the free fatty acid and triglyceride fractions of SC-CO_2 extracted husk oil samples.

The corresponding free fatty acids solubilities are shown in figure 4, at 313.6 K. As the major constituent of the free fatty acid fraction is by far oleic acid, with about 60 % in weight (followed by palmitic and linoleic acids in amounts that do not exceed 16 % , as given in table 4), we compared our results with data of several authors for pure oleic acid.

It can be seen in figure 4 that, as for triolein, the results of Chrastil (8) and of King et al. (17) are in close agreement with our own. The measurements of Peter et al. (9) give somewhat higher solubilities.

As to the results of Brunetti et al. (7), they are once again higher than those of most other authors, as found previously for pure triolein. For oleic acid, however, a recent paper by Zou et al. (18) gives

solubilities in carbon dioxide that are even higher. As to the triglyceride fraction, solubilities at 308.65 K and 313.65 K are similar but slightly lower than the solubility of triolein, as measured in this work or as reported by Chrastil (8), at 313.15 K.

Triolein is not as prevailing among triglycerides in husk oil as oleic acid is among free fatty acids. After triolein (with about 45% weight), the most abundant constituent of the triglyceride fraction is 1-palmitil diolein (approximately 30% weight); other triglycerides are present in amounts lower than 10 % weight. We do not have data on the solubility of pure 1-palmitil diolein, but since it is reported (8) that tripalmitin has a lower solubility in SC-CO_2 than triolein, it is reasonable to suppose that the presence of a palmitic group in 1-palmitil diolein will be associated with a lower solubility of this triglyceride.

In figure 5 we can see how free fatty acids are more easily extracted than triglycerides from the oil , at 313.6 K. This difference between the solubility of free fatty acids and triglycerides was also detected at 308.6 K. The enrichment in free fatty acids is clear, if we compare the chromatograms of crude and SC-CO_2 extracted oils shown respectively in figures 6 and 7. Therefore, application of SC-CO_2 extraction to deacidify vegetable oils, particulary husk and olive oil, seems to be feasible in relatively mild operational conditions. This is the same conclusion as reached recently by Brunetti et al. (7), but based on substantially different results.

As mentioned above, the conventional refining processes used to deacidify either olive and husk oils may introduce changes in the triglyceride composition, producing a decrease in the nutricional qualities of the oil.

The results in table 5 show that the SC-CO_2 extracted husk oil, the crude oil and the two olive oils have a similar triglyceride composition; refined husk oil presents some considerable differences from all others, particulary in the weight % of triglycerides that contain oleate or linoleate groups. This is shown in figure 8. As no detectable differences were found between the crude oil and the extracts, it is reasonable to assume that contact with high pressure carbon dioxide, oppositely to classic refining processes, does not affect the organoleptic qualities of husk oil.

Therefore, the results obtained in this work indicate that SC-CO_2 extraction can achieve a deacidification of olive and husk oils, retaining their triglyceride composition and consequently preserving their nutritional characteristics.

ACKNOWLEDGEMENTS

We thank J.N.I.C.T., Lisbon (grant nº 886·86·119), A.I.D. Washington, D.C. (grant nº DPE-5542-G-SS-7048-00) and I.N.V.O.T.A.N. (N.A.T.O. grant PO-837-Lisbonfood) for financial support. One of us, (M. Gonçalves) thanks J.N.I.C.T. for a grant (BIC nº185).

REFERENCES

1. Friedrich, J.P., G.R. List and A.J. Heakin, J. Am. Oil Chem. Soc. 59:288 (1982)
2. List, G.R., and J.P. Friedrich, J. Am. Oil Chem. Soc. 66:98 (1989)
3. Sthal, E., E. Schutz and H.K. Mangold, J. Agri. Food Chem. 28:1153 (1980)
4. Sthal,E.,K.W. Quirin and Gerard , Fette . Seifen. Anstrichmittel85:458 (1983)
5. Sthal, E., K.-W. Quirin and D. Gerard, Dense Gases for Extraction and Refining, ed. Springer-Verlag, 1987
6. King, M.B., T.R. Bott, M.J. Barr and R.S. Mahmud Separation Science and Technology 22:1103 (1987)
7. Brunetti, L., A. Daghetta, E. Fedeli, I. Kikic and L. Zanderighi J. Am. Oil Chem. Soc. 66:209 (1989)
8. Chrastil, J., J. Phys. Chem. 86:3016 (1982)
9. Peter, S., M. Seekamp and A. Bayer in Proceedings of the International Symposium on Supercritical Fluids, Nice, 1988, p.99
10. DAS 23 32 038 (23.6.1973) Studiengesellschaft Kohle mbH, Mulheim. Inventor: Zosel, K.
11. DOS 2843 920 (9.10.1978) F. Krupp GmbH, Essen. Inventors: Coenen, H., Kriegel, E.
12. Brunner,G., S. Peter Ger. Chem. Eng. 5: 181 (1982)
13. Giovachino, L. Di, M. Solinas, V. Brandani, G. del Re and G. Di Giacomo, Industrie Alimentari 28:925 (1989)
14. Vasconcelos, A.M.P., M. Gonçalves, E.J.S. Gomes de Azevedo, M.Nunes da Ponte and H.J. Chaves das Neves , HRC 12:244 (1989)
15. Matos, H.A., E. Gomes de Azevedo, P.C. Simões, M.T. Carrondo and M. Nunes da Ponte , Fluid Phase Equilibria 52:357 (1989)
16. Klein, T., and S. Schulz, Ind. Eng. Chem. Res. 28:1073 (1989)
17. King, M.B., D.A. Alderson, F.H. Fallaha, D.M. Kassim, J.R. Sheldon and R.S. Mahmud, Chapter 2 in Chemical Engineering at Supercritical Fluid Conditions, M.E. Paulaitis et al., 1983, p. 31
18. Zou, M., Z.R. Yu, P. Kashulines, S.S.H. Rizvi and J. Zollweg, J. Supercritical Fluids 3: 23 (1990)

TABLES

Table 1 - Solubility (S) of glycerol trioleate in carbon dioxide, at pressure P and at 308.15 K.

P MPa	S mg/nL	P MPa	S mg/nL
9.6	1.1	12.2	3.8
9.9	1.9	14.0	4.4
10.0	2.2	15.0	5.6
10.3	1.9	18.9	6.2
11.3	3.6	22.0	7.7

Table 2 - Solubility of husk oil in carbon dioxide, at pressure P and temperature T = 308.65 K and 313.65 K. The oil was extracted from: a) solid phase - husk flakes , b) liquid phase - crude husk oil

P MPa	T/K 308.65		313.65
	a) solid	b)liquid	b) liquid
9.0		5.0	
10.0	4.7	5.5	
10.5		6.1	5.5
11.3		7.5	7.3
12.0	6.2	8.9	7.8
12.5		9.3	
13.0		10.0	10.5
14.2		11.7	11.2
15.3		11.9	13.7
16.0	6.4	12.3	
16.8		13.4	15.9
17.6		14.6	17.0
18.0	8.1	15.8	
18.6		16.9	
19.5		18.8	17.5
19.8		19.1	
20.7			17.5
21.7			18.4

Table 3 - Comparison between the solubility S, in carbon dioxide, of crude husk oil (S_{Oil}), and of the corresponding triglyceride (S_{Tri}) and free fatty acid (S_{FFA}) fractions, at pressure P and at temperatures of 308.6 K and 313.6 K.

T/K	P MPa	S mg/nL		
		S_{Oil}	S_{Tri}	S_{FFA}
308.65	11.3	7.5	3.7	3.4
	12.5	9.3	4.2	4.6
	14.2	11.7	3.5	7.1
	15.3	11.9	3.4	7.1
	17.6	14.6	3.6	9.2
	19.8	19.1	3.4	14.3
313.65	10.5	5.5	1.7	3.4
	13.0	10.5	1.6	7.4
	14.2	11.2	2.0	8.2
	15.3	13.7	3.7	8.8
	17.6	17.0	5.3	10.3
	20.7	17.5	3.9	12.1
	21.7	18.4	6.0	10.7

Table 4 - Characterization of the free fatty acid fractions from oil samples obtained by extraction of crude husk oil with SC-CO_2, at pressure P and temperatures of 308.6 K and 313.6 K. Individual free fatty acid concentration is given as the weight percent of the total free fatty acid fraction.

T/K	P MPa	Individual FFA Weight Percent			
		Palmitic (C16:0)	Stearic (C18:0)	Oleic (C18:1)	Linoleic (C18:2)
308.65	11.3	7.7	5.5	57.5	11.2
	12.5	10.4	1.7	61.3	5.3
	17.6	8.0	2.0	63.7	7.3
	19.8	14.7	4.6	71.5	3.7
313.65	10.5	7.7	5.2	62.5	9.4
	11.5	6.4	51.7	15.8	13.0
	17.6	9.6	2.4	57.7	12
	20.7	7.7	1.6	59.5	7.2

Table 5 - Characterization of the triglyceride fractions corresponding to: SC-CO_2 extracted husk oil, crude husk oil, refined husk oil and two olive oils; the SC-CO_2 extracted oil samples were obtained at pressure P and temperatures of 308.6 K and 313.6 K. Individual triglyceride concentration is given as the weight percent of the total triglyceride fraction.

Oil Samples	P MPa	Individual Triglyceride Weight Percent								
		POP	PLP	POO	PLO	PLL	OOO	OLO	OOL	OLL
SC-CO_2 extracts										
1	11.3	4.3	2.7	24.8	8.1	3.7	42.4	9.4	4.5	0.0
2	12.5	4.9	2.3	30.2	6.6	1.6	46.5	6.4	1.5	0.0
3	17.6	7.0	7.0	30.1	10.3	0.0	37.5	8.0	0.0	0.0
4	19.8	5.5	2.9	29.2	8.0	1.7	43.1	7.5	2.1	0.0
5	17.6	6.3	2.3	33.4	6.1	0.2	45.2	4.9	0.5	0.0
6	20.7	6.4	2.3	32.2	5.9	0.3	45.0	5.5	0.8	0.0
crude husk oil		4.6	1.8	28.9	6.8	0.2	45.6	6.8	0.9	0.2
refined husk oil		3.1	1.0	14.0	7.2	7.7	21.8	8.8	9.7	13.2
olive oil 1		4.2	2.4	32.0	6.0	2.9	47.0	8.5	0.0	0.0
olive oil 2		4.2	2.3	28.1	6.0	2.9	43.4	8.5	0.0	0.0

The temperature at which the extracts were obtained was : extracts 1 to 4 - 308.65 K; extracts 5 and 6 - 313.65 K.

FIGURES

FIGURE 1 - Schematic diagram of the SC-CO_2 extraction apparatus.

FIGURE 2 - Solubility of glycerol trioleate in SC-CO_2 , at 308.6 K (●); Comparison with measurements reported by: King et al.(*), at 308.15 K; J. Chrastil (△) and Brunetti et al. (◊), at 313.15 K.

FIGURE 3 - Solubility of husk oil in SC-CO_2, at 308.6 K, when extraction is performed from crude husk oil (○) or from olive husk flakes (◐).

FIGURE 4 - Comparison between : a) solubility in SC-CO_2 of free fatty acids from husk oil (◐), at 313.6 K; b) other authors reports on the solubility in SC-CO_2 of oleic acid - Chrastil (△), Peter et al. (▽), Brunetti et al. (◊), Zou et al. (○), at 313.15 K and King et al. (*) at 308.15 K.

FIGURE 5 - Solubility of : crude husk oil(◐), the free fatty acid(○) and the triglyceride (△) fractions from the same oil, in SC-CO_2 , at 313.6 K.

FIGURE 6 - Typical chromatographic profile of a crude husk oil.

FIGURE 7 - Chromatogram of a SC-CO_2 extract obtained from crude husk oil, at 17.6 MPa and 313.6 K.

FIGURE 8 - Triglyceride composition of SC-CO_2 extracts obtained in different pressure and temperature conditions; comparison with olive and husk oils.

Fig 1

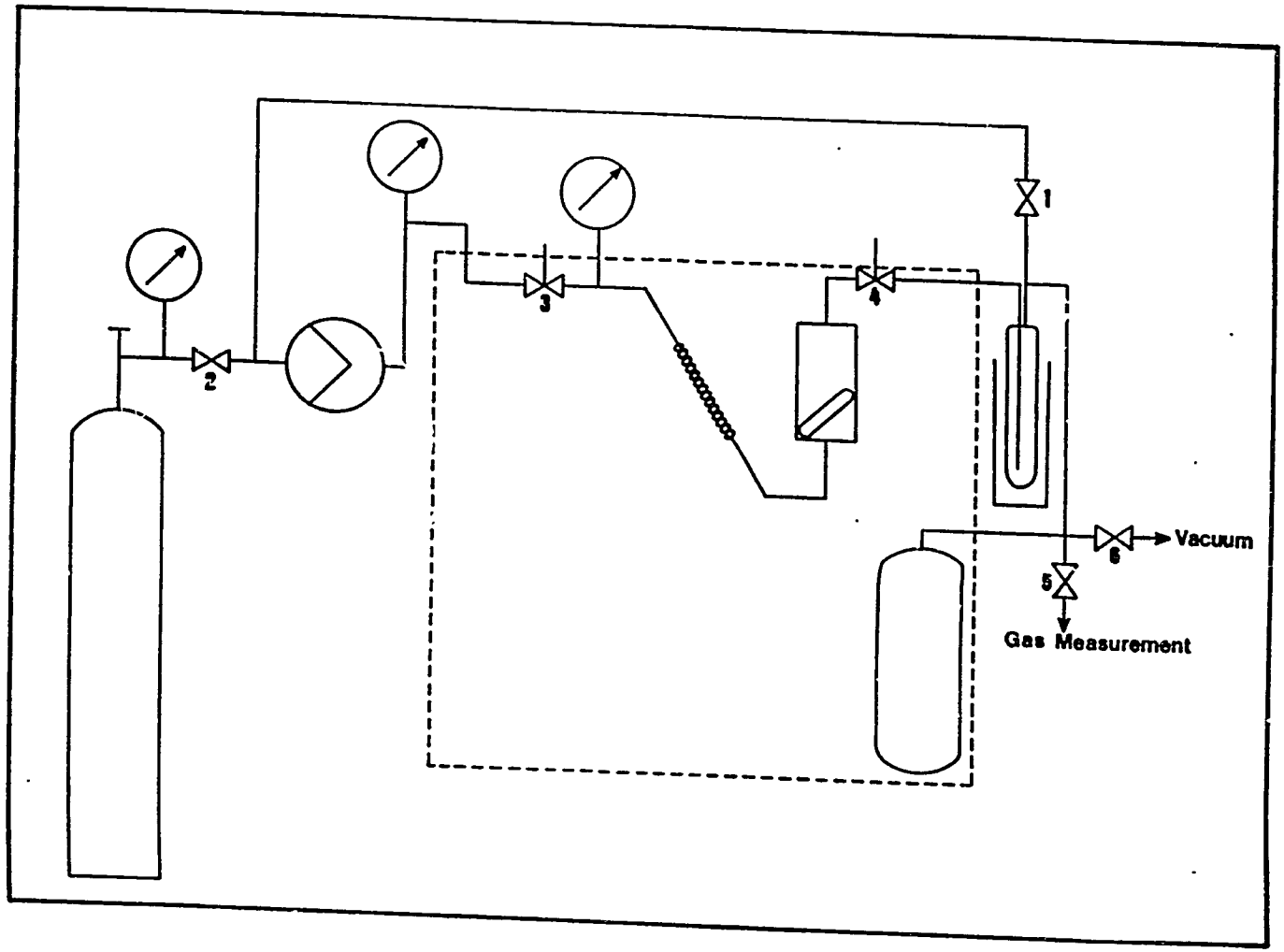

2/

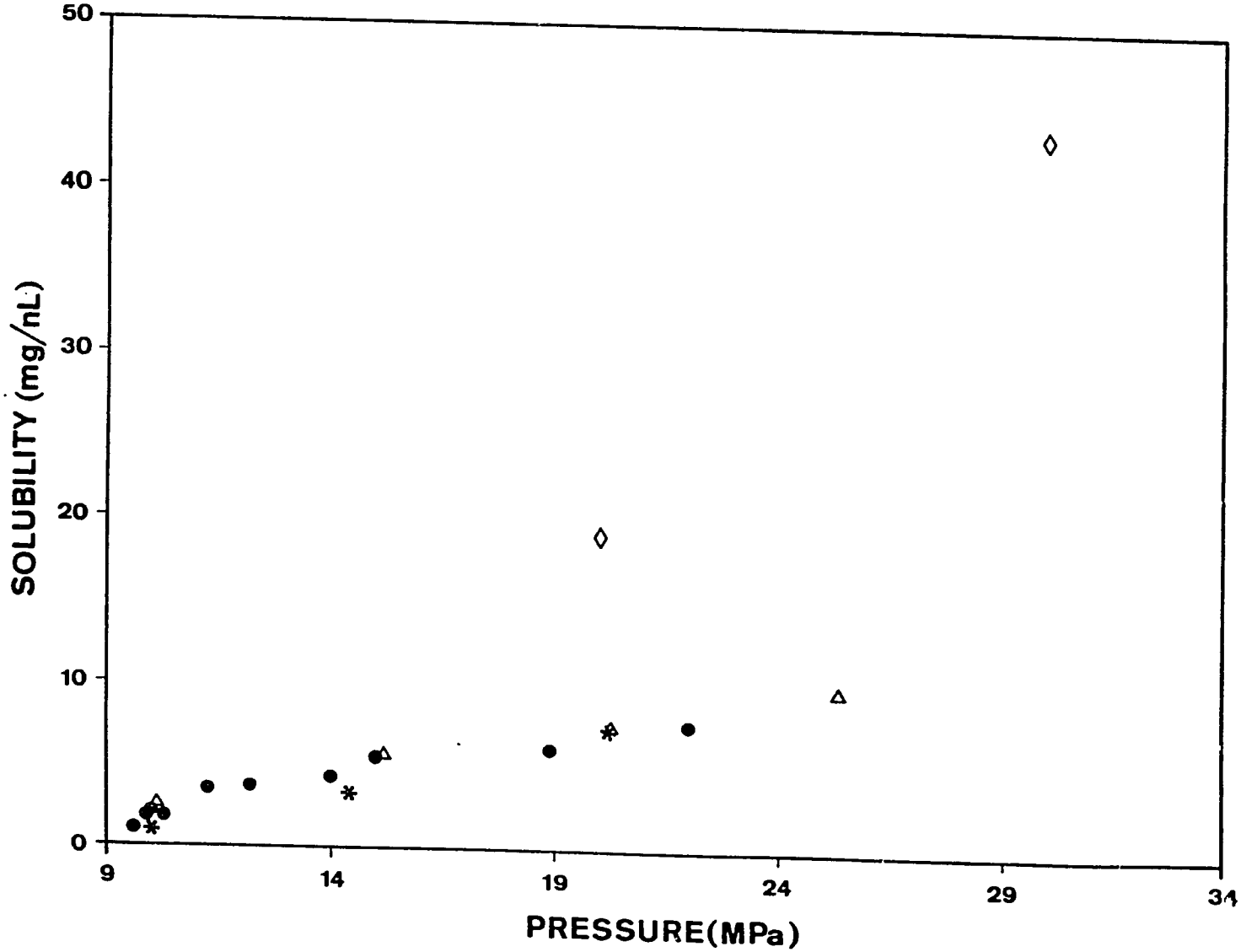
50
40
30
20
10
0
SOLUBILITY (mg/nL)
9
14
19
24
29
34
PRESSURE(MPa)

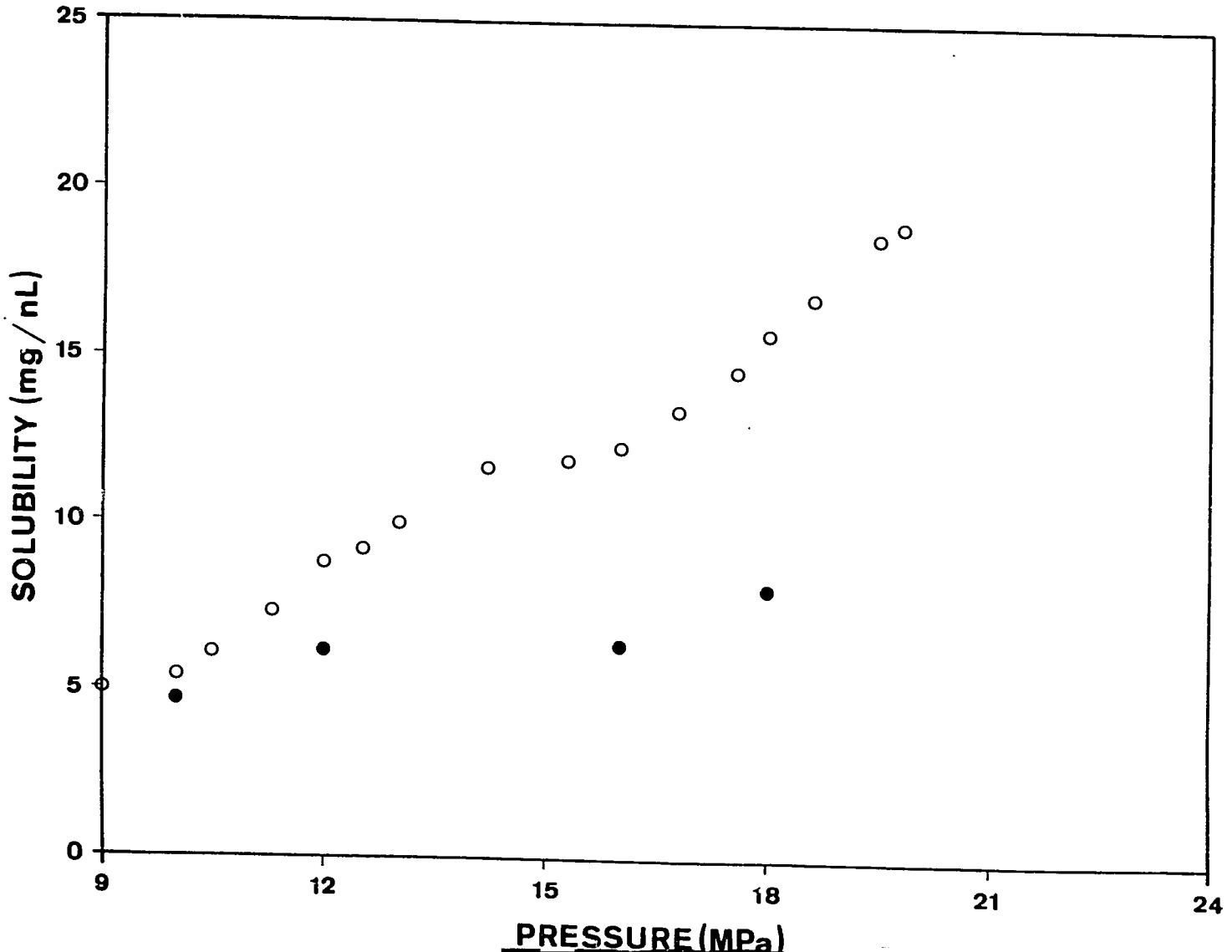
SOLUBILITY (mg/nL)
25
20
15
10
5
0
9
12
15
18
21
24
PRESSURE (MPa)

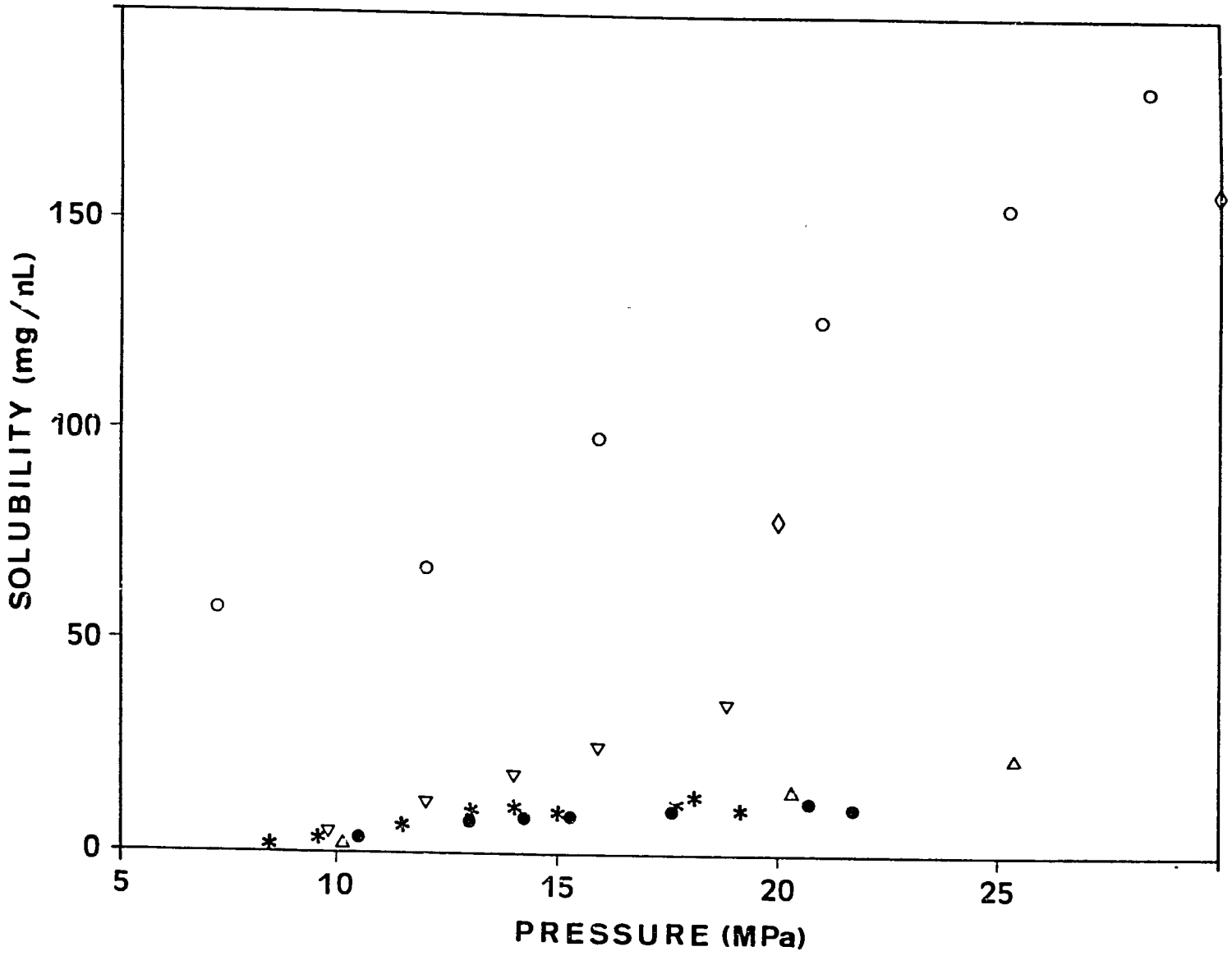
SOLUBILITY (mg/nL)
150
100
50
0
5
10
15
20
25
PRESSURE (MPa)

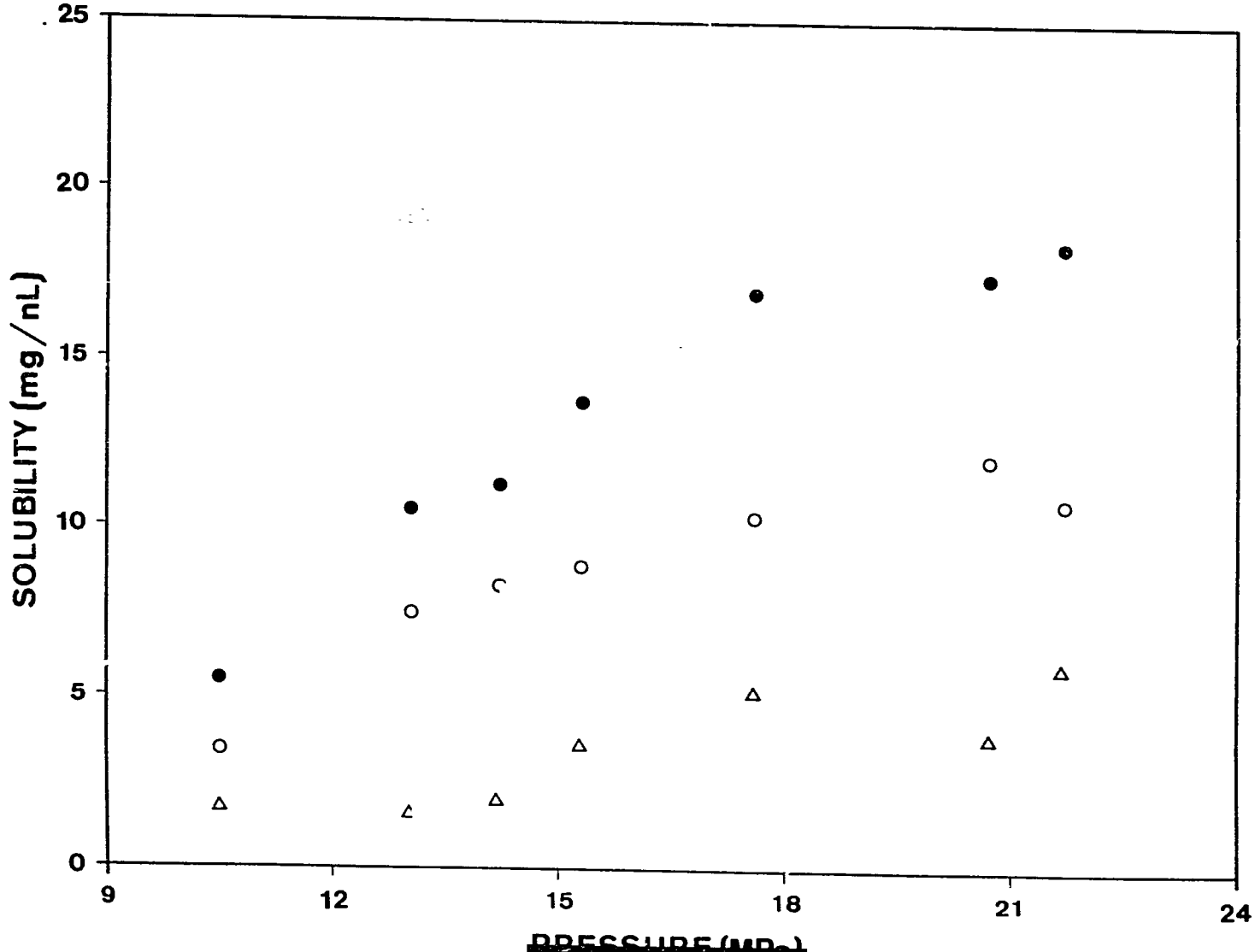
SOLUBILITY (mg/nL)
25
20
15
10
5
0
9
12
15
18
21
24
PRESSURE (MPa)

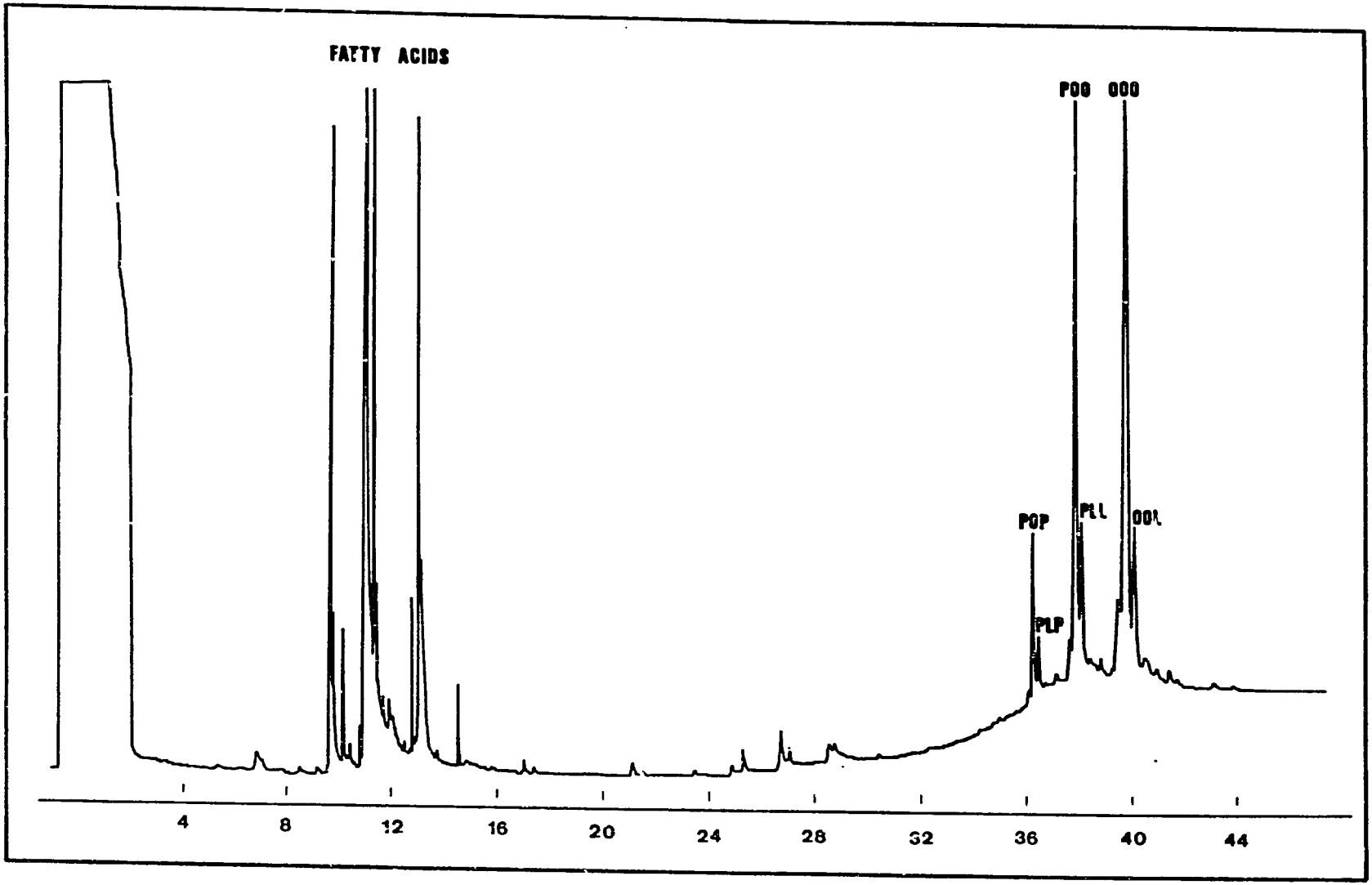
FATTY ACIDS
POO
OOO
POP
PLL
OOL
PLP
4
8
12
16
20
24
28
32
36
40
44

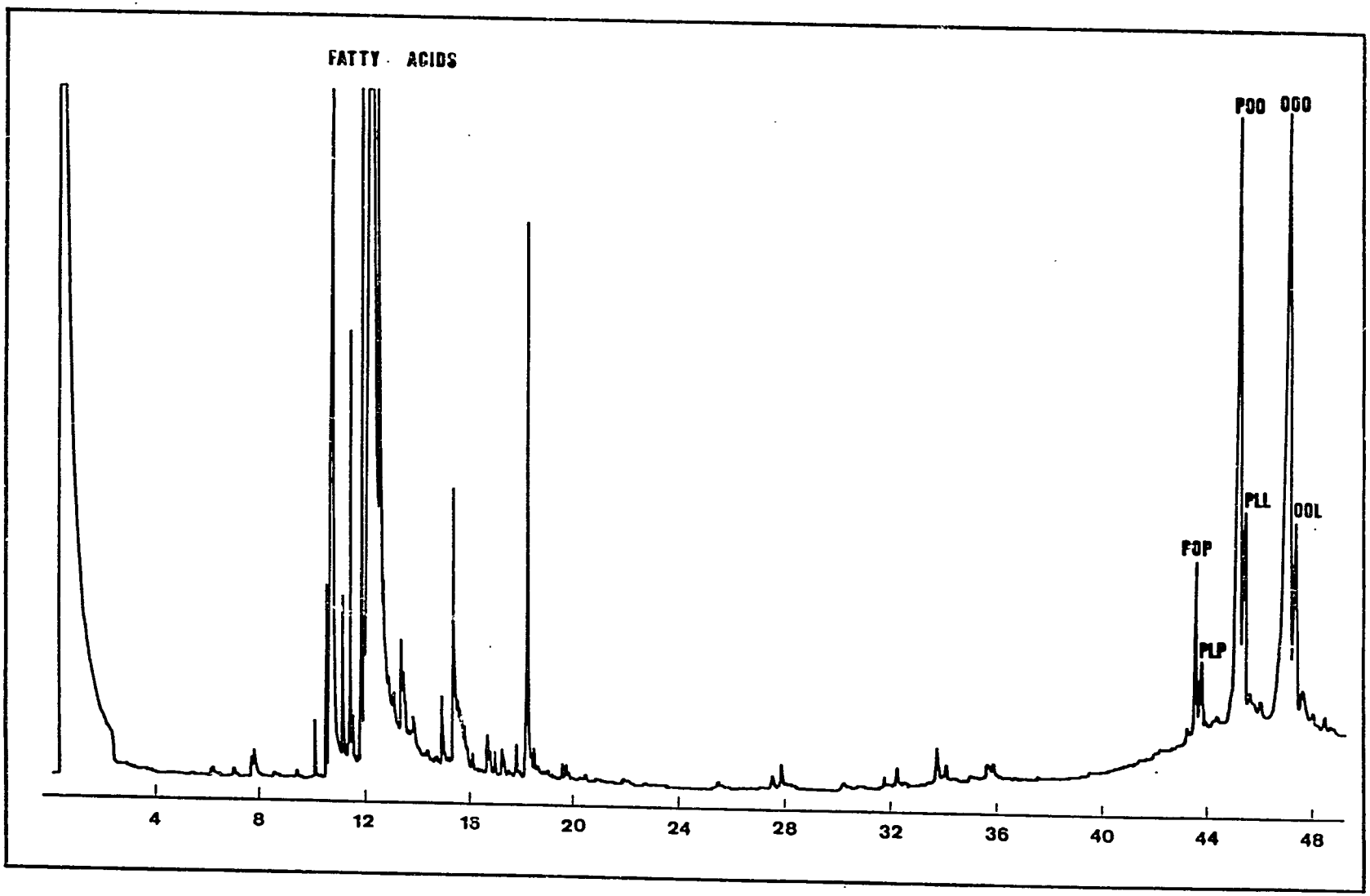
FATTY ACIDS
POO
OOO
PLL
OOL
FOP
PLP
4
8
12
16
20
24
28
32
36
40
44
48

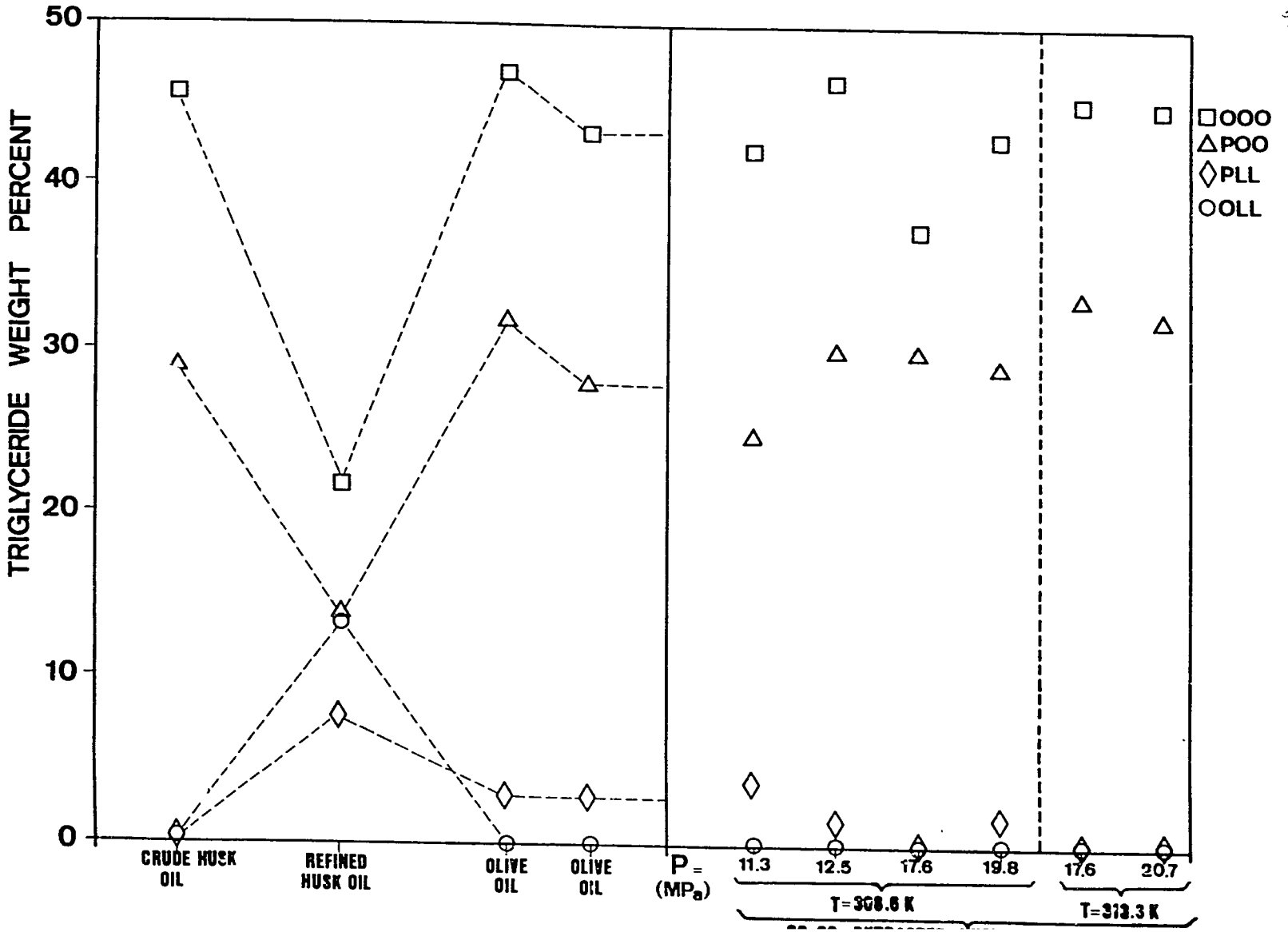
TRIGLYCERIDE WEIGHT PERCENT
50
40
30
20
10
0
CRUDE HUSK OIL
REFINED HUSK OIL
OLIVE OIL
OLIVE OIL
P = (MPa)
11.3
12.5
17.6
19.8
17.6
20.7
T=308.6 K
T=313.3 K
OOO
POO
PLL
OLL

Use of Computerized Pattern Recognition of Triglyceride Profiles in Monitoring SCF-CO_2 Extraction of Fatty Oils

A. M. P. Vasconcelos
Departamento de Fitotecnia, Universidade de Évora, 7000 Évora, Portugal

M. Gonçalves, E. J. S. Gomes de Azevedo, M. Nunes da Ponte, and H. J. Chaves das Neves
Departamento de Química, Faculdade de Ciências e Tecnologia, Universidade Nova de Lisboa, 2825 Monte de Caparica, Portugal

Key Words:

High temperature CGC
SF CO_2 extraction
Pattern recognition
Fatty oils

Summary

High pressure extraction of vegetable fatty oils by supercritical fluid carbon dioxide was investigated. Pressures from 9 to 20 MPa at 40°C were used. The extracts were monitored by high temperature capillary gas chromatography for sterol and triglyceride composition. The quality of the extracted oils was evaluated by numerical taxonomy methods. The extraction products compared well with the characteristics of commercial fatty oils of the same vegetable origin. No significant qualitative variation was detected in the pressure range studied.

1 Introduction

The applicability of supercritical fluid extraction (SCFE) to the recovery of vegetable fatty oils has been reported by several authors. The solubility of vegetable fatty oils in SCF-CO_2 as well as the advantages of this technology over conventional methods of fatty oils extraction have been described [1-5]. However, in many instances characterization of the extracts is made solely on the basis of gravimetric methods by which product quality can hardly be assessed [1-4]. Gas chromatography of the fatty acid content has been used [2]. Data on fatty acid composition of fatty oils is often biased by the fact that the values obtained may still be within the accepted range, in spite of contaminations. Therefore, on the basis of fatty acid content alone, the oils cannot be adequately characterized.

In the present work, high temperature capillary gas chromatography was used to monitor the triglyceride and sterol composition of the fatty oils obtained by SCF-CO_2 extraction of soybean seeds and oils, carried out in a home-made extractor. The data were treated by computerized pattern recognition methods in order to characterize the different extracts obtained from the same material under different extraction conditions. The results were compared with identical data obtained from crude and refined commercial oils of identical plant origin. The results presented show that SCF-CO_2 extraction leads to products that are quantitatively and qualitatively comparable to the ones obtained by traditional techniques. The application of high temperature capillary gas chromatography, associated with pattern recognition techniques, for rapid assessment of product quality in monitoring the extraction procedure is illustrated.

Presented at the Ninth International Symposium on Capillary Chromatography

2 Materials and Methods

2.1 Materials

The CO_2 used was of commercial grade obtained in cylinders purchased from Companhia Portuguesa do Ar Líquido. The seeds were obtained directly from vegetable oil manufacturers as being the same raw materials as used in fatty oil production. Crude and refined oils were obtained from the same industrial sources. The seeds were milled in a coffee mill, producing flakes of 0.5 to 1.5 mm thickness. All solvents were of analytical grade obtained from E. Merck (Darmstadt).

2.2 Instruments

Gas chromatography was performed with a Carlo Erba instrument of the Mega Series, model 5300, equipped with a split-splitless injector and a flame ionization detector (FID). Quantitative calculations were made with a Shimadzu CR3A computing integrator equipped with a floppy disk unit and a CRT display. Triglycerides were identified by comparision with oils of known composition and the sterols were identified by GC-MS with a Shimadzu model QP-1000 instrument from EI mass spectra. Computerized treatment of the data was performed on an IBM and an Apple IIe microcomputer.

2.3 Capillary Gas Chromatography and GC-MS

GC of triglycerides from oils and SCF extracts was carried out with a 25 m × 0.25 mm i.d. steel-armored fused silica capillary column coated with OV-17-OH purchased from Rescom. 0.1 µl aliquots of 0.01% solutions of the oils in *n*-heptane were injected in splitless injection mode. For this purpose, the injector was equipped with a 8 cm × 2.5 mm i.d. glass liner (0.25 ml) and injection was carried at elevated carrier gas flow rate (6 ml/min). A splitless period of 40 s was used. The initial oven temperature during injection was 40°C. After ballistic heating to 240°C the oven temperature was linearly programmed at a heating rate of 8°/min until the final temperature of 370°C was reached. Hydrogen was used as carrier gas, P_i = 120 KPa. Injector temperature, 400°C; FID temperature 400°. Raw data of all analyses were stored on floppy disk for subsequent integration.

Sterols were analyzed underivatized on a home-made 6 m × 0.25 mm i.d. borosilicate glass capillary, coated with OV-17-OH, under isothermal conditions at 260°C. Carrier gas, hydrogen P_i =

© 1989 Dr. Alfred Huethig Publishers

100

40 kPa Injector and FID temperature, 350°C The same gas chromatographic conditions were used for GC-MS of the sterol fractions obtained from the unsaponifiable fractions. The mass spectra (EI, 70 eV) were obtained under the following mass spectrometer conditions, ion source temperature 250°C, interface temperature, 350°C, multiplier, 2,100 V The capillary column was directly connected to the ion source by means of a 1 m piece of 0 25 mm i d deactivated fused silica column, connected to the capillary by means of a low dead volume butt connector (Supelco)

2.4 Pattern Analysis

Each oil sample was regarded as an assembly of variables, each variable being the mean value of five replicates for the percentage integrated peak areas of the peaks of interest The triglycerides composition and the sterol composition for each sample, formed two arrays of data vectors, representing that sample Principal component analysis and the "star plot" diagrams were made by an IBM PC processor, by means of STATGRAPHICS® (Statistical Graphics Corporation, Rockville, Maryland) Dendograms were made by an Apple IIe by means of CLUE® (Elsevier Scientific Software, Amsterdam)

2.5 Supercritical CO_2 Extraction

The apparatus used in SCF-CO_2 extraction is schematically represented in **Figure 1** Carbon dioxide, from cylinder 1 is brought to the desired pressure by a diaphragm compressor (3) and injected in a high pressure cell (5) The cell has an internal volume of approximately 30 ml and is immersed in a water bath The connections at both ends of the cell 5 are made of flexible steel capillary tubing, thus allowing vigorous shaking of the cell The shaking is necessary for ensuring a good contact between the supercritical fluid and the materials inside One-hour shaking periods were used before sampling The end caps of the cell 5 are designed for easy removal Pressure is measured by a Bourdon tube manometer (4), with an accuracy of ± 100 kPa Valve 6 is a pressure valve which opens to a glass container were the extract left behind by the depressurized CO_2 gas is collected Valve 8 leads the gas to a thermostated cylinder, of calibrated volume, connected to a mercury manometer This arrangement allows the measurement of the amount of CO_2 that dissolved the recovered extract.

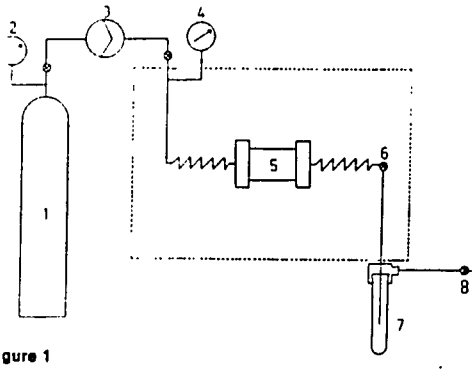

Figure 1

SCF-CO_2 Extraction apparatus. 1 = CO_2 cylinder; 2 and 4 = manometers; 3 = compressor; 5 = high pressure cell; 6 = pressure reducing valve; 7 = glass container; 8 = valves.

3 Results and Discussion

The apparatus represented schematically in Figure 1 was constructed for the supercritical fluid carbon dioxide (SCF-CO_2) extraction of soybean oil The cell was immersed in a water bath at constant temperature (40 6°C ± 0 5°) After temperature equilibration for one hour the sample is kept in contact with supercritical CO_2, also for one hour, with vigorous shaking. Extractions were performed at 8 9, 11 9, 12, 14.4 (3 samples), 14 9, and 18 4 MPa Within the pressure range of 11 9 to 18 4 MPa the extraction yields correlates linearly with the extraction pressure (r = 0.9978) The oils obtained were analyzed by high temperature capillary gas chromatography for triglycerides and sterols composition All samples showed similar gas chromatographic profiles (**Figure 2**).

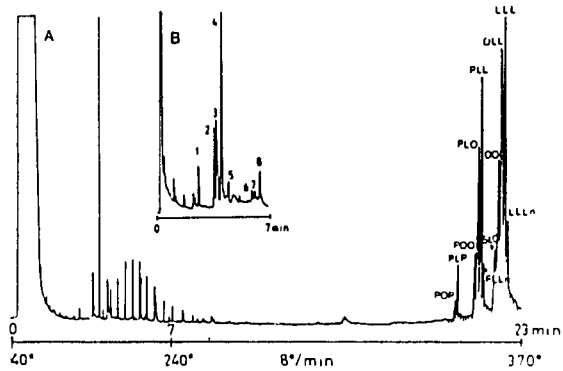

Figure 2

Typical high temperature capillary GC profile for triglycerides (A) and unsaponifiable matter sterols (B) of SCF-CO_2 extracts of soybean oil: A = triglycerides (for nomenclature see [6]); B = sterols; 1 = Δ^5-campesterol; 2 = stigmasterol; 3 = Δ^7-campesterol; 4 = sitosterol; 5 = fucosterol; 6 = Δ^5-avenasterol; 7 = stigmastenol; 8 = citrostadienol.

The extraction pressure showed no significant effect on the triglyceride composition of the oils For each extracted oil, the relative concentration of the individual triglycerides was calculated as the percentage peak areas [6] A tridimensional plot of the relative percent composition of each triglyceride *vs* extraction pressure is shown in **Figure 3** It can be seen that the different SCF-CO_2 extracts have similar qualitative and quantitative triglyceride compositions Under the isothermal conditions used, SCF-CO_2 does not seem to possess selective solvent properties for any particular triglyceride.

The percent relative composition of triglycerides was also determined for commercial soybean oils, of which two were refined products and the other two were crude industrial extracts, obtained by traditional solvent extraction techniques The results were compared with those obtained from SCF-CO_2 extraction Two kinds of SCF-CO_2 soybean oil extracts were obtained: direct SCF-CO_2 extraction of the seeds, and direct extraction from commercial soybean oil. Both kinds of extracts were obtained at the described working pressures The mean concentrations of the individual triglycerides are compared with the corresponding values for commercial refined and crude

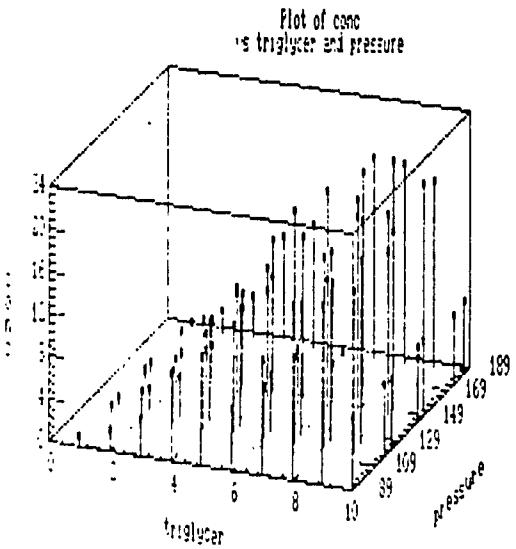

Figure 3

Tridimensional plot of percent relative concentrations of individual triglycerides present in the SCF-CO_2 extracted soybean oils, at different pressures (kPa × 10^{-2}). Triglycerides: 1 = POP; 2 = PLP; 3 = POO; 4 = PLO; 5 = PLL; 6 = SLO; 7 = OOL; 8 = OLL; 9 = LLL; 10 = LLLn (for nomenclature, see [6]).

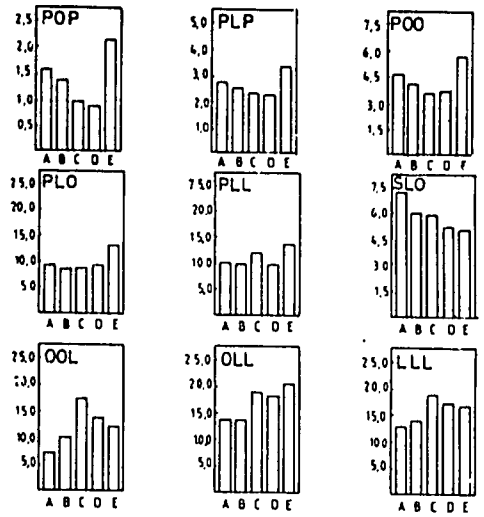

Figure 4

Histograms for the individual triglyceride composition in percentage peak areas for different soybean oils: A = commercial crude oil; B = commercial refined; C = residual oil in the extraction cell after SCF-CO_2 extraction; D = SFC-CO_2 oil extracted from commercial oil; E = SCF-CO_2 oil extracted directly from the milled seeds.

soybean oils in **Figure 4** Except for POP in the SCF-CO_2 soybean seed extract, the samples have very similar triglyceride composition (Figure 4) When the SCF-CO_2 extraction is performed on the soybean oil itself, the triglyceride composition of the extract does not differ significantly from the composition of the oil remaining behind in the extraction cell

Although these results show the similarity between the current commercial soybean oils obtained by solvent extraction techniques and those obtained by SCF-CO_2 extraction, as well as the minute influence of the extraction pressure on the triglyceride composition, it is not suprinsing that classification of the oils may not always be easily achieved on the basis of triglyceride analysis alone A better correlation between gas chromatographic triglyceride profiles and the nature of the fatty oils can be achieved by the use of pattern recognition methods

The application of pattern recognition methods to the characterization of fatty oils is reported elsewhere [7] **Figure 5** shows the results of hierarchical clustering of different vegetable fatty oils including the soybean oils obtained by SCF-CO_2 extraction. The dendogram was drawn by the CLUE® program (Elsevier Scientific Software). The percentage integrated peak areas of triglycerides (Figure 2), were used as variables without any previous treatment. The oils are well grouped together according to their origin All soybean oils are grouped together under the same cluster. It is interesting to note, however, that two independent sub-clusters are formed by the commercial soybean oils, on one side, and the oils obtained by SCF-CO_2 extraction, on the other.

These observations show that high temperature capillary gas chromatography is the method of choice for monitoring SCF-CO_2 extraction of fatty oils through their triglyceride profiles. No sample preparation is required Solutions of the oils (0 01%) in *n*-heptane can be directly analyzed under splitless conditions. The percentage integrated peak areas for the individual triglycerides are used as object (oil) characterizing features (variables). Straightforward information may be obtained from these data, if treated by the "star symbol plot" sub-routine of the

Figure 5

Dendogram of plant fatty oil classification according to triglyceride percentage integrated peak areas from high temperature capillary gas chromatographic assay. Fatty oils (sample no.): S = soybean; C = corn; SF = sunflower; GS = grapestone; MX = commercial mixture; O = olive; OH = olive-husks; SCF (extraction pressure in bars) = SCF-CO_2 extracted soybean oil.

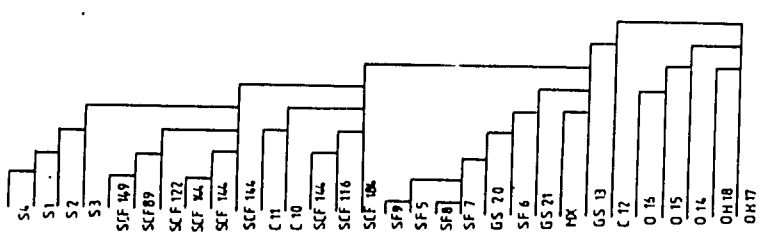

Figure 6

Star symbol plot of capillary GC percentage integrated peak areas of triglycerides for quality control of SCF-CO_2 extracted soybean oils at different pressures. Comparison with current commercial oils originating from the same seeds.

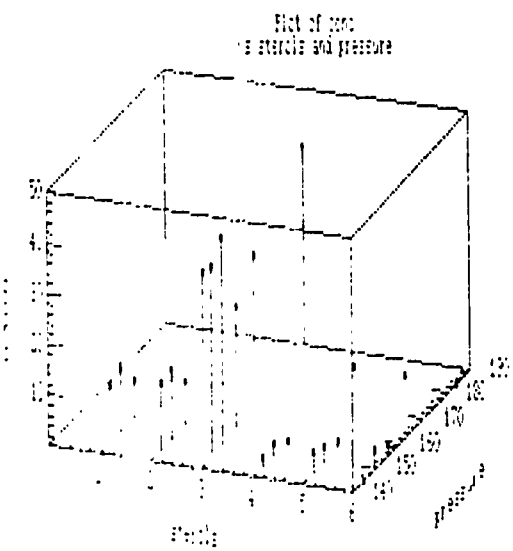

Figure 7

Three-dimensional plot of sterol relative composition (%) of SCF-CO_2 extracted soybean oils at different pressures (kPa × 10^{-2}). Sterols: 1 = Δ^5-campesterol; 2 = stigmasterol; 3 = sitosterol; 4 = Δ^5-avenasterol; 5 = stigmastenol; 6 = citrostadienol.

STATGRAPHICS® program (**Figure 6**). This is an interesting way of graphing multivariate data, allowing visual comparison of the different observations The "star" is formed from a series of rays drawn from a center point, each ray representing the magnitude of each variable in the matrix In this case, no special knowledge of pattern recognition techniques is required. The similarities and differences between the different oils and their comparison with the plots obtained from current soybean oils are recognized directly (Figure 6).

Additional information may be obtained from capillary gas chromatography of the unsaponifiable matter sterols. However, in contrast to triglycerides, the individual sterols seem to be somehow irregularly affected by the extraction pressure (**Figure 7**). For these reasons, and also owing to the smaller overall concentrations and sample preparation procedures, the role of sterol analysis is limited to complementary qualitative information as far as the extraction monitoring is concerned.

4 Conclusions

Capillary gas chromatography of fatty oils is an adequate technique for the monitoring of SCF-CO_2 extraction of fatty oils, as demonstrated for soybean oil. Treatment of the data by methods of pattern recognition permits assessment of comparative quality.

Acknowledgments

This work was partially supported by Junta Nacional de Investigação Científica e Tecnológica under research contract no 886 86.119, and by Smith Kline & French through a research grant.

References

[1] *J P Friedrich, G R List,* and *A J Heakin,* J Am Oil Chem Soc. **7** (1982) 288

[2] *E Stahl, E Schutz,* and *H K Mangold,* J Agric Food Chem **28** (1980) 1153

[3] *N R Bulley, M Fatton, A Meisenand,* and *L Moyls,* J Am Oil Chem Soc **61** (1984) 1302

[4] *E Stahl, K W Quirin,* and *D Gerard,* Fette Seifen Anstrichmittel **12** (1983) 458

[5] *M MacHugh, V Krukonis,* "Supercritical Fluid Extraction", Butterworths, Stoneham (1986) Chapter X

[6] *E Geeraert* in *P Sandra* (Ed), "Proc Sixth International Symposium on Capillary Chromatography", Riva del Garda, May 14-16, 1985, Huthig, Heidelberg (1985) p 174.

[7] *H J Chaves das Neves* and *A M P Vasconcelos* in *P Sandra* (Ed), "Proc Ninth International Symposium on Capillary Chromatography", Monterey, May 16-19, 1988, Huthig, Heidelberg (1988), p 643